UNITED STATES AIR FORCE

SUMMER RESEARCH PROGRAM – 1998

SUMMER FACULTY RESEARCH PROGRAM FINAL REPORTS

VOLUME 6

ARNOLD ENGINEERING DEVELOPMENT CENTER

UNITED STATES AIR FORCE ACADEMY

AIR LOGISTIC CENTERS

WILFORD HALL MEDICAL CENTER

RESEARCH & DEVELOPMENT LABORATORIES

5800 Uplander Way

Culver City, CA 90230-6608

Program Director, RDL
Gary Moore

Program Manager, AFOSR
Colonel Jan Cerveny

Program Manager, RDL
Scott Licoscos

Program Administrator, RDL
Johnetta Thompson

Program Administrator, RDL
Rebecca Kelly-Clemmons

Submitted to:

AIR FORCE OFFICE OF SCIENTIFIC RESEARCH

Bolling Air Force Base

Washington, D.C.

December 1998

AQM01-06-1208

PREFACE

Reports in this volume are numbered consecutively beginning with number 1. Each report is paginated with the report number followed by consecutive page numbers, e.g., 1-1, 1-2, 1-3; 2-1, 2-2, 2-3.

This document is one of a set of 15 volumes describing the 1998 AFOSR Summer Research Program. The following volumes comprise the set:

VOLUME	TITLE
1	Program Management Report
	Summer Faculty Research Program (SFRP) Reports
2	Armstrong Laboratory
3	Phillips Laboratory
4	Rome Laboratory
5A & 5B	Wright Laboratory
6	Arnold Engineering Development Center, Air Logistics Centers, United States Air Force Academy and Wilford Hall Medical Center
	Graduate Student Research Program (GSRP) Reports
7	Armstrong Laboratory
8	Phillips Laboratory
9	Rome Laboratory
10	Wright Laboratory
11	Arnold Engineering Development Center, and Wilford Hall Medical Center
	High School Apprenticeship Program (HSAP) Reports
12	Armstrong Laboratory
13	Phillips Laboratory
14	Rome Laboratory
15A, 15B & 15C	Wright Laboratory

REPORT DOCUMENTATION PAGE

AFRL-SR-BL-TR-00-

0782

1. AGENCY USE ONLY (Leave blank)	2. REPORT DATE December, 1998	3. RE. ... .

4. TITLE AND SUBTITLE
1998 Summer Research Program (SRP), Summer Faculty Research Program (SFRP), Final Reports, Volume 6, Arnold Eng. Development Center, US Air Force Academy, Air Logistic Centers, and Wilford Hall Medical Center

5. FUNDING NUMBERS
F49620-93-C-0063

6. AUTHOR(S)
Gary Moore

7. PERFORMING ORGANIZATION NAME(S) AND ADDRESS(ES)
Research & Development Laboratories (RDL)
5800 Uplander Way
Culver City, CA 90230-6608

8. PERFORMING ORGANIZATION REPORT NUMBER

9. SPONSORING/MONITORING AGENCY NAME(S) AND ADDRESS(ES)
Air Force Office of Scientific Research (AFOSR)
801 N. Randolph St.
Arlington, VA 22203-1977

10. SPONSORING/MONITORING AGENCY REPORT NUMBER

11. SUPPLEMENTARY NOTES

12a. DISTRIBUTION AVAILABILITY STATEMENT
Approved for Public Release

12b. DISTRIBUTION CODE

13. ABSTRACT (Maximum 200 words)
The United States Air Force Summer Research Program (USAF-SRP) is designed to introduce university, college, and technical institute faculty members, graduate students, and high school students to Air Force research. This is accomplished by the faculty members (Summer Faculty Research Program, (SFRP)), graduate students (Graduate Student Research Program (GSRP)), and high school students (High School Apprenticeship Program (HSAP)) being selected on a nationally advertised competitive basis during the summer intersession period to perform research at Air Force Research Laboratory (AFRL) Technical Directorates, Air Force Air Logistics Centers (ALC), and other AF Laboratories. This volume consists of a program overview, program management statistics, and the final technical reports from the SFRP participants at the Arnold Engineering Development Center, US Air Force Academy, Air Logistic Centers, and Wilford Hall Medical Center

14. SUBJECT TERMS
Air Force Research, Air Force, Engineering, Laboratories, Reports, Summer, Universities, Faculty, Graduate Student, High School Student

15. NUMBER OF PAGES

16. PRICE CODE

17. SECURITY CLASSIFICATION OF REPORT	18. SECURITY CLASSIFICATION OF THIS PAGE	19. SECURITY CLASSIFICATION OF ABSTRACT	20. LIMITATION OF ABSTRACT
Unclassified	Unclassified	Unclassified	UL

GENERAL INSTRUCTIONS FOR COMPLETING SF 298

The Report Documentation Page (RDP) is used in announcing and cataloging reports. It is important that this information be consistent with the rest of the report, particularly the cover and title page. Instructions for filling in each block of the form follow. It is important to *stay within the lines* to meet *optical scanning requirements.*

Block 1. Agency Use Only *(Leave blank).*

Block 2. Report Date. Full publication date including day, month, and year, if available
(e.g. 1 Jan 88). Must cite at least the year.

Block 3. Type of Report and Dates Covered. State whether report is interim, final, etc. If applicable, enter inclusive report dates (e.g. 10 Jun 87 - 30 Jun 88).

Block 4. Title and Subtitle. A title is taken from the part of the report that provides the most meaningful and complete information. When a report is prepared in more than one volume, repeat the primary title, add volume number, and include subtitle for the specific volume. On classified documents enter the title classification in parentheses.

Block 5. Funding Numbers. To include contract and grant numbers; may include program element number(s), project number(s), task number(s), and work unit number(s). Use the following labels:

C - Contract	**PR** - Project
G - Grant	**TA** - Task
PE - Program	**WU** - Work Unit
Element	Accession No.

Block 6. Author(s). Name(s) of person(s) responsible for writing the report, performing the research, or credited with the content of the report. If editor or compiler, this should follow the name(s).

Block 7. Performing Organization Name(s) and Address(es). Self-explanatory.

Block 8. Performing Organization Report Number. Enter the unique alphanumeric report number(s) assigned by the organization performing the report.

Block 9. Sponsoring/Monitoring Agency Name(s) and Address(es). Self-explanatory.

Block 10. Sponsoring/Monitoring Agency Report Number. *(If known)*

Block 11. Supplementary Notes. Enter information not included elsewhere such as: Prepared in cooperation with....; Trans. of....; To be published in.... When a report is revised, include a statement whether the new report supersedes or supplements the older report.

Block 12a. Distribution/Availability Statement. Denotes public availability or limitations. Cite any availability to the public. Enter additional limitations or special markings in all capitals (e.g. NOFORN, REL, ITAR).

DOD -	See DoDD 5230.24, "Distribution Statements on Technical Documents."
DOE -	See authorities.
NASA -	See Handbook NHB 2200.2.
NTIS -	Leave blank.

Block 12b. Distribution Code.

DOD -	Leave blank.
DOE -	Enter DOE distribution categories from the Standard Distribution for Unclassified Scientific and Technical Reports.
	Leave blank.
NASA -	Leave blank.
NTIS -	

Block 13. Abstract. Include a brief *(Maximum 200 words)* factual summary of the most significant information contained in the report.

Block 14. Subject Terms. Keywords or phrases identifying major subjects in the report.

Block 15. Number of Pages. Enter the total number of pages.

Block 16. Price Code. Enter appropriate price code *(NTIS only)*.

Blocks 17. - 19. Security Classifications. Self- explanatory. Enter U.S. Security Classification in accordance with U.S. Security Regulations (i.e., UNCLASSIFIED). If form contains classified information, stamp classification on the top and bottom of the page.

Block 20. Limitation of Abstract. This block must be completed to assign a limitation to the abstract. Enter either UL (unlimited) or SAR (same as report). An entry in this block is necessary if the abstract is to be limited. If blank, the abstract is assumed to be unlimited.

SFRP FINAL REPORT TABLE OF CONTENTS   i-x

SFRP FINAL REPORTS

SRP Final Report Table of Contents

SRP Final Report Table of Contents

SRP Final Report Table of Contents

SRP Final Report Table of Contents

SRP Final Report Table of Contents

SRP Final Report Table of Contents

SRP Final Report Table of Contents

SRP Final Report Table of Contents

SRP Final Report Table of Contents

SRP Final Report Table of Contents

1. INTRODUCTION

The Summer Research Program (SRP), sponsored by the Air Force Office of Scientific Research (AFOSR), offers paid opportunities for university faculty, graduate students, and high school students to conduct research in U.S. Air Force research laboratories nationwide during the summer.

Introduced by AFOSR in 1978, this innovative program is based on the concept of teaming academic researchers with Air Force scientists in the same disciplines using laboratory facilities and equipment not often available at associates' institutions.

The Summer Faculty Research Program (SFRP) is open annually to approximately 150 faculty members with at least two years of teaching and/or research experience in accredited U.S. colleges, universities, or technical institutions. SFRP associates must be either U.S. citizens or permanent residents.

The Graduate Student Research Program (GSRP) is open annually to approximately 100 graduate students holding a bachelor's or a master's degree; GSRP associates must be U.S. citizens enrolled full time at an accredited institution.

The High School Apprentice Program (HSAP) annually selects about 125 high school students located within a twenty mile commuting distance of participating Air Force laboratories.

AFOSR also offers its research associates an opportunity, under the Summer Research Extension Program (SREP), to continue their AFOSR-sponsored research at their home institutions through the award of research grants. In 1994 the maximum amount of each grant was increased from $20,000 to $25,000, and the number of AFOSR-sponsored grants decreased from 75 to 60. A separate annual report is compiled on the SREP.

The numbers of projected summer research participants in each of the three categories and SREP "grants" are usually increased through direct sponsorship by participating laboratories.

AFOSR's SRP has well served its objectives of building critical links between Air Force research laboratories and the academic community, opening avenues of communications and forging new research relationships between Air Force and academic technical experts in areas of national interest, and strengthening the nation's efforts to sustain careers in science and engineering. The success of the SRP can be gauged from its growth from inception (see Table 1) and from the favorable responses the 1997 participants expressed in end-of-tour SRP evaluations (Appendix B).

AFOSR contracts for administration of the SRP by civilian contractors. The contract was first awarded to Research & Development Laboratories (RDL) in September 1990. After completion of the 1990 contract, RDL (in 1993) won the recompetition for the basic year and four 1-year options.

2.   PARTICIPATION IN THE SUMMER RESEARCH PROGRAM

The SRP began with faculty associates in 1979; graduate students were added in 1982 and high school students in 1986. The following table shows the number of associates in the program each year.

YEAR	SRP Participation, by Year			TOTAL
	SFRP	GSRP	HSAP	
1979	70			70
1980	87			87
1981	87			87
1982	91	17		108
1983	101	53		154
1984	152	84		236
1985	154	92		246
1986	158	100	42	300
1987	159	101	73	333
1988	153	107	101	361
1989	168	102	103	373
1990	165	121	132	418
1991	170	142	132	444
1992	185	121	159	464
1993	187	117	136	440
1994	192	117	133	442
1995	190	115	137	442
1996	188	109	138	435
1997	148	98	140	427
1998	85	40	88	213

Beginning in 1993, due to budget cuts, some of the laboratories weren't able to afford to fund as many associates as in previous years. Since then, the number of funded positions has remained fairly constant at a slightly lower level.

3. RECRUITING AND SELECTION

The SRP is conducted on a nationally advertised and competitive-selection basis. The advertising for faculty and graduate students consisted primarily of the mailing of 8,000 52-page SRP brochures to chairpersons of departments relevant to AFOSR research and to administrators of grants in accredited universities, colleges, and technical institutions. Historically Black Colleges and Universities (HBCUs) and Minority Institutions (MIs) were included. Brochures also went to all participating USAF laboratories, the previous year's participants, and numerous individual requesters (over 1000 annually).

RDL placed advertisements in the following publications: *Black Issues in Higher Education, Winds of Change,* and *IEEE Spectrum.* Because no participants list either *Physics Today* or *Chemical & Engineering News* as being their source of learning about the program for the past several years, advertisements in these magazines were dropped, and the funds were used to cover increases in brochure printing costs.

High school applicants can participate only in laboratories located no more than 20 miles from their residence. Tailored brochures on the HSAP were sent to the head counselors of 180 high schools in the vicinity of participating laboratories, with instructions for publicizing the program in their schools. High school students selected to serve at Wright Laboratory's Armament Directorate (Eglin Air Force Base, Florida) serve eleven weeks as opposed to the eight weeks normally worked by high school students at all other participating laboratories.

Each SFRP or GSRP applicant is given a first, second, and third choice of laboratory. High school students who have more than one laboratory or directorate near their homes are also given first, second, and third choices.

Laboratories make their selections and prioritize their nominees. AFOSR then determines the number to be funded at each laboratory and approves laboratories' selections.

Subsequently, laboratories use their own funds to sponsor additional candidates. Some selectees do not accept the appointment, so alternate candidates are chosen. This multi-step selection procedure results in some candidates being notified of their acceptance after scheduled deadlines. The total applicants and participants for 1998 are shown in this table.

1998 Applicants and Participants			
PARTICIPANT CATEGORY	TOTAL APPLICANTS	SELECTEES	DECLINING SELECTEES
SFRP	382	85	13
(HBCU/MI)	(0)	(0)	(0)
GSRP	130	40	7
(HBCU/MI)	(0)	(0)	(0)
HSAP	328	88	22
TOTAL	840	213	42

4. SITE VISITS

During June and July of 1998, representatives of both AFOSR/NI and RDL visited each participating laboratory to provide briefings, answer questions, and resolve problems for both laboratory personnel and participants. The objective was to ensure that the SRP would be as constructive as possible for all participants. Both SRP participants and RDL representatives found these visits beneficial. At many of the laboratories, this was the only opportunity for all participants to meet at one time to share their experiences and exchange ideas.

5. HISTORICALLY BLACK COLLEGES AND UNIVERSITIES AND MINORITY INSTITUTIONS (HBCU/MIs)

Before 1993, an RDL program representative visited from seven to ten different HBCU/MIs annually to promote interest in the SRP among the faculty and graduate students. These efforts were marginally effective, yielding a doubling of HBCI/MI applicants. In an effort to achieve AFOSR's goal of 10% of all applicants and selectees being HBCU/MI qualified, the RDL team decided to try other avenues of approach to increase the number of qualified applicants. Through the combined efforts of the AFOSR Program Office at Bolling AFB and RDL, two very active minority groups were found, HACU (Hispanic American Colleges and Universities) and AISES (American Indian Science and Engineering Society). RDL is in communication with representatives of each of these organizations on a monthly basis to keep up with the their activities and special events. Both organizations have widely-distributed magazines/quarterlies in which RDL placed ads.

Since 1994 the number of both SFRP and GSRP HBCU/MI applicants and participants has increased ten-fold, from about two dozen SFRP applicants and a half dozen selectees to over 100 applicants and two dozen selectees, and a half-dozen GSRP applicants and two or three selectees to 18 applicants and 7 or 8 selectees. Since 1993, the SFRP had a two-fold applicant increase and a two-fold selectee increase. Since 1993, the GSRP had a three-fold applicant increase and a three to four-fold increase in selectees.

In addition to RDL's special recruiting efforts, AFOSR attempts each year to obtain additional funding or use leftover funding from cancellations the past year to fund HBCU/MI associates.

SRP HBCU/MI Participation, By Year				
YEAR	SFRP		GSRP	
	Applicants	Participants	Applicants	Participants
1985	76	23	15	11
1986	70	18	20	10
1987	82	32	32	10
1988	53	17	23	14
1989	39	15	13	4
1990	43	14	17	3
1991	42	13	8	5
1992	70	13	9	5
1993	60	13	6	2
1994	90	16	11	6
1995	90	21	20	8
1996	119	27	18	7

6.   SRP FUNDING SOURCES

Funding sources for the 1998 SRP were the AFOSR-provided slots for the basic contract and laboratory funds. Funding sources by category for the 1998 SRP selected participants are shown here.

1998 SRP FUNDING CATEGORY	SFRP	GSRP	HSAP
AFOSR Basic Allocation Funds	67	38	75
USAF Laboratory Funds	17	2	13
Slots Added by AFOSR (Leftover Funds)	0	0	0
HBCU/MI By AFOSR (Using Procured Addn'l Funds)	0	0	N/A
TOTAL	84	40	88

7.   COMPENSATION FOR PARTICIPANTS

Compensation for SRP participants, per five-day work week, is shown in this table.

1998 SRP Associate Compensation

PARTICIPANT CATEGORY	1991	1992	1993	1994	1995	1996	1997	1998
Faculty Members	$690	$718	$740	$740	$740	$770	$770	$793
Graduate Student (Master's Degree)	$425	$442	$455	$455	$455	$470	$470	$484
Graduate Student (Bachelor's Degree)	$365	$380	$391	$391	$391	$400	$400	$412
High School Student (First Year)	$200	$200	$200	$200	$200	$200	$200	$200
High School Student (Subsequent Years)	$240	$240	$240	$240	$240	$240	$240	$240

The program also offered associates whose homes were more than 50 miles from the laboratory an expense allowance (seven days per week) of $52/day for faculty and $41/day for graduate students. Transportation to the laboratory at the beginning of their tour and back to their home destinations at the end was also reimbursed for these participants. Of the combined SFRP and GSRP associates, 65 % claimed travel reimbursements at an average round-trip cost of $730.

Faculty members were encouraged to visit their laboratories before their summer tour began. All costs of these orientation visits were reimbursed. Forty-three percent (85 out of 188) of faculty associates took orientation trips at an average cost of $449. By contrast, in 1993, 58 % of SFRP associates elected to take an orientation visits at an average cost of $685; that was the highest percentage of

6

associates opting to take an orientation trip since RDL has administered the SRP, and the highest average cost of an orientation trip.

Program participants submitted biweekly vouchers countersigned by their laboratory research focal point, and RDL issued paychecks so as to arrive in associates' hands two weeks later.

This is the third year of using direct deposit for the SFRP and GSRP associates. The process went much more smoothly with respect to obtaining required information from the associates, about 15% of the associates' information needed clarification in order for direct deposit to properly function as opposed to 7% from last year. The remaining associates received their stipend and expense payments via checks sent in the US mail.

HSAP program participants were considered actual RDL employees, and their respective state and federal income tax and Social Security were withheld from their paychecks. By the nature of their independent research, SFRP and GSRP program participants were considered to be consultants or independent contractors. As such, SFRP and GSRP associates were responsible for their own income taxes, Social Security, and insurance.

8.   CONTENTS OF THE 1998 REPORT

The complete set of reports for the 1998 SRP includes this program management report (Volume 1) augmented by fifteen volumes of final research reports by the 1998 associates, as indicated below:

1998 SRP Final Report Volume Assignments

LABORATORY	SFRP	GSRP	HSAP
Armstrong	2	7	12
Phillips	3	8	13
Rome	4	9	14
Wright	5A, 5B	10	15
AEDC, ALCs, USAFA, WHMC	6	11	

APPENDIX A – PROGRAM STATISTICAL SUMMARY

A. Colleges/Universities Represented

Selected SFRP associates represented 169 different colleges, universities, and institutions, GSRP associates represented 95 different colleges, universities, and institutions.

B. States Represented

SFRP -Applicants came from 47 states plus Washington D.C. Selectees represent 44 states.

GSRP - Applicants came from 44 states. Selectees represent 32 states.

HSAP - Applicants came from thirteen states. Selectees represent nine states.

Total Number of Participants	
SFRP	85
GSRP	40
HSAP	88
TOTAL	213

Degrees Represented			
	SFRP	GSRP	TOTAL
Doctoral	83	0	83
Master's	1	3	4
Bachelor's	0	22	22
TOTAL	186	25	109

SFRP Academic Titles	
Assistant Professor	36
Associate Professor	34
Professor	15
Instructor	0
Chairman	0
Visiting Professor	0
Visiting Assoc. Prof.	0
Research Associate	0
TOTAL	85

Source of Learning About the SRP		
Category	Applicants	Selectees
Applied/participated in prior years	177	47
Colleague familiar with SRP	104	24
Brochure mailed to institution	101	21
Contact with Air Force laboratory	101	39
IEEE Spectrum	12	1
BIIHE	4	0
Other source	117	30
TOTAL	616	162

APPENDIX B – SRP EVALUATION RESPONSES

1. OVERVIEW

Evaluations were completed and returned to RDL by four groups at the completion of the SRP. The number of respondents in each group is shown below.

Table B-1. Total SRP Evaluations Received

Evaluation Group	Responses
SFRP & GSRPs	100
HSAPs	75
USAF Laboratory Focal Points	84
USAF Laboratory HSAP Mentors	6

All groups indicate unanimous enthusiasm for the SRP experience.

The summarized recommendations for program improvement from both associates and laboratory personnel are listed below:

A. Better preparation on the labs' part prior to associates' arrival (i.e., office space, computer assets, clearly defined scope of work).

B. Faculty Associates suggest higher stipends for SFRP associates.

C. Both HSAP Air Force laboratory mentors and associates would like the summer tour extended from the current 8 weeks to either 10 or 11 weeks; the groups state it takes 4-6 weeks just to get high school students up-to-speed on what's going on at laboratory. (Note: this same argument was used to raise the faculty and graduate student participation time a few years ago.)

2. 1998 USAF LABORATORY FOCAL POINT (LFP) EVALUATION RESPONSES

The summarized results listed below are from the 84 LFP evaluations received.

1. LFP evaluations received and associate preferences:

Table B-2. Air Force LFP Evaluation Responses (By Type)

Lab	Evals Recv'd	How Many Associates Would You Prefer To Get ?								(% Response)			
		SFRP				GSRP (w/Univ Professor)				GSRP (w/o Univ Professor)			
		0	1	2	3+	0	1	2	3+	0	1	2	3+
AEDC	0	-	-	-	-	-	-	-	-	-	-	-	-
WHMC	0	-	-	-	-	-	-	-	-	-	-	-	-
AL	7	28	28	28	14	54	14	28	0	86	0	14	0
USAFA	1	0	100	0	0	100	0	0	0	0	100	0	0
PL	25	40	40	16	4	88	12	0	0	84	12	4	0
RL	5	60	40	0	0	80	10	0	0	100	0	0	0
WL	46	30	43	20	6	78	17	4	0	93	4	2	0
Total	84	32%	50%	13%	5%	80%	11%	6%	0%	73%	23%	4%	0%

LFP Evaluation Summary. The summarized responses, by laboratory, are listed on the following page. LFPs were asked to rate the following questions on a scale from 1 (below average) to 5 (above average).

2. LFPs involved in SRP associate application evaluation process:
    a. Time available for evaluation of applications:
    b. Adequacy of applications for selection process:
3. Value of orientation trips:
4. Length of research tour:
5   a. Benefits of associate's work to laboratory:
    b. Benefits of associate's work to Air Force:
6.   a. Enhancement of research qualifications for LFP and staff:
    b. Enhancement of research qualifications for SFRP associate:
    c. Enhancement of research qualifications for GSRP associate:
7.   a. Enhancement of knowledge for LFP and staff:
    b. Enhancement of knowledge for SFRP associate:
    c. Enhancement of knowledge for GSRP associate:
8. Value of Air Force and university links:
9. Potential for future collaboration:
10.   a. Your working relationship with SFRP:
    b. Your working relationship with GSRP:
11. Expenditure of your time worthwhile:

12. Quality of program literature for associate:
13.   a. Quality of RDL's communications with you:
      b. Quality of RDL's communications with associates:
14. Overall assessment of SRP:

Table B-3. Laboratory Focal Point Reponses to above questions

	AEDC	AL	USAFA	PL	RL	WHMC	WL
# Evals Recv'd	0	7	1	14	5	0	46
Question #							
2	-	86 %	0 %	88 %	80 %	-	85 %
2a	-	4.3	n/a	3.8	4.0	-	3.6
2b	-	4.0	n/a	3.9	4.5	-	4.1
3	-	4.5	n/a	4.3	4.3	-	3.7
4	-	4.1	4.0	4.1	4.2	-	3.9
5a	-	4.3	5.0	4.3	4.6	-	4.4
5b	-	4.5	n/a	4.2	4.6	-	4.3
6a	-	4.5	5.0	4.0	4.4	-	4.3
6b	-	4.3	n/a	4.1	5.0	-	4.4
6c	-	3.7	5.0	3.5	5.0	-	4.3
7a	-	4.7	5.0	4.0	4.4	-	4.3
7b	-	4.3	n/a	4.2	5.0	-	4.4
7c	-	4.0	5.0	3.9	5.0	-	4.3
8	-	4.6	4.0	4.5	4.6	-	4.3
9	-	4.9	5.0	4.4	4.8	-	4.2
10a	-	5.0	n/a	4.6	4.6	-	4.6
10b	-	4.7	5.0	3.9	5.0	-	4.4
11	-	4.6	5.0	4.4	4.8	-	4.4
12	-	4.0	4.0	4.0	4.2	-	3.8
13a	-	3.2	4.0	3.5	3.8	-	3.4
13b	-	3.4	4.0	3.6	4.5	-	3.6
14	-	4.4	5.0	4.4	4.8	-	4.4

3. 1998 SFRP & GSRP EVALUATION RESPONSES

The summarized results listed below are from the 120 SFRP/GSRP evaluations received.

Associates were asked to rate the following questions on a scale from 1 (below average) to 5 (above average) - by Air Force base results and over-all results of the 1998 evaluations are listed after the questions.

1. The match between the laboratories research and your field:
2. Your working relationship with your LFP:
3. Enhancement of your academic qualifications:
4. Enhancement of your research qualifications:
5. Lab readiness for you: LFP, task, plan:
6. Lab readiness for you: equipment, supplies, facilities:
7. Lab resources:
8. Lab research and administrative support:
9. Adequacy of brochure and associate handbook:
10. RDL communications with you:
11. Overall payment procedures:
12. Overall assessment of the SRP:
13.   a. Would you apply again?
        b. Will you continue this or related research?
14. Was length of your tour satisfactory?
15. Percentage of associates who experienced difficulties in finding housing:
16. Where did you stay during your SRP tour?
        a.   At Home:
        b.   With Friend:
        c.   On Local Economy:
        d.   Base Quarters:
17. Value of orientation visit:
        a.   Essential:
        b.   Convenient:
        c.   Not Worth Cost:
        d.   Not Used:

SFRP and GSRP associate's responses are listed in tabular format on the following page.

Table B-4. 1997 SFRP & GSRP Associate Responses to SRP Evaluation

	Arnold	Brooks	Edwards	Eglin	Griffis	Hanscom	Kelly	Kirtland	Lackland	Robins	Tyndall	WPAFB	average
# res	6	48	6	14	31	19	3	32	1	2	10	85	257
1	4.8	4.4	4.6	4.7	4.4	4.9	4.6	4.6	5.0	5.0	4.0	4.7	4.6
2	5.0	4.6	4.1	4.9	4.7	4.7	5.0	4.7	5.0	5.0	4.6	4.8	4.7
3	4.5	4.4	4.0	4.6	4.3	4.2	4.3	4.4	5.0	5.0	4.5	4.3	4.4
4	4.3	4.5	3.8	4.6	4.4	4.4	4.3	4.6	5.0	4.0	4.4	4.5	4.5
5	4.5	4.3	3.3	4.8	4.4	4.5	4.3	4.2	5.0	5.0	3.9	4.4	4.4
6	4.3	4.3	3.7	4.7	4.4	4.5	4.0	3.8	5.0	5.0	3.8	4.2	4.2
7	4.5	4.4	4.2	4.8	4.5	4.3	4.3	4.1	5.0	5.0	4.3	4.3	4.4
8	4.5	4.6	3.0	4.9	4.4	4.3	4.3	4.5	5.0	5.0	4.7	4.5	4.5
9	4.7	4.5	4.7	4.5	4.3	4.5	4.7	4.3	5.0	5.0	4.1	4.5	4.5
10	4.2	4.4	4.7	4.4	4.1	4.1	4.0	4.2	5.0	4.5	3.6	4.4	4.3
11	3.8	4.1	4.5	4.0	3.9	4.1	4.0	4.0	3.0	4.0	3.7	4.0	4.0
12	5.7	4.7	4.3	4.9	4.5	4.9	4.7	4.6	5.0	4.5	4.6	4.5	4.6
Numbers below are percentages													
13a	83	90	83	93	87	75	100	81	100	100	100	86	87
13b	100	89	83	100	94	98	100	94	100	100	100	94	93
14	83	96	100	90	87	80	100	92	100	100	70	84	88
15	17	6	0	33	20	76	33	25	0	100	20	8	39
16a	-	26	17	9	38	23	33	4	-	-	-	30	
16b	100	33	-	40	-	8	-	-	-	-	36	2	
16c	-	41	83	40	62	69	67	96	100	100	64	68	
16d	-	-	-	-	-	-	-	-	-	-	-	0	
17a	-	33	100	17	50	14	67	39	-	50	40	31	35
17b	-	21	-	17	10	14	-	24	-	50	20	16	16
17c	-	-	-	-	10	7	-	-	-	-	-	2	3
17d	100	46	-	66	30	69	33	37	100	-	40	51	46

4. 1998 USAF LABORATORY HSAP MENTOR EVALUATION RESPONSES

Not enough evaluations received (5 total) from Mentors to do useful summary.

5. 1998 HSAP EVALUATION RESPONSES

The summarized results listed below are from the 23 HSAP evaluations received.

HSAP apprentices were asked to rate the following questions on a scale from
1 (below average) to 5 (above average)

1. Your influence on selection of topic/type of work.
2. Working relationship with mentor, other lab scientists.
3. Enhancement of your academic qualifications.
4. Technically challenging work.
5. Lab readiness for you: mentor, task, work plan, equipment.
6. Influence on your career.
7. Increased interest in math/science.
8. Lab research & administrative support.
9. Adequacy of RDL's Apprentice Handbook and administrative materials.
10. Responsiveness of RDL communications.
11. Overall payment procedures.
12. Overall assessment of SRP value to you.
13. Would you apply again next year?   Yes (92 %)
14. Will you pursue future studies related to this research?   Yes (68 %)
15. Was Tour length satisfactory?   Yes (82 %)

	Arnold	Brooks	Edwards	Eglin	Griffiss	Hanscom	Kirtland	Tyndall	WPAFB	Totals
# resp	5	19	7	15	13	2	7	5	40	113
1	2.8	3.3	3.4	3.5	3.4	4.0	3.2	3.6	3.6	3.4
2	4.4	4.6	4.5	4.8	4.6	4.0	4.4	4.0	4.6	4.6
3	4.0	4.2	4.1	4.3	4.5	5.0	4.3	4.6	4.4	4.4
4	3.6	3.9	4.0	4.5	4.2	5.0	4.6	3.8	4.3	4.2
5	4.4	4.1	3.7	4.5	4.1	3.0	3.9	3.6	3.9	4.0
6	3.2	3.6	3.6	4.1	3.8	5.0	3.3	3.8	3.6	3.7
7	2.8	4.1	4.0	3.9	3.9	5.0	3.6	4.0	4.0	3.9
8	3.8	4.1	4.0	4.3	4.0	4.0	4.3	3.8	4.3	4.2
9	4.4	3.6	4.1	4.1	3.5	4.0	3.9	4.0	3.7	3.8
10	4.0	3.8	4.1	3.7	4.1	4.0	3.9	2.4	3.8	3.8
11	4.2	4.2	3.7	3.9	3.8	3.0	3.7	2.6	3.7	3.8
12	4.0	4.5	4.9	4.6	4.6	5.0	4.6	4.2	4.3	4.5
Numbers below are percentages										
13	60%	95%	100%	100%	85%	100%	100%	100%	90%	92%
14	20%	80%	71%	80%	54%	100%	71%	80%	65%	68%
15	100%	70%	71%	100%	100%	50%	86%	60%	80%	82%

Effect of Environmental Variables on Aging Aircraft

F. N. Albahadily
Associate Professor
Department of Chemistry

University of Central Oklahoma
100 North University Drive
Edmond, Oklahoma 73034

Final Report for:
Summer Faculty Research Program
Tinker Air Force Base

August 1998

Effect of Environmental Variables on Aging Aircraft

F. N. Albahadily
Associate Professor
Department of Chemistry
University of Central Oklahoma

Abstract

This report is intended to evaluate environmental data collected by ARING from six Air Force Bases, Hickam, Kadena, Macdill, Mildenhall, Pease, and Seymour-Johnson for the period between January 1997 and April 1998. The environmental variables measured were air temperature, surface temperature, rainfall, rain pH, time-of wetness, and concentrations of NO_2 and Cl_2. Time domain plots (plots of sensor responses as a function of time) are the bases for the finding in this report.

Effect of Environmental Variables on Aging Aircraft

F. N. Albahadily

Corrosion is a natural process by which some metals are converted to a thermodynamically stable state (natural ore). This natural process has a major impact on the world economy. It has been estimated that 4 to 5% of the national gross incomes of industrial or technologically advanced nations are spent to deal with corrosion problems. In the United States, the various agencies of the Department of Defense (DoD) spend about $1 billion a year to deal with corrosion related problems on their fleet of aircraft, ships, vehicles and weapon systems. The Air Force is one of the DoD agencies with a large holding of aging aircraft (KC-135, B-52, and E-3). A Large number of the aging aircraft are severely affected by corrosion and the Air Force has to invest significant amount of money and manpower in dealing with the problem. The Air Force corrosion maintenance program is far from being perfect, however, the invested efforts are commendable in terms of minimizing fatalities due corrosion damages. The corrosion maintenance program involves two steps, detection and repair. Neither of the two steps is simple to conduct and both are expensive to perform. As a common protective measure against corrosion, all aircraft are painted from outside and are primed from inside. The protective coatings make corrosion detection by visual inspection a challenging task unless structural damage is evident. There is a pressing need for a device that is simple to operate yet powerful to detect hidden corrosion in its early development stages. Due to the unique shape, size and structure complexity of aircraft, such device is not exist. Few instrumental techniques are developed for the detection purposes. These techniques are used for Non-Destructive Evaluation (NDE) and include, eddy current, pulse-echo ultrasonic, thermography, optical methods, acoustic emission, X-rays radiography and neutron radiography. A specific set of circumstances must be satisfied to insure successful applicability of each of the techniques on aircraft fuselages and wings. Eddy current based devices appear to have few advantages over the other approaches. Consequently, the technique has been utilized with limited success by few air depots including the Oklahoma

City Air Logistic Center (OC-ALC). The technique requires highly trained personal for operation and data interpretation.

A large number of the aging aircraft have relatively low flying hours (20,000 or less) and are expected to remain in service until the year 2040 (KC-135). The Air Logistic Centers are expected to insure that the aircraft remain structurally sound. Corrosion is the source for structure failure often and controlling its rate of growth is greatly sought. It is believed that most of the corrosion problems start and propagate while the aircraft are stationed in air bases. A comprehensive corrosion maintenance program requires understanding the role of environmental variables on the corrosion process. Knowing the history of the aircraft and documentation of local environmental variables around the air force bases should provide the necessary tool to develop a successful program for detecting corrosion and estimating its severity. The OC-ALC is leading the efforts in this direction currently. The OC-ALC had contracted ARINC Incorporated, Oklahoma City Engineering and Research Center to gather environmental variable data from six Air Force bases. The bases selected for the program are Hickam, Kadena, Macdill, Mildenhall, Pease and Seymour-Johnson. The geographical areas where Hickam, Kadena, Mildenhall and Pease are located considered to be severe corrosion zones while Macdill and Seymour-Johnson are located in moderate corrosion zones. The contract with ARINC is for five years period starting at the beginning of 1997. This report is intended to evaluate the data collected by ARINC for the period from January, 1997 to April, 1998. Time domain plots (plots of sensor responses as a function of time) are the bases for the findings in this report.

Atmospheric Data Collected by ARINC

The data files obtained from ARINC are saved using text format and read by Microsoft Excel. As indicated earlier, the data files reflect measurements from six Air Force bases, Hickam, Kadena, Macdill, Mildenhall, Pease, and Seymour-Johnson. The atmospheric variable measured are relative humidity, air temperature, surface temperature, rainfall, rain pH, time of wetness (TOW1 and TOW2), NO_2 concentration, and Cl_2 concentration. The data acquisition systems, data loggers, and the control devices are powered by a

combination of a 14volt batteries and solar panels. The output voltages of the power suppliers are also reported. Information regarding wind direction and speed are included on few data files. The responses of the sensors are recorded every one-half hour. A summary table is included in each data file. The table reports the minimum and maximum reading for each variable together with an average representing the time period monitored. The data sets examined represent blocks of times ranging from few days to few months within the time period from January, 1997 to April, 1998.

Data Analysis

<u>Air temperature</u>

The measurements are accomplished with aid of Camptus Inc. (New Boston, NH) sensors model A70-HA. The sensors produce voltages from 0.0 volt to 1.0 volt in response to temperature variation from -4 to 167 °F. The sensors are protected from direct sunlight using a passive radiation shield from Comptus Inc. model A76-HTB. Temperature readings from all the six air force bases are reliable and follow expected trends in terms of daytime, nighttime, or the season of the year. No unjustifiable variations are observed. The readings appear to be insensitive to wind speed, rainfall, or power fluctuations. Figure 1 is an example these data. The Figure shows air temperature variation over a four days period (Hickam AFB).

<u>Surface temperature</u>

The measurements are accomplished with a thermocouple wire inserted between two aluminum plates resembling a lap joint of an aircraft skin. The thermocouple-plates assembly is exposed to the atmosphere without shielding from the sun. The responses of the thermocouples are monitored using Omega (Stamford, CT) model TX91A mini temperature transmitters. Surface temperature measurements appear to be reliable more often than not. However, the measurements are very sensitive to power fluctuations and rainfalls. As shown in Figure 2, voltage fluctuation causes surface temperature to appear at much lower levels. However, rainfalls seem to cause surface temperature to appear at

Figure 1. Air temperature variation over Hicham AFB for the period from Jan. 22, 1998 to Jan. 26, 1998
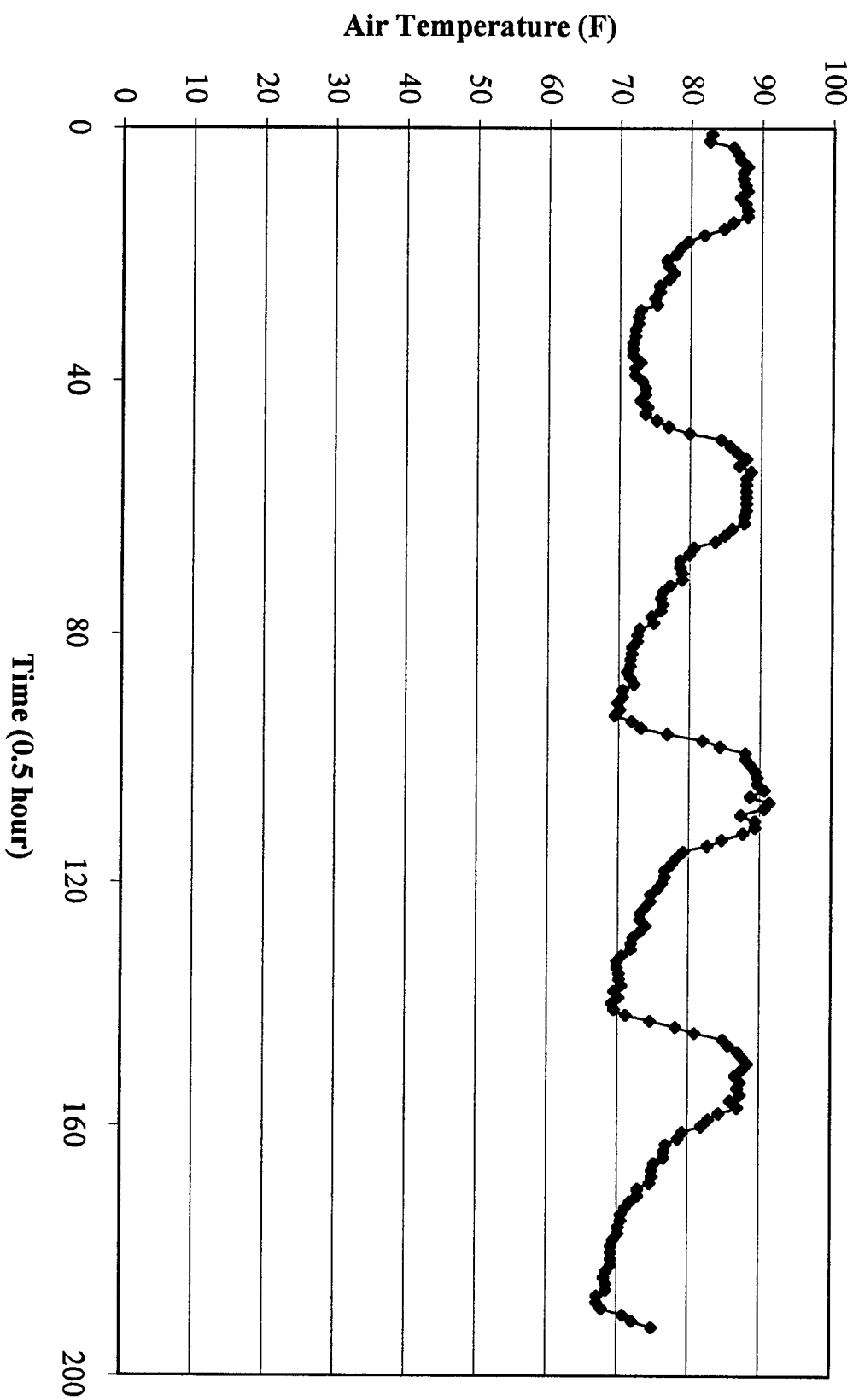
Figure 2. Fluctuation of surface temperature measurements due to fluctuation in power supply.
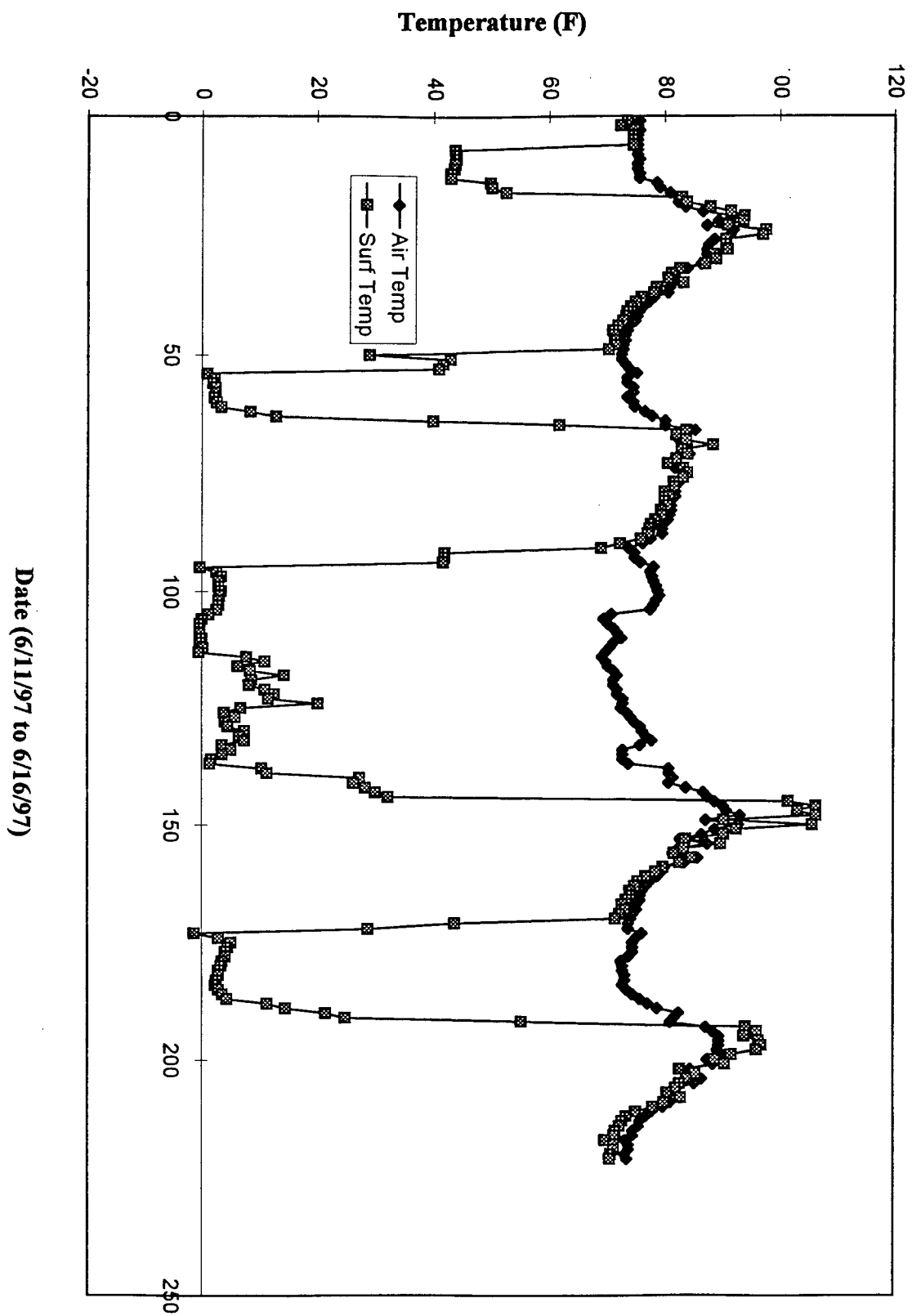
higher levels (see Figure 3). Some data sets from Kadena suggest that wind speed above 15 mph causes surface temperature to appear at higher levels. Figure 4 shows the response of surface temperature to wind speed. Questionably low (-43 °F) surface temperatures are reported on few data sets. These low readings are assumed to be due to bad electrical contacts or circuit shortenings.

Rainfall

The measurements are accomplished using a two-tip-buckets assembly. An orifice is used to collect the rain into one of the two buckets. When the rain reaches a specific level (a calibrated level of 0.01 in is usually used), the bucket tips and the second bucket is positioned under the orifice. After filling to the calibration level, the second bucket tips and the first bucket is repositioned under the orifice and so on. Repositioning of the buckets under the orifice are monitored electronically. Total rainfall is calculated by multiplying the calibration volume times the number of buckets repositioning. The experimental set up for rainfall measurements appear to be reliable and there is no reason to question the validity of the data.

Rain pH

Glass electrodes immersed in rain collecting buckets are used to measure the rain pH (pH is a measure of solution acidity and is related to the number of hydrogen ions with in a given volume). Rain pH data from Kadena, Mildenhall, Pease and Seymour-Johnson suggest rain pH averages around 5 to 6. Rain pH readings lower than 4 are seen often in data sets from Pease. The average rain pH readings for Hickam and Macdill are slightly higher than the expected level. Reading of pH 8 or higher are seen often on data files from the two bases. Data sets from Hickam suggest that rain pH drop to normal levels (about 6) when significant amount of rainfall is reported. Questionable rain pH variations are observed in some data sets from Macdill. Figure 5 indicates that rain pH can change by 4 units or higher within a 24 hours period. Macdill data also indicate that pH readings are slightly sensitive to high wind speeds (see Figure 6). All data examined indicate that daytime rain pH readings are noticeably lower than nighttime readings. Many of the

Figure 3. Effect of rainfall on surface temperature measuremants
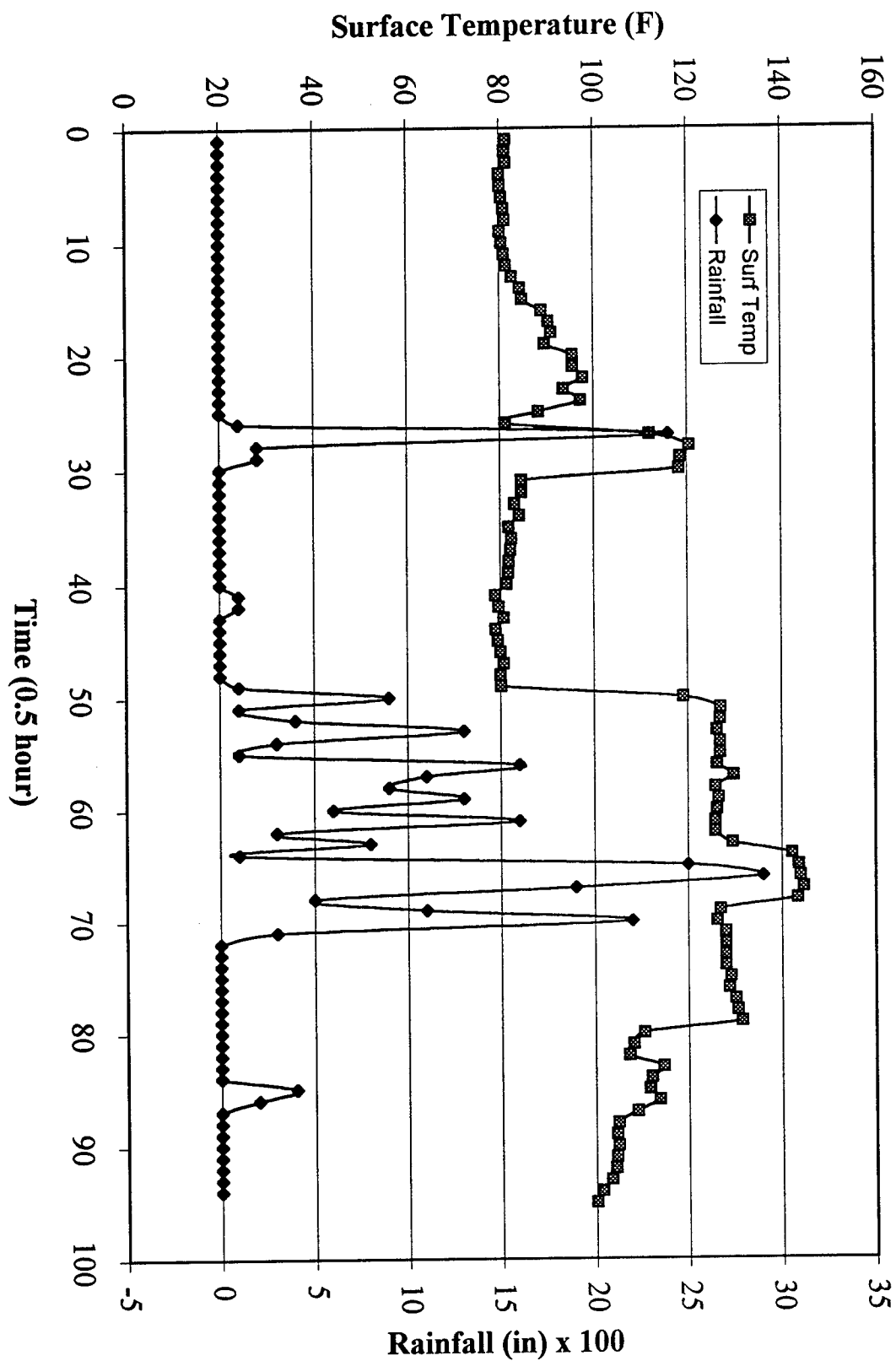
Figure 4. Effect of wind speed on surface temperature measurements
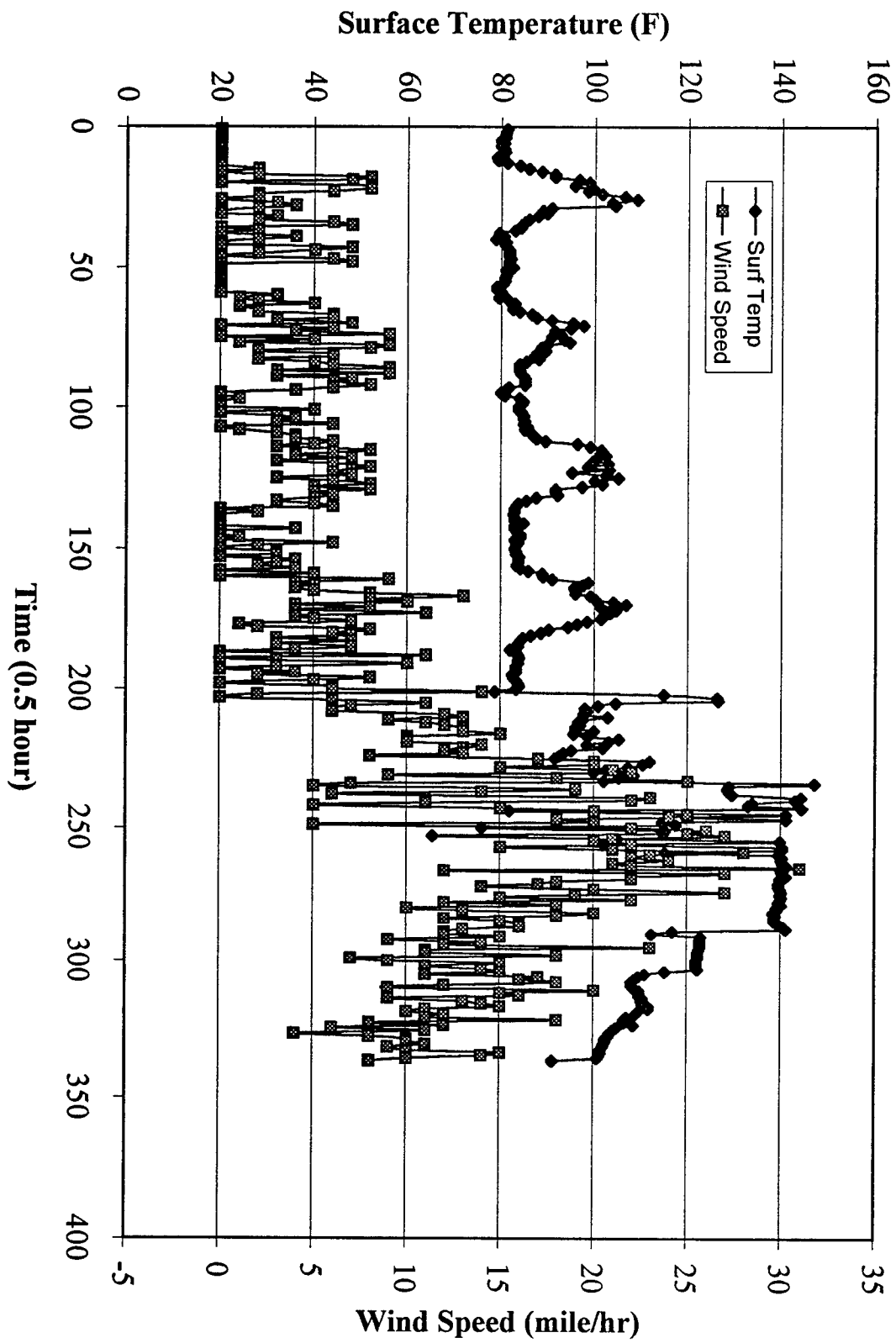
Figure 5. Rain pH variation over Macdill AFB for the period from April 6, 1998 to April 10, 1998
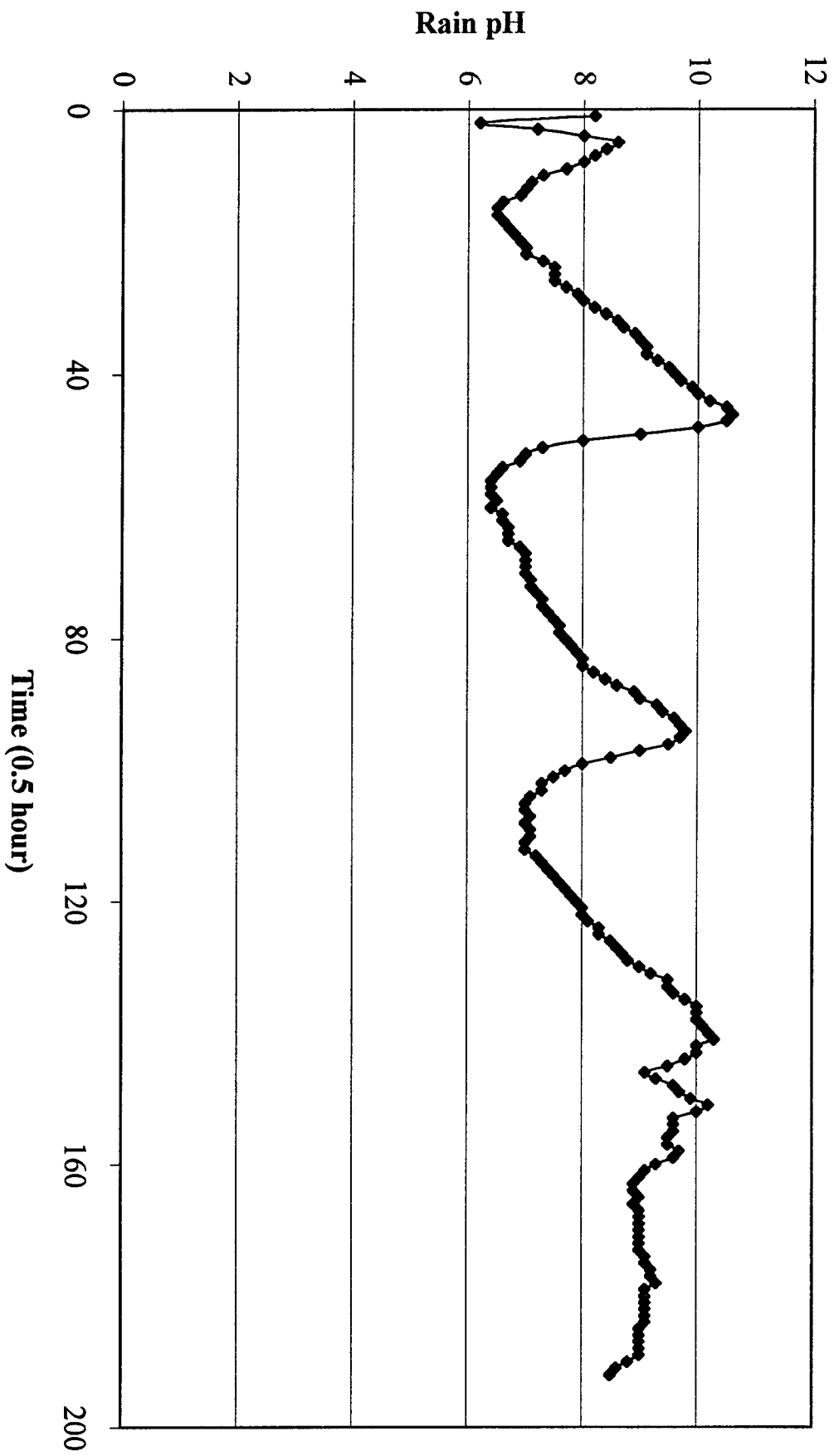
Figure 6. Correlation between Time-of-Wetness (TOW1 and TOW2) measurements
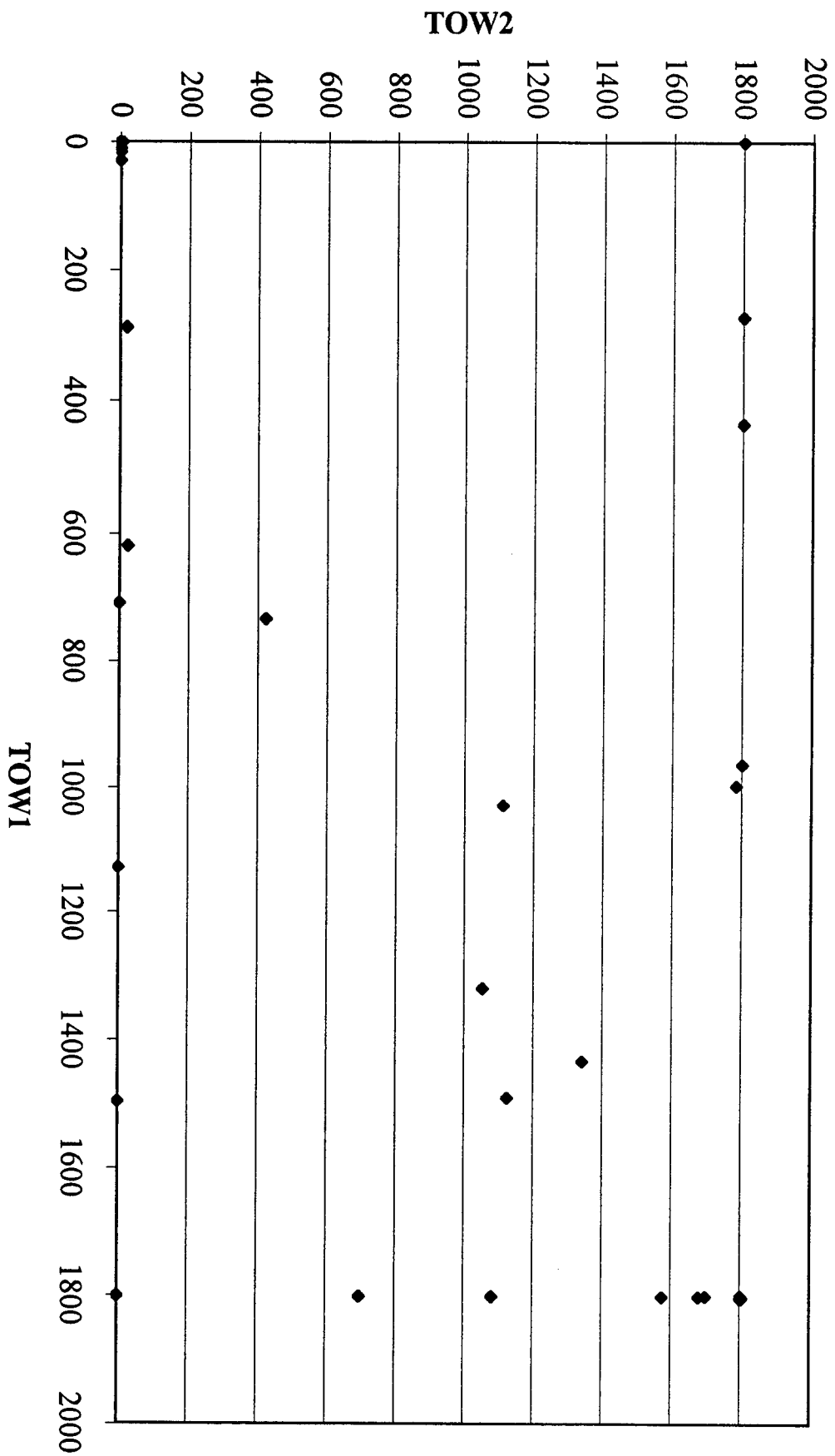
observations above are unexpected and cannot be explained without ispecting the experimental set up. However, our experience with pH measurements leeds us to believe that these problems arise because the glass electrodes used for the measurements are not calibrated periodically and remain dry between rainfalls.

Time-of-wetness

Time-of wetness data represnt the number of seconds over which the sensors remain wet with in a period of one-half hour. For example, TOW reading of 1800 indicates that the sensor remained wet for one-half hour. The measurements are accomplished using moisture sensor devices (EPITEK model SMMS-01). The devices are based on ASTM designation G84-89. The sensors are simple galvanic cells with gold/copper or gold/zinc electrodes. The electrodes are spaced about 100-200 μm apart. The galvanic activities are initiated when moisture accumulates in the cavity between the electrodes. Two kinds of time-of-wetness measurements are reported on each data file, TOW1 and TOW2. The operation principles of TOW1 and TOW2 sensors are basically the same except for the activation voltages, 20 mV and 50 mV respectively. Despite of the similarities between the two sensors, their outputs can not be correlated in an understandable manner often. Typically, the sensors are activated during rainfalls and certain levels of relative humidity. A minimum relative humidity of about 70% is needed for the TOW1 sensors to record any data. Relative humidity of 80% or higher is required to activate the TOW2 sensors. It should be recognized that relative humidity readings as high as 100% do not always guaranty TOW readings from the sensors. No TOW data are reported for Macdill or Mildenhall. Data sets from Pease show minimal recording of TOW1. Some data sets suggest nice correlation between rainfall and TOWs. However, less clear correlation is observed in other data sets.

NO_2 and Cl_2

Sensors from McNeill (Mentor, Ohio) models 6130 and 6140 are used to monitor the activities of NO_2 and Cl_2 respectively. The detection limits (lowest detectable ativities) of the sensors are rated at 1 part-per-million (ppm). None of the sensors have functioned

properly since installation. Negative activities for NO_2 and Cl_2 are reported as often as the positive readings. Simple statistical analysis shows that the standard deviations associate with the activity measurements are as high or even higher than the average readings for NO_2 or Cl_2. These observations indicate that either the apparatus are not installed correctly or they are not functioning as described by vendor. McNeill recommends that the sensors operate off a 24VDC source. However, voltages as low as 15VDC or as high as 36VDC can be used to operate the sensors. ARINC records indicate that the DC voltage sources used on all the bases are rated at 14VDC or lower. The power limitation may need to be considered in explaining the poor performance of the NO_2 and Cl_2 sensors. It should be pointed out that Cl_2 activities in the atmosphere are in the part-per-billion (ppb). The experimental set ups used for measuring the activities of CL_2 are not adequate.

Conclusion:

Except for NO_2 and Cl_2 activity measurements, the data collected by ARINC appear to be satisfactory. Acceptable routines can be utilized to reject or minimize questionable surface temperature and pH measurements assuming that the interested is in the long-range effect of these variables instead of the instantaneous ones. It appears to us that most the problems or the limitations associated with measurements discussed in this report are due to the power system used. The dual power systems currently in use should be replaced with 120 volt power lines. The excess power will expand the capabilities of the apparatus used for measurements and increase data acquisition capabilities.

Suggestions for Future Data Collection:

1. The data file need to be rearranged to insure that relative humidity data appear in separate column instead of appearing in the same column with date and time.

2. The data collection programs need to be modified to insure that TOW2 data appear in one column. It has been observed often that the first digits from TOW2 column appear in the column where TOW1 data is reported..

1-14

3. Smoother time domain plots can be obtained if the data are collected every minute or two and the average from ½ or 1 hour period is recorded.

4. Develop a routine to insure that pH data are reported only when the pH electrode is immersed in enough rain water.

5. Modify the interface between the main battery and the solar panel.

6. Report wind speed for all six Air Force Bases.

7. Insure that all data files reflect a fixed time period. Time periods of ten or twelve days are ideal.

8. Develop a better instrumental set up to measure atmospheric NO_2.

Acknowledgment

A STUDY OF SCHEDULING AND TRACKING OF
PARTS IN THE PLATING SHOP AT
WARNER ROBINS AIR LOGISTICS CENTER

Shelia K. Barnett
Assistant Professor
Industrial Engineering Department

Mercer University
1400 Coleman Ave.
Macon, GA 31207

A STUDY OF SCHEDULING AND TRACKING OF
PARTS IN THE PLATING SHOP AT
WARNER ROBINS AIR LOGISTICS CENTER

Shelia K. Barnett
Assistant Professor
Industrial Engineering
Mercer University

Abstract

This study focuses on the Plating Shop within the Industrial Products Division of Manufacturing (TINM) at Warner Robins Air Logistics Center (WR-ALC). The objective is to determine the feasibility of improving the workflow through the shop and to determine the extent to which the Plating Shop will benefit from the manufacturing information system being installed in the near future.

It was determined through this study that the Plating Shop is operating at 107% (year-to-date) efficiency for 1998, as more work is processed through the shop than is scheduled. (The excess is attributable to the arrival of unexpected parts needing work at the shop.) This figure takes into account such things as overhead, absenteeism and overtime. As it is difficult to improve a system operating above 100% efficiency, it was determined that the method of scheduling work in the Plating Shop should not be altered until further study of individual processes can be completed.

A change in layout for incoming parts and a color-coding scheme for log-ins were suggested to assist the scheduler in updating the Plating Shop's information system. An updated information system will benefit the Plating Shop when TINM incorporates the Plating Shop's data into the manufacturing information system.

At this time, the manufacturing information system does not consider the needs of schedulers for any area other than manufacturing. It is hoped that by first concentrating on the manufacturing area and eliminating problems with scheduling there, problems for the back shops such as Plating will diminish. As such, the Plating Shop will not immediately benefit from such a system and will be better served by keeping the information system currently used.

A STUDY OF SCHEDULING AND TRACKING OF PARTS IN THE PLATING SHOP AT WARNER ROBINS AIR LOGISTICS CENTER

Shelia K. Barnett

Introduction

The purpose of this study is to determine the feasibility of improving the workflow of the Plating Shop and to determine if an information system would improve the shop's performance. As the Plating Shop is considered a back or supporting shop of the manufacturing area, the information system currently being considered for the manufacturing area will be reviewed to determine if it will contain the necessary information for the Plating Shop to utilize the information system.

The Plating Shop currently inspects all parts for airplanes manufactured and repaired at WR-ALC. Parts are "recycled" in that they are repaired, cleaned, inspected and re-coated for various planes. There are currently three shifts operating, with one scheduler and one assistant scheduler during the day shift; there is no scheduler for the two other shifts.

Parts arrive periodically throughout the day and are recorded as received as soon as possible. Operators then process the part(s) according to the attached paperwork. When processing is complete, the part(s) is recorded as complete and is ready to leave the shop.

The shop is divided into three areas: blasting, non-destructive inspection (NDI) and plating. Blasting is used to clean the various parts of rust, corrosion, paint, sealant, etc. before any processing takes place. NDI is a non-destructive means of inspecting parts for defects; such as cracks. Plating is a coating process used to protect metals and is divided into two processes: ion vapor deposit (IVD) and chemical. IVD is an electrical process used to provide protective covering for certain metals, such as steel and aluminum. The chemical

processes uses various chemical compounds to coat parts with materials such as chrome, silver, tin, etc.

The Plating Shop is considered a job-shop in that parts from various customers come in needing different repairs or processes. For example, the shop may receive two parts that are identical but each needs a different set of processes performed. Batch jobs are seldom received. The average number of items needing repairs or inspection for 1996 was 25,581 and for 1997 was 19,983. Appendix A shows the monthly breakdown of the number of items received by the shop for these years.

The Plating Shop currently has a dBase program on a non-networked computer to track items in the shop area; however, the shop needs to be able to communicate resources, delivery dates, machine downtime, etc. to other areas of WR-ALC. This is currently done by phone or in person. Also, due to the large number of items received by the Plating Shop from these various customers, the method of scheduling parts arriving and leaving is a matter of concern.

Methodology

This study of the Plating Shop begins by determining the current workflow of the shop in terms of customers and basic types of processes performed. To look at items received and their time in the shop is beyond the scope of this work, as it would require a detailed study following specific parts and processes over a period of several months. However, this would provide a more complete picture of the Plating Shop and its operation, providing important information for use in improving flow of specific processes or part families in the future, and this is suggested for future studies.

It is also necessary to determine the capabilities in terms of a computer information system for scheduling and what information needs to be included for the Plating Shop to effectively schedule incoming work. The database currently being considered for manufacturing will be reviewed to determine if the Plating Shop can use it for scheduling. Finally, any recommendations for improvement in the flow of the Plating Shop will be considered.

Results

Workflow and Priorities

Figure 1 shows the current workflow for the Plating Shop in relation to customers served. "Other" relates to both on- and off-base customers not specifically listed. The number in parentheses is the building number at WR-ALC associated with the customers and is how customers are referenced in the computer database.
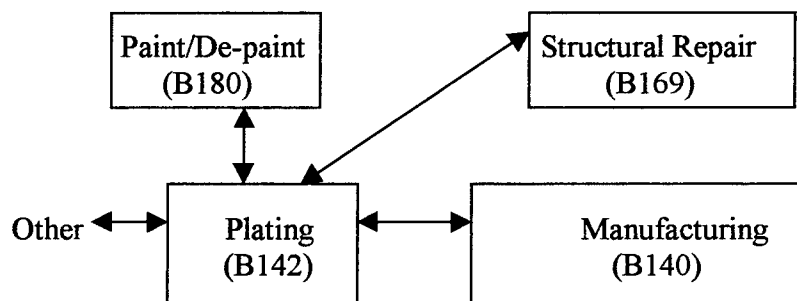
Figure 1: Movement of Parts

Note that the Plating Shop receives and returns items from every customer shown. The shop may also receive an item several times before it is completely repaired. For instance, when an older part comes in needing repairs, it is first degreased and blasted to clean any corrosion and/or sealant from the part. If repairable, it is processed through the shop, sent to manufacturing to verify tolerances, and then returned for inspection using NDI.

It is important to note that the Plating Shop does not declare parts defective; for this, they are referred to the engineering department.

The type of work order for parts is determined by the customer from a select list: shoe tags (ST), mission capability (MICAP), surge, items from aircraft companies, electronic components, and management of items subject to repair (MISTR). ST are "hot" items needing immediate attention by the shop. In most cases, ST are simple parts that are typically hand carried through the shop, sometimes being finished the same day received. MICAP indicates those parts needed to support a specific mission. Surge items are those items needed for wartime conditions and take priority over all other work received by Plating. Aircraft companies send parts that are for a specific type of airplane. MISTR items are those items received from supply or from the wing shops needing repair, and are typically miscellaneous items. These are reworked and returned to supply or the wing shops.

Current scheduling priorities for the Plating Shop are 1) ST, 2) MICAP and surge, 3) items from aircraft companies, 4) electronics, 5) MISTR, and 6) Other bases. ST, MICAP and surge items make up approximately 20% of Plating's workload, while items from aircraft companies make up around 40%, electronic components make up roughly 1%, and MISTR items make up about 39%. Work received from other bases is included with MICAP, surge, and items from aircraft companies.

Critical Processes

Two processes needed by approximately 90% of the parts arriving in the Plating Shop are blasting and degreasing. The two most critical blasting processes are walnut hull and glass bead. Other blasting processes typically used are aluminum oxide, aluminum glass,

shop peen, and glass peen. Actual blasting time varies per item depending on the amount of corrosion, rust, paint removal needed, sealant needing removed, etc.

It is important that the walnut hull process operate daily. If one of the blasters is not operational, Plating has the ability to use one of the other blasters for a backup. If more than one blaster is not working, there is a problem scheduling the work through the shop efficiently. Also, the shop has only one degreaser, which must be operational at all times, as most items must be degreased before other processes can be completed. Overall, the shop has a total of 45 processes that can be done on any given part (see Appendix B).

Figure 2 shows a general layout of the processes and where parts are to be delivered. There are two designated delivery points for incoming items, but parts are currently being deposited throughout the shop, which makes it difficult for the scheduler to track newly arriving items. A great deal of time is spent on the shop floor trying to locate newly received items, which are often mixed with previously logged items.

Outside Receiving Area

Blasting	IVD	Small Blasting		NDI	
		Other Equipment			
		Outgoing Area		To B140 ⟶	
	Inside Receiving Area		Offices	
Plating (Chemical Area)				
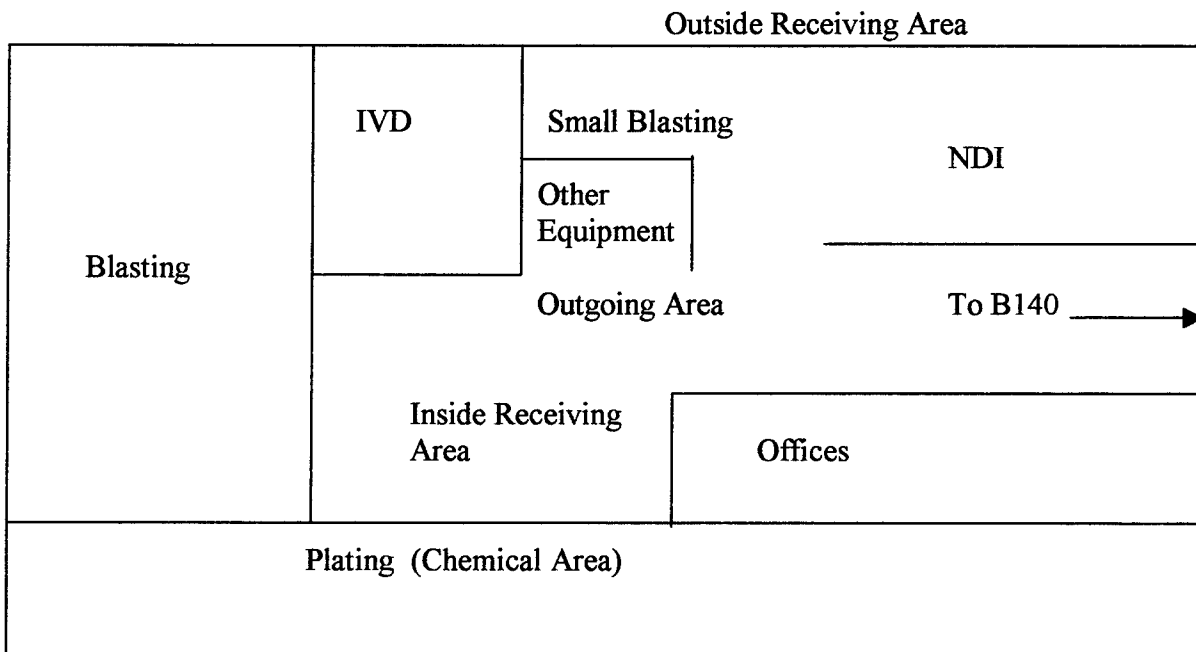
Figure 2: Current Layout of Plating Shop (Not to Scale)

Current Tracking System

Currently, the scheduler and assistant scheduler use a combination of manual and computerized methods to track items through the shop. The item is first recorded manually into a notebook and the date written on the paperwork that comes with the part. This indicates that the part has been logged into the shop. The scheduler or his assistant then inputs this data into a dBase program as time allows. When work on the part is completed, the date on the paperwork is crossed out and the finish date is entered in the notebook. Unfortunately, as parts arrive sporadically, it is difficult for either the scheduler or assistant scheduler to consistently enter the data into the database and sometimes the data are not entered until later in the day, when the parts may have already left the shop. As most of the operators take the initiative when they see parts needing work, it is imperative that the parts are logged in at least manually.

The dBase program allows the scheduler to search for parts by shoe tag (ST), plane type, part number, control number, or part name. It is menu-driven, simple to use, and flexible. The program was designed by the scheduler to answer typical customer questions quickly, such as if an item has arrived, what processes are being done on the item, where the item is at the time, and, if it is no longer in the shop, where it went after leaving the shop. In addition, this program can provide a history of work done on a particular plane, a history of any process done in the shop area, and flow data (the average days) for parts in the shop.

Challenges

Typical problems associated with scheduling parts through the shop include parts arriving unannounced (ST), before or without complete paperwork attached, placed in a non-receiving area, or placed in a receiving area without notifying the scheduler of its arrival.

2-8

When parts are received before or with incomplete paperwork, the scheduler is unable to schedule the part or must locate the part later when the paperwork does arrive, resulting in wasted time and effort. Also, failure to notify the scheduler of arrivals causes delays in scheduling.

Even with the challenges the scheduler and his assistant face, the productivity for the Plating Shop is excellent. Productivity is the number of hours earned divided by the adjusted scheduled hours. Adjusted scheduled hours takes into consideration overtime, absenteeism and overhead. Figure 3 shows a graphical representation of the monthly productivity for 1996 and 1997. Plating's overall productivity for 1996 and 1997 were 106.0% and 107.9%, respectively. Appendix C shows the data used to calculate productivity. As of May 1998, the year-to-date productivity is 107.0%.
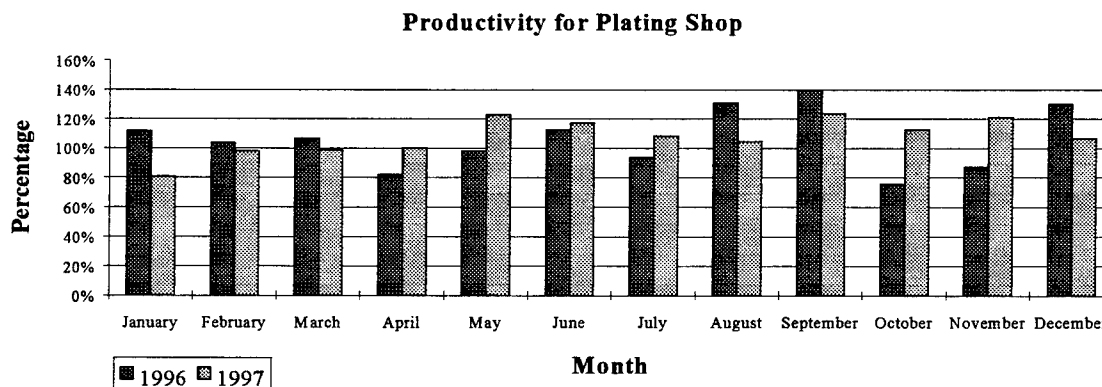
Figure 3: Summary of Productivity Data for the Plating Shop for 1996 and 1997.

Although the Plating Shop's productivity is 107%, indicating no obvious need for improvement, a couple of simple improvements can make scheduling easier. For instance, it is recommended that the shop have three receiving areas instead of two: one for small parts

only, another for large parts and intermediate work, and the outside area for very large parts (see Figure 4). The area for finished parts leaving the shop should remain the same.
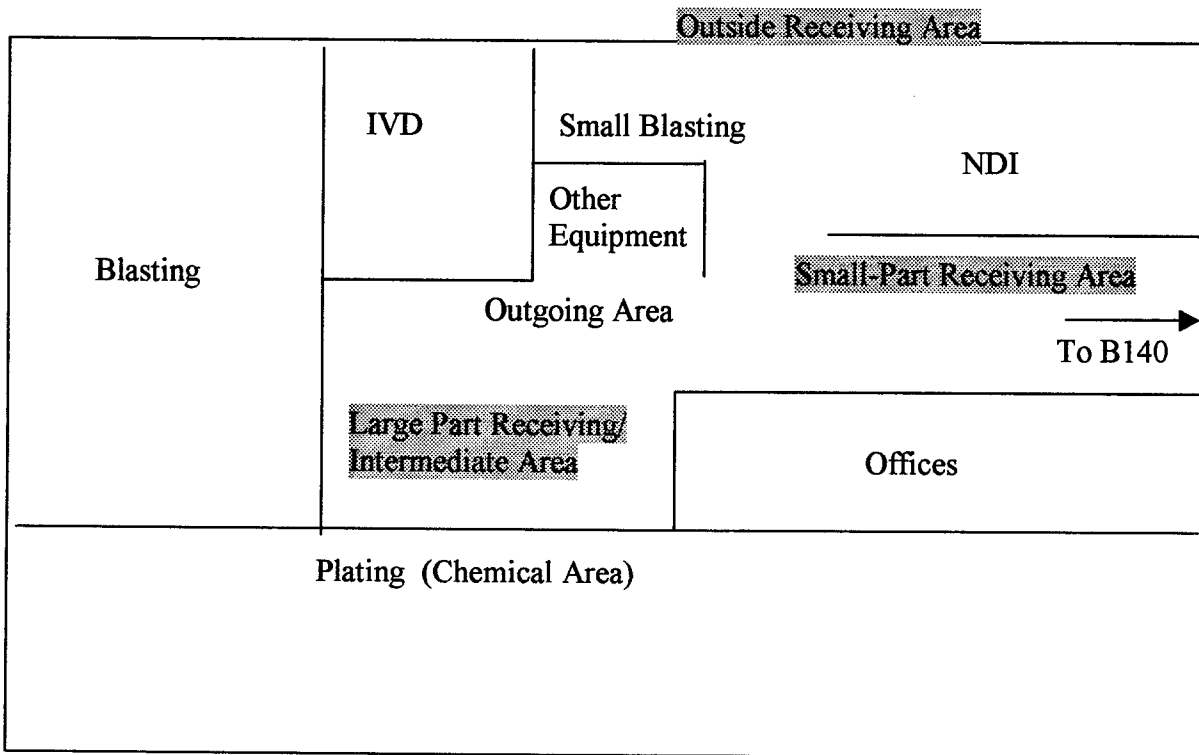
Figure 4: New drop-off areas for incoming parts (Not to Scale).

ST items should still be dropped off directly with the scheduler or assistant scheduler in the office. The small parts area would be located directly in front of the offices, allowing the scheduler an easier view of these parts when they arrive. This should help in preventing misplaced items and keep missed items to a minimum.

Manufacturing Information System

The primary purpose of the manufacturing information system is eliminating scheduling and resource allocation problems in the manufacturing area. By utilizing a currently used database at WR-ALC, DO12, in conjunction with a new database program, Resonance, TINM hopes to correct these problems. Resonance, also referred to as Through-put, uses the data collected and stored by DO12 to provide schedulers with accurate

information on priorities, resource availability, arrival and completion dates, etc., in a more user-friendly environment. DO12 has the capability to perform some of these operations, but not to the degree needed by the schedulers. For example, DO12 readily reveals the process to be performed on a part but does not provide the scheduler with the date of arrival of the item in the shop for processing.

The Facility Process Engineering (TINPE) department at WR-ALC is currently working to correct programming deficiencies in the DO12 program to make it compatible with Resonance. Until this can be accomplished, Resonance cannot be tested properly in manufacturing. For this reason, the Plating Shop and other back shops will not be considered at this time for the manufacturing information system. Resonance will eventually include information needed by the back shops, but this is a future goal of TINPE.

Conclusions

As the manufacturing information system is not ready to go online in the format the Plating Shop needs for scheduling purposes, it is recommended that the Plating Shop keep the existing database. In order for this database to be viewed online by other departments, the dBase program used by Plating would need to be converted to an Access database. However, since Access is currently in the process of being phased out at WR-ALC, converting the dBase program to Access for viewing is not practical.

Until the manufacturing information system is tested and ready to incorporate the back shops' needs, it is imperative that the Plating Shop keep their existing database intact. The scheduler will need an assistant available at all times, as the Plating Shop will be susceptible to an inability to track items brought through the shop if the scheduler is unavailable.

In addition to the utilization of the small part drop-off area in the Plating Shop, another method of indicating a part has been recorded needs to be adopted. This method must be easily identifiable, usable and easy to track. One suggestion is the use of color codes. For example, when a part is logged in, a colored sticker could be quickly placed on the paperwork and when logged out, a different colored sticker could be placed on the paperwork. This is a very quick and simple method, which is also immediately visible to the operators and individuals leaving or picking up the work. No sticker would indicate the scheduler has not processed the part. This would also allow the scheduler to quickly determine which parts have not been logged into the shop.

A second suggestion would be the installation of a bar coding system. This option requires further study to determine the types of bar coding technology that already exists on base, technology that could be used with the proposed manufacturing information system, costs associated with installation and implementation, training requirements, and the impact on scheduling and tracking.

It is hoped with these minor changes, the scheduler or the assistant scheduler will be able to capture most of the incoming parts before they are processed. Since the shop's productivity is already above 100%, these changes will not have a significant effect on productivity. However, it will improve the scheduler's chances of keeping adequate records. Also, once TINPE is ready to incorporate information from the back shops for scheduling with Resonance, they will need to review the dBase program already being used in Plating to adequately provide scheduling information needed by this particular shop.

Future Research

There are at least two areas needing further research in the Plating Shop area not directly related to scheduling: floor layout and investigation of the individual processes. First, for the floor layout, an example problem is the small blasting area, which allows dust particles to escape into the shop area. This machine is located next to an expensive piece of equipment which is sensitive to dust particles. Second, although the overall efficiency of the Plating Shop is above 100%, there may be individual processes, which need improvement. These processes could be investigated to determine improvements needed to increase individual process efficiencies.

References

Abney, Tony, Industrial Products Division – Operations (TINO), Warner Robins Air Logistics Center (WR-ALC), 1998.

Best, Bill, Manufacturing (TINM), WR-ALC, 1998.

Pickney, Robert, Process Shop (TINMP), WR-ALC, 1998.

Ragan, Louis, Process Shop (TINMP), WR-ALC, 1998.

Singletary, Lott, Facility Process Engineering (TINPE), WR-ALC, 1998.

Appendix A: Number of Items and Workorders Received per Month

Number of Items and Workorders Received per Month

Date	Nr. Items	Nr. Orders	Total/Mth			
Jan-96	22,062	1,103	23,165			
Feb-96	25,968	824	26,792			
Mar-96	20,573	970	21,543			
Apr-96	22,261	1,041	23,302			
May-96	24,193	1,070	25,263	AVG 96 =	25,581	per month
Jun-96	19,229	899	20,128			
Jul-96	24,091	1,111	25,202			
Aug-96	32,701	1,383	34,084			
Sep-96	25,808	1,272	27,080			
Oct-96	30,838	1,245	32,083			
Nov-96	25,149	921	26,070			
Dec-96	21,672	591	22,263			
Total 96	294,545	12,430				
Jan-97	15,154	988	16,142			
Feb-97	15,854	921	16,775			
Mar-97	26,461	949	27,410			
Apr-97	17,899	887	18,786			
May-97	26,297	1,076	27,373	AVG 97 =	19,983	per month
Jun-97	14,419	986	15,405			
Jul-97	12,854	987	13,841			
Aug-97	12,532	1,013	13,545			
Sep-97	28,754	1,454	30,208			
Oct-97	18,187	1,228	19,415			
Nov-97	16,660	716	17,376			
Dec-97	22,639	878	23,517			
Total 97	227,710	12,083				

Data provided by TINMP

Appendix B: Plating Shop Processes

Record Number	Code	Process	Uses
1	ALO	Alodine	Coating
2	ANO	Anodize	Coating
3	BO	Black Oxide	Coating
4	IVD	Ion Vapor Deposit	Coating
5	CHR	Chrome	Coating
6	SIL	Silver	Coating
7	GLD	Gold	Coating
8	TIN	Tin	Coating
9	NIC	Nickel	Coating
10	PHS	Phosphate	Coating
11	CLN	Clean	Cleaning
12	CML	Chem Mill	Metal reduction
13	LOB	Lubon	Spray-on lubricant
14	CCT	G14S	Coating
15	BKE	Bake	Baking
16	SEL	Selective Plate	Coating
17	PAS	Passivate	Cleaning of Stainless Steel
18	STP	Strip	Removal of Coatings
19	FCC	Final Clean & Cap	Clean inside of tubes
20	DGR	Degrease	Removal of grease
21	MAG	Magnesium Coat	Coating
22	PHO	Photo Etch	Photo developing of parts
23	ETCH	Etch	Roughing of parts
24	COP	Copper	Coating
25	CAH	Cetyl Alcohol	Lubricant
26	BDP	Bright Dip	Cleaning process
27	WH	Walnut Hull	Removal of paint & sealant
28	GL	Glass Bead	Removal of rust & corrosion
29	SND	Sand	Discontinued
30	SPN	Shot Peen	Stress relief
31	AOX	Aluminum Oxide	See GL uses & prep of IVD parts
32	VB	Vapor Blast	Discontinued
33	MP	Magnetic Particle	Check steel for cracks
34	DP	Dye Penetrant	Check Aluminum & SS for cracks
35	TE	Temper Etch	Check metal structure after grind.
36	CPC	Corros. Prev. Comound	Lubricant
37	TST	Hardness/Conduct. Test	Check AL alloy that is IVD'd
38	ANC	Anodize-Chromic	Coating
39	CLT	Clean-Titanium	Cleaning titanium
40	CAU	Caustic Soda Etch	Cleaning
41	AP	Acid Pickle	Cleaning
42	NDI	Non-Destructive Inspection	Non-destructive inspection
43	FGL	Fastener Glass Blast	Cleaning of fasteners
44	SSTP	Silver Strip	Removal of Silver from steel
45	GPN	Glass Peen	Smooth IVD surfaces

Data Provided by TINMP

Appendix C: Plating Shop Monthly Productivity Numbers for 1996 and 1997

	Paid Hrs	-0.14	Tot Pd Hrs	Bud T Au	BO T	-0.14	Bud T Au	Factor	Bud DPSH	Flex DPSH	Earn Hrs	Prod.
Jan 96	6,622	53	6,569	8,648	432	108	8,972	0.7321	6,355	4,653	5,201	111.8%
Feb 96	5,445	51	5,394	7,896	394	108	8,182	0.6592	6,028	3,974	4,117	103.6%
Mar 96	5,235	55	5,180	7,896	394	108	8,182	0.6331	6,310	3,995	4,256	106.5%
Apr 96	5,596	56	5,540	8,096	404	108	8,392	0.6602	6,135	4,050	3,326	82.1%
May 96	5,971	53	5,918	8,464	423	108	8,779	0.6741	6,193	4,175	4,092	98.0%
Jun 96	5,314	51	5,263	7,360	368	108	7,620	0.6907	5,642	3,897	4,386	112.5%
Jul 96	6,053	55	5,998	8,464	423	108	8,779	0.6832	6,197	4,234	3,975	93.9%
Aug 96	6,843	51	6,792	8,096	404	108	8,392	0.8093	6,523	5,279	6,920	131.1%
Sep 96	6,481	99	6,382	7,392	369	108	7,653	0.8339	5,653	4,714	6,573	139.4%
Oct 96	6,415	51	6,364	8,464	423	108	8,779	0.7249	6,462	4,685	3,545	75.7%
Nov 96	6,332	51	6,281	7,728	386	108	8,006	0.7846	5,204	4,083	3,562	87.2%
Dec 96	6,315	51	6,264	8,096	404	108	8,392	0.7465	5,244	3,914	5,088	130.0%
Jan 97	6,451	52	6,399	8,464	423	108	8,779	0.7289	6,304	4,595	3,706	80.7%
Feb 97	5,273	51	5,222	7,360	368	108	7,620	0.6853	5,722	3,921	3,838	97.9%
Mar 97	6,066	108	5,958	7,728	386	108	8,006	0.7442	6,417	4,776	4,720	98.8%
Apr 97	6,065	52	6,013	8,096	402	108	8,390	0.7167	6,345	4,547	4,551	100.1%
May 97	6,575	55	6,520	8,096	402	108	8,390	0.7771	6,026	4,683	5,753	122.9%
Jun 97	5,662	53	5,609	7,560	383	108	7,835	0.7158	6,083	4,354	5,109	117.3%
Jul 97	6,550	51	6,499	8,280	395	108	8,567	0.7586	6,178	4,686	5,076	108.3%
Aug 97	5,576	102	5,474	7,560	360	108	7,812	0.7008	6,276	4,398	4,595	104.5%
Sep 97	6,151	52	6,099	7,920	394	108	8,206	0.7433	6,274	4,663	5,769	123.7%
Oct 97	6,097	54	6,043	5,888	298	108	6,078	0.9942	4,470	4,444	5,002	112.5%
Nov 97	5,328	67	5,261	5,120	260	108	5,272	0.9979	3,335	3,328	4,031	121.1%
Dec 97	6,305	54	6,251	5,888	298	108	6,078	1.0284	3,785	3,892	4,141	106.4%

*Data provided by TINO

NATURAL ATTENUATION EVALUATION SUMMARY
FOR A
CHLORINATED SOLVENT PLUME, OU1, HILL AFB, UTAH

R. Ryan Dupont
Professor
Civil and Environmental Engineering

Utah Water Research Laboratory
8200 Old Main Hill, UMC-8200
Utah State University
Logan, UT 84322-8200

NATURAL ATTENUATION EVALUATION SUMMARY
FOR A
CHLORINATED SOLVENT PLUME, OU1, HILL AFB, UTAH

R. Ryan Dupont
Professor
Department of Civil and Environmental Engineering
Utah State University

Abstract

An evaluation of the natural attenuation of chlorinated solvents (TCE and its daughter products) was conducted for a contaminated groundwater system at Hill Air Force Base, OU1, using a quantitative natural attenuation evaluation protocol. As part of this evaluation protocol the following plume characteristics were determined: stability of the parent compound dissolved plume via centerline, dissolved plume mass, and center of mass estimates; geochemical indicator parameter results for plume terminal electron acceptors and degradation products; free product evaluation and dissolved plume composition estimates; parent compound and intermediate product degradation rates; plume lifetime predictions; and long-term monitoring and site management recommendations. Using this evaluation protocol it was determined that the OU1 dissolved plume is actually declining in mass, being indicative of a pulse or weathered free product source. Contaminant pseudo-first order degradation rates within the dissolved plume were estimated to range from -0.0002 to -0.0068/d for cis-DCE and trans-DCE, respectively. Required timeframes for plume management ranged from 2 to 33 years, with cis-DCE requiring the longest time before reaching MCLs required for site closure.

The methods used in this evaluation protocol are described in this final report along with results specific for OU1. A long-term monitoring strategy is defined, as is a recommended management approach for this dissolved plume. Finally, recommendations are provided for the investigation of methods that can be used for the acceleration of natural degradation processes DCE dechlorination taking place throughout the site.

NATURAL ATTENUATION EVALUATION SUMMARY FOR A CHLORINATED SOLVENT PLUME, OU1, HILL AFB, UTAH

R. Ryan Dupont

Introduction

Natural attenuation describes the physical/chemical/biological processes that result in the attenuation and ultimate destruction of contaminant mass within impacted aquifer systems independent of active, external intervention. These processes have been intensively studied over the last 10 years at fuel-impacted sites, and have recently been investigated at chlorinated solvent sites as part of the development of risk-based management strategies for these sites. As a result of this work a number of protocols have been developed that provide guidance regarding the assessment and documentation of natural attenuation processes. These protocols include that by Wiedemeier et al. {1} for petroleum hydrocarbons, Wiedemeier et al. {2} for chlorinated solvents, the *Principles and Practices Manual for Natural Attenuation of Chlorinated Solvents* by the RTDF {3}, and a quantitative protocol generally applicable to all contaminated groundwater systems in Dupont {4}. It is with this latter protocol that the chlorinated solvent site at Hill AFB, OU1, was evaluated.

Discussion of Problem

Historical waste disposal practices at U.S. industrial facilities has resulted in significant groundwater contamination and environmental impact at many sites. Department of Defense facilities are no exception, and Hill AFB in particular hosts a number of Superfund sites because of the prominent role it has played in the maintenance and refurbishing of U.S. Air Force aircraft over the last 50+ years. One of these sites, OU1, consists of several landfills, chemical disposal pits, fire training areas, a waste phenol/oil pit, and a waste oil storage tank that lie adjacent to the base property boundary as indicated in Figure 1. A mixture of waste solvents, industrial sludges, residues from solvent cleaning operations, domestic solid waste, sulfuric and chromic acid residues, methyl ethyl ketone, jet fuel, and waste oils were deposited in these disposal areas from 1940 until 1975. The northern portion of the site, in the location of the chemical disposal pits, represents the most significant source of contamination, with a dissolved chlorinated solvent plume that has left the base boundary and has migrated approximately 2,700 ft down gradient from the disposal pits into the adjacent Weber Valley {5}.

Figure 1. Topographic and disposal site location map, OU1, Hill AFB, UT {6}
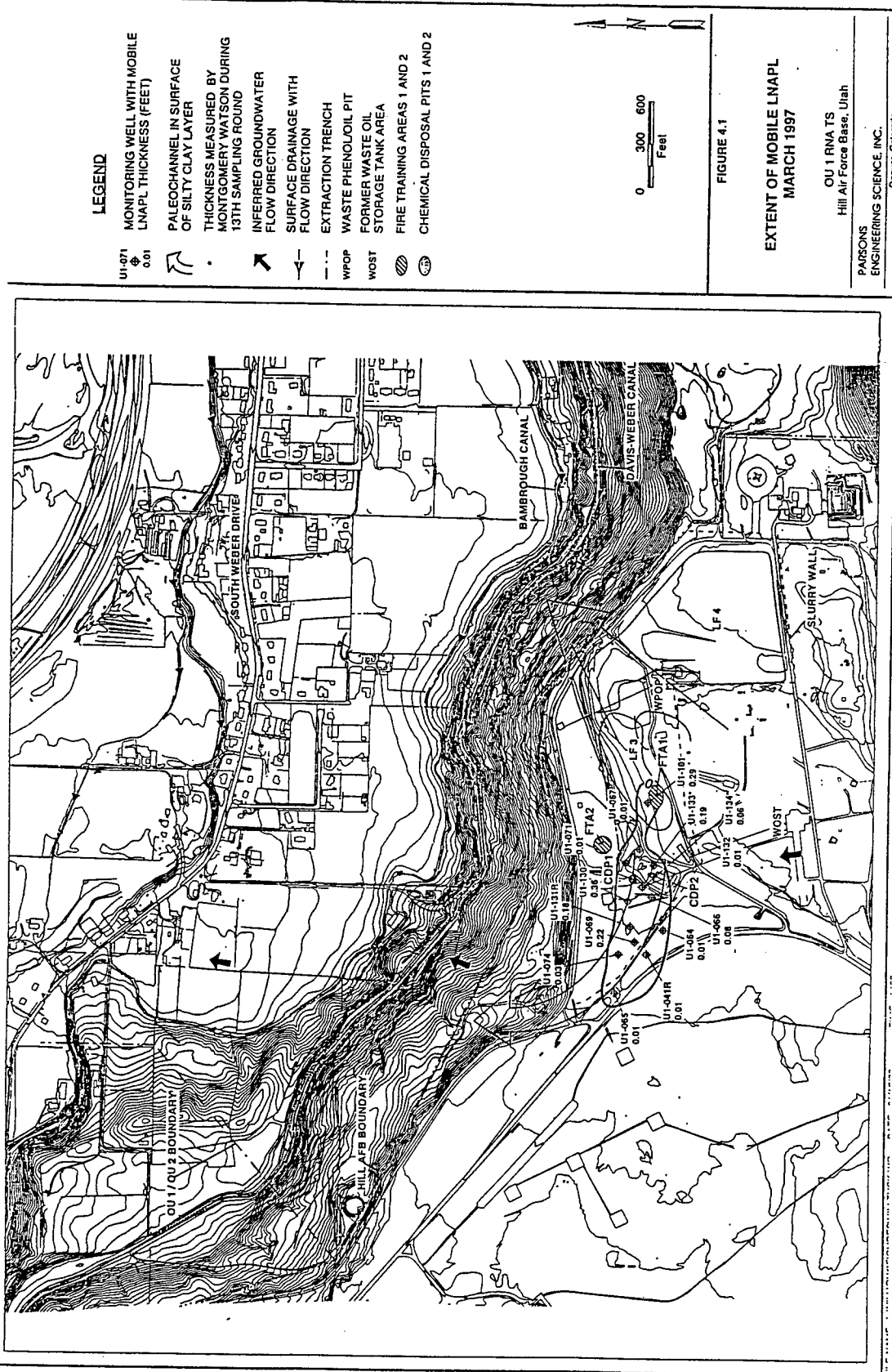
<u>Initial investigations and remedial actions {7}</u>. Investigations of soil and groundwater contamination at OU1 were initiated as early as 1976, and continued through 1982 to 1988 when the IRP program was begun at Hill. Interim Remedial Actions were initiated in 1984 in response to a Cease and Desist Order from the Utah DEQ to eliminate landfill leachate discharge below LF4. Remedial actions have included: capping of Landfills 3 &4 to limit infiltration into the landfill areas; installation of a slurry wall upgradient of OU1 to eliminate groundwater recharge into the contaminated area; and installation of an extraction well/cut-off trench system to dewater hillside springs that existed downgradient of the fire training and landfill areas. An analysis of the effectiveness of these measures has indicated that "...Although the actions appear to have decreased infiltration and recharge into the OU1 area, several inadequacies in design or construction have limited their effectiveness..." {7}.

<u>Existing site contamination</u>. The most comprehensive evaluation of contamination at OU1 was recently completed by Parsons Engineering Science, Inc. {6}, and indicates that as shown in Figure 1, a NAPL phase continues to persist west of FTA1 and the two chemical disposal pits. The composition of this free product is described below, and is believed to be the source of the contaminant plume that has migrated north, off-base and into the Weber River valley.

The primary contaminants of concern in the dissolved phase are chlorinated solvents, primarily TCE and its daughter products, and to a lesser extent 1,1,1-TCA and 1,1-DCA produced from dechlorination reactions in the aquifer. Table I summarizes when and where maximum contaminant concentration data were observed in the western plume at OU1 for these contaminants of interest. DCE and TCA show the most significant migration downgradient from the source area, but have also been stable over time as discussed below:

Table I. Summary of maximum concentrations observed over time for contaminants of concern in the western groundwater plume at OU1, Hill AFB, Utah.

Contaminant	Maximum Conc. (µg/L)	Date Observed	Last Monitored	Well Location
TCE	28	10/95	7/96	U1-151
cis-DCE	1,500	2/93	12/97	U1-108
VC	940	2/93	12/97	U1-089
TCA	14	2/93	12/97	U1-108
DCA	41	12/94	7/96	U1-104
Benzene	6.1	8/94	12/97	U1-089
ΣBTEX	200	7/96	12/97	U1-105

Methodology

The methodology used in the evaluation of natural attenuation processes in contaminated ground-water below OU1 is based on procedures that have been developed for the hydrocarbon and chlorinated solvent contaminated groundwater systems as described by Dupont {4}. It has been used at a number of hydrogeologically simple sites at Hill and Eielson AFBs, and application to OU1 at Hill provided an opportunity to evaluate its utility at a more complex, intensely studied site. This methodology was also not well known, and implementation at OU1 provided a vehicle for transferring this information to the Hill AFB EM staff and for comparison with a natural attenuation study recently completed for OU1 by Parsons Engineering Science {6}.

The methodology described by Dupont {4} involves the sequential analysis of contaminant migration, degradation, and plume stability using the approach summarized in Figure 2. Procedures applicable to each step in the process are detailed in Dupont {4}, and the reader is referred to this document for specific details. Methods appropriate to the OU1 contaminant plume are describe below along with the results of each step in this intrinsic remediation assessment protocol.

```
                    ┌─────────────────────┐
                    │ Intrinsic Remediation│
                    │ Assessment Approach  │
                    └─────────────────────┘
        ┌──────────────────────┐   ┌──────────────────────┐
        │ 1. Steady-State Plume │   │ 5. Long-Term Behavior │
        │    Conditions?        │   │                       │
        └──────────────────────┘   └──────────────────────┘
        ┌──────────────────────┐   ┌──────────────────────┐
        │ 2. Estimate          │   │ 6. Intrinsic          │
        │    Contaminant       │   │    Remediation for Site?│
        │    Degradation Rate  │   │                       │
        └──────────────────────┘   └──────────────────────┘
        ┌──────────────────────┐   ┌──────────────────────┐
        │ 3. Estimate Source   │   │ 7. Long-Term          │
        │    Mass              │   │    Monitoring for Site │
        └──────────────────────┘   └──────────────────────┘
        ┌──────────────────────┐
        │ 4. Estimate Souce    │
        │    Lifetime          │
        └──────────────────────┘
```
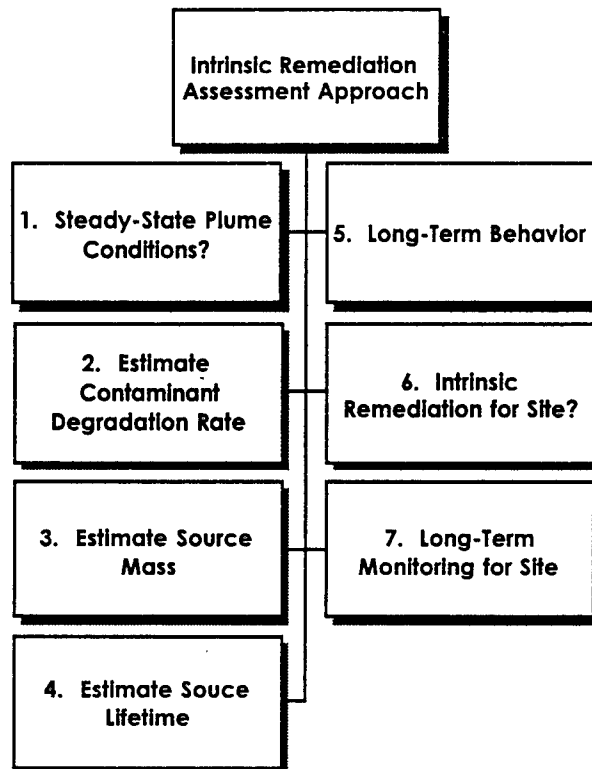
Figure 2. Intrinsic remediation assessment protocol from Dupont {4}.

Results

Steady-state plume conditions. Steady-state plume conditions have classically been determined in natural attenuation assessments through an evaluation of plume centerline concentration changes over time. This method is susceptible to miss-interpretation due to variability in groundwater elevation, groundwater direction, etc., and an improved method integrates contaminant concentrations over the entire plume, accounting for variability in plume thickness due to changes in groundwater elevations over time. The method involves designating an outer plume boundary from historical groundwater data, assigning areas of the plume to each sampling location within the plume boundary (the Thiessen Area Method {8} is used in this methodology), determining a contaminated aquifer thickness based on groundwater elevation measurements recorded at each sampling interval, extrapolating measured contaminant concentrations to the aquifer volume assigned to each sampling location, determining the total plume mass and center of mass locations over time, and comparing total mass and mass center locations to determine the status of the contaminant plume being monitored. This process was carried out for the shallow (10 to 35 ft BGS), western plume at OU1. The results of the Thiessen Area Method are shown in Figure 3, while the center of mass plots for chlorinated alkenes and chloride are shown in Figure 4.
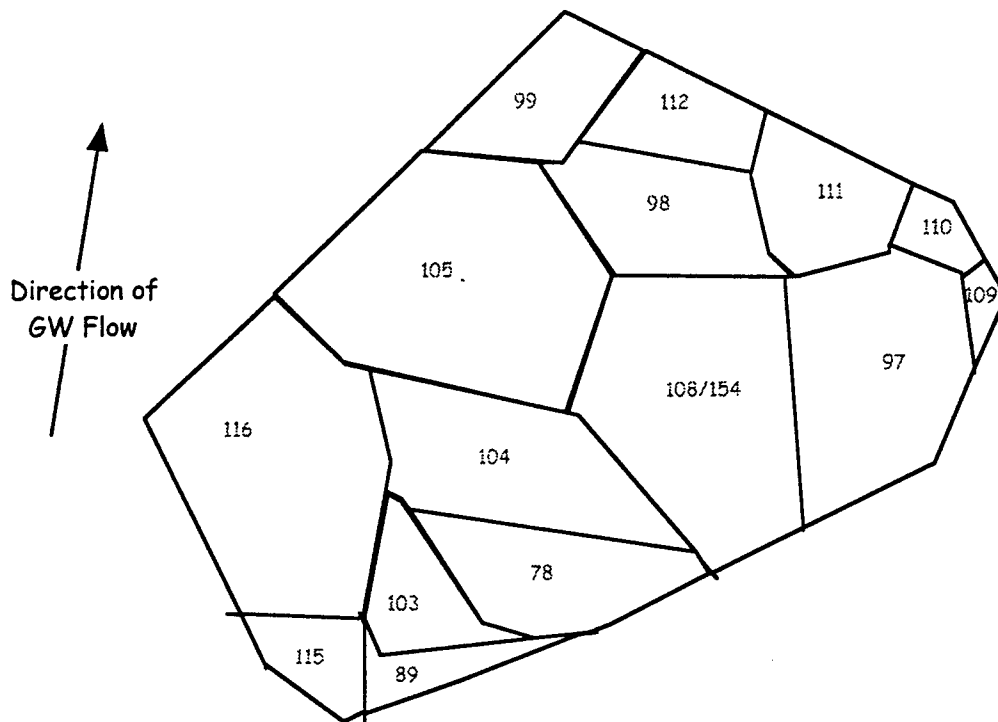

Figure 3. Thiessen area method results for dissolved plumes at OU1. Numbers within each area indicates monitoring well to which each area is applied.
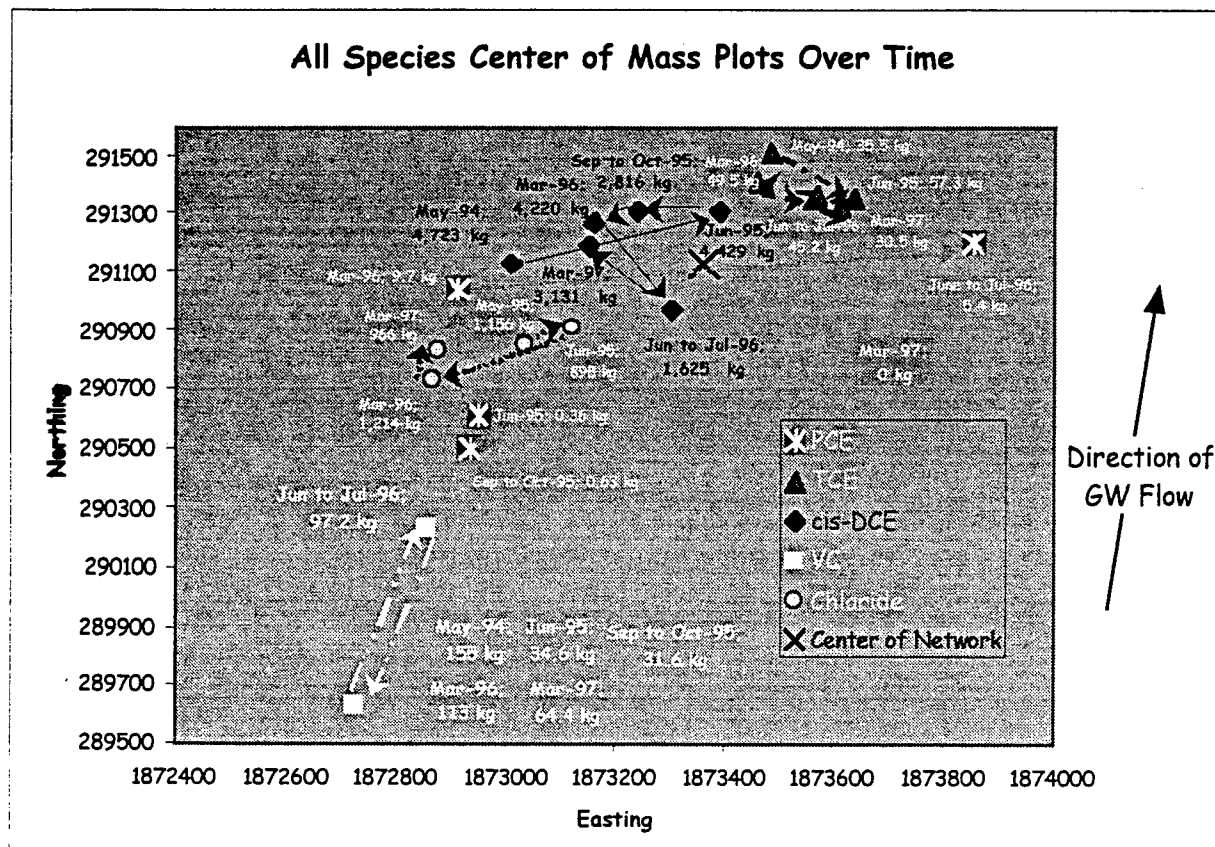
3-7

Figure 4. Center of mass plots for chlorinated alkenes and chloride in dissolved plumes at OU1, Hill AFB, Utah, May 1994 through March 1997.

Based on both the total mass estimates and changes in position of the center of mass over time for these chlorinated alkenes in the dissolved plume at OU1 it was found that: 1) consistent reductions in contaminant mass has occurred over time for all constituents of interest; 2) anaerobic dechlorination is indicated based on the existence of degradation products (cis-DCE and vinyl chloride) and their relative position within the plume; 3) as has been observed in other field sites, cis-DCE appears to be the most persistent intermediate at the site, with VC rapidly being transformed as indicated by its near-source position and lack of accumulation within the dissolved plume; 4) mass center positions indicate no net, downgradient migration between May 1994 and March 1997; and 5) these results are indicative of a "pulse" source of contamination {4} which is indicative of a weathered source area no longer providing a supply of contaminant into the dissolved plume.

Estimate of contaminant degradation rate. Using the methodology presented in Figure 2, once a pulse source of contamination has been documented, the estimation of contaminant degradation

rates is made based on an analysis of changes in the dissolved plume mass over time. The governing equation is shown below:

$$M = M_0\, e^{-k_1 t} \qquad (1)$$

where M = contaminant mass at time t, mass; M_0 = the initial contaminant mass at time $t = 0$, mass; and k_1 = first order degradation rate constant, 1/time. A plot of the natural log of contaminant mass versus time should yield a linearized relationship with slope equal to k_1.

Using Equation 1 and the dissolved plume mass data generated from the Thiessen area estimates described above, first order contaminant degradation rate estimates were made for the plumes at OU1. An example of these regression relationships is shown in Figure 5 for vinyl chloride, while all of the calculated results are summarized in Table II along with statistical descriptors for each relationship.

ln(VC mass) = -0.0016 (Δ Time) + 5.7781, r^2 = 0.9997; p = 0.0116
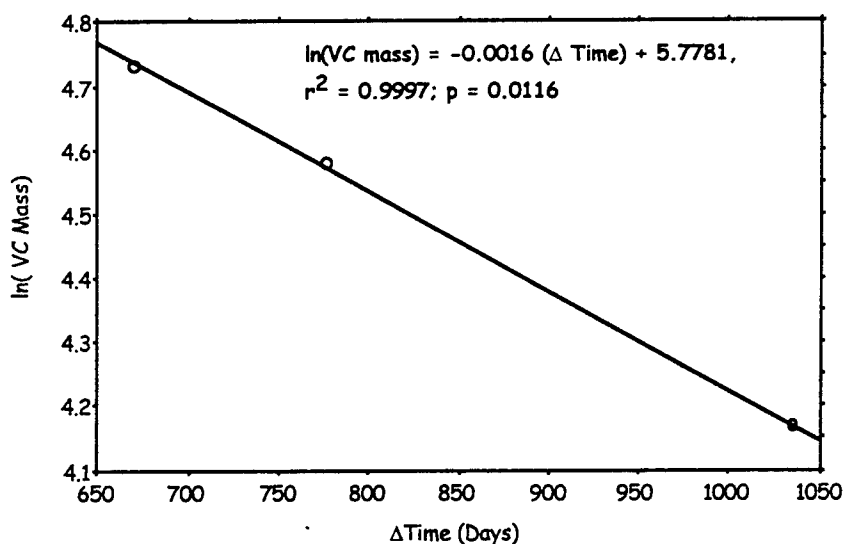
Figure 5. First order degradation rate estimate for vinyl chloride at OU1 based on dissolved mass changes over time.

Table II. Summary of first order degradation rates estimated for contaminants of concern in the western groundwater plume at OU1, Hill AFB, Utah.

Contaminant	First Order Rate (1/d)	Half-Life (yr)	r^2	p Value
PCE	-0.0055	0.35	2 pt. Regression	1
TCE	-0.0010	1.9	0.9213	0.0401
cis-DCE	-0.0002	9.5	0.9994	0.0150
trans-DCE	-0.0068	0.28	0.9360	0.1628
VC	-0.0016	1.2	0.9997	0.0116

The estimated degradation rates presented in Table II are consistent with those reported elsewhere in the literature, and indicate, as is common at most sites, that cis-DCE is the contaminant with the slowest degradation rate, controlling the overall duration of management required for the site.

Source mass and source lifetime estimates. The issues of source mass and source lifetime estimates are critical in the evaluation of contaminant plumes emanating from a continuous source, as the mass of contaminant that is available for dissolution into the aquifer governs the duration of the dissolved plume that is generated from this source. These site characteristics are less important for pulse sources as by the very definition of a pulse source, it is inferred that the source mass has either been removed or isolated from the aquifer system so that the dissolved plume is no longer fed by a source of groundwater contamination.

What is of interest at OU1, however, is analysis of data that can provide independent verification of the weathered nature of the source material, strengthening the conclusions of the plume mass and mass center estimates. Analytical data describing the composition of the free product observed in the source area from OU1 can provide this weathering information.

Only three true free product sample analyses are available from OU1. These samples include data collected from monitoring wells U1-004A (9/25/92), U1-065 (10/1/92), and U1-101 (9/24/92). An additional mobile free product sampling was reported in the natural attenuation evaluation study conducted by Parsons Engineering Science and the U.S. EPA Kerr Lab in March 1997 {6}, however, these data from well U1-130 were reported as water headspace samples, not purge-and-trap nor solvent extractable concentrations of the free product itself, and are only indirect estimates of free product composition.

The true free product data from the 1992 sampling event are shown in Table III, and indicate that at the time the product contained high concentrations of petroleum constituents - toluene, ethylbenzene, xylenes; and a variety of chlorinated organics including chlorobenzene; 1.1.1-TCA; 1,2-DCE; and to a much lesser extent PCE.

Analyses from monitoring well U1-130 were used to estimate free product composition in 1997 using the reported water concentration data from headspace analyses (Table III) along with the assumption that the groundwater concentrations in equilibrium with the free product in U1-130 can be described by Raoult's Law as follows:

Water Concentration = (Mole Fraction in Product) (Compound Aqueous Solubility)   (2)

3-10

TABLE III. Analytical Results for Free Product Samples from OU1, 1992, and estimated composition from equilibrium aqueous phase concentrations measured in 1997.

Constituent	Well U1-004A 09/25/92 Concentration (µg/kg)	Well U1-065 10/01/92 Concentration (µg/kg)	Well U1-101 09/24/92 Concentration (µg/kg)	Well U1-130 3/97 Concentration (µg/L)	GMW (g/gmol)	Aqueous Solubility (mg/L)	Estimated Product Concentration (mole fraction)	Estimated Product Concentration (mass fraction)	Estimated Product Concentration (ppb)
1,1,1-TRICHLOROETHANE	92,000	ND	ND	20.2	133.42	1.33E+03	1.51E-05	1.55E-05	15,502
1,1,2,2-TETRACHLOROETHANE	ND	ND	ND	–					
1,1,2-TRICHLOROETHANE	ND	ND	ND	–					
1,1-DICHLOROETHANE	ND	ND	ND	23.2	98.97	5.50E+03	4.22E-06	3.21E-06	3,211
1,1-DICHLOROETHENE	ND	ND	ND	ND					
1,2,3-TRICHLOROPROPANE	ND	ND	ND	–					
1,2-DICHLOROBENZENE	NR	NR	NR	939	147.01	1.85E+02	5.08E-03	5.75E-03	5,748,239
1,3-DICHLOROBENZENE	NR	NR	NR	ND					
1,4-DICHLOROBENZENE	NR	NR	NR	118	147	6.24E+01	1.89E-03	2.14E-03	2,140,838
1,2-DICHLOROETHANE	ND	ND	ND	ND					
1,2-DICHLOROPROPANE	ND	ND	ND	--					
2-CHLOROETHYL VINYL ETHER	ND	ND	ND	–					
2-HEXANONE	ND	ND	ND	–					
ACETONE	ND	1,100,000	ND	--					
ACROLEIN	ND	ND	ND	–					
ACRYLONITRILE	ND	ND	ND	–					
BENZENE	ND	ND	ND	--					
BROMODICHLOROMETHANE	ND	ND	ND	--					
BROMOFORM	ND	ND	ND	--					
BROMOMETHANE	ND	ND	ND	–					
CARBON DISULFIDE	ND	ND	ND	--					
CARBON TETRACHLORIDE	ND	ND	ND	ND					
CHLOROBENZENE	ND	2,300,000	ND	16.5	112.56	1.35E+02	1.22E-04	1.06E-04	105,505
CHLOROETHANE	ND	ND	ND	–					
CHLOROFORM	ND	ND	ND	ND					
CHLOROMETHANE	ND	ND	ND	--					
cis-1,3-DICHLOROPROPENE	ND	ND	ND	–					
DIBROMOCHLOROMETHANE	ND	ND	ND	–					
DIBROMOMETHANE	ND	ND	ND	–					
ETHYL METHACRYLATE	ND	ND	ND	--					
ETHYLBENZENE	210,000	ND	210,000	--	106.17	1.35E+02	–		
IODOMETHANE (METHYL IODIDE)	ND	ND	ND	--					
METHYL ETHYL KETONE (2-BUTANONE)	ND	ND	ND	--					
METHYL ISOBUTYL KETONE (4-METHYL-2-PENTANONE)	ND	ND	ND	--					
METHYLENE CHLORIDE	ND	ND	ND	--					
STYRENE	ND	ND	ND	--					
TETRACHLOROETHYLENE (PCE)	38,000	ND	ND	0.90	165.85	1.35E+02	6.67E-06	8.51E-06	8,505
TOLUENE	770,000	ND	ND	--	92.13	1.35E+02	–		
TOTAL 1,2-DICHLOROETHENE	87,000	ND	ND	124	96.95	8.00E+02	1.55E-04	1.16E-04	115,594
trans-1,3-DICHLOROPROPENE	ND	ND	ND	–					
trans-1,4-DICHLORO-2-BUTENE	ND	ND	ND	--					
TRICHLOROETHENE	ND	ND	ND	ND					
TRICHLOROFLUOROMETHANE	ND	ND	ND	–					
VINYL ACETATE	ND	ND	ND	–					
VINYL CHLORIDE	ND	ND	ND	16.4	62.5	1.10E+00	1.49E-02	7.15E-03	7,145,979
XYLENES, TOTAL	1,400,000	ND	540,000	–					

ND = below method detection limit, NR = not reported.

The results in Table III indicate that the product at OU1 does appear to be highly weathered, particularly of the parent chlorinated solvent constituents of original concern at the site, i.e., PCE and TCE. There is evidence from the headspace data collected in 1997 that the product in the source area may still contain high levels of some constituents of concern, however, particularly 1,2- and 1,4-dichlorobenzene, and vinyl chloride (produced from dechlorination of the higher molecular weight chlorinated alkenes). There appears to be significant variation in product analyses that have been conducted to date, and it is recommended that further analysis of the product via extraction/purge and trap methods should be conducted so that an adequate determination of

3-11

current product composition can be made for long-term product weathering and remedial design purposes. It does appear from these data, however, that product weathering has occurred, and that the findings of the plume mass and center of mass calculations are supported by the data summarized in Table III.

Long-term plume behavior. Based on the natural attenuation assessment protocol shown in Figure 2, analysis of long-term plume behavior for a pulse source involves the analysis of the degradation of contaminant within the dissolved plume over time until the remedial objectives for contaminated groundwater are reached. This amounts to an analysis of the lifetime of the dissolved plume based on an extrapolation of contaminant degradation rates presented in Table II. Equation 1 is modified to be expressed in concentration terms assuming linear partitioning within the aquifer to the form shown in Equation 3:

$$C = Co\ e^{-k_1 t} \qquad\qquad (3)$$

where C = the contaminant concentration representing the remedial clean-up objective, and Co = the maximum concentration observed within the dissolved plume at the site. Using this approach, the time, t, required to reach clean-up objectives can be easily estimated by solving Equation 3. The contaminant governing requirements for site management, then, is the one yielding the longest time to reach remedial clean-up goals.

Table IV summarizes calculations for the required time to reach remedial goals for each of the contaminants of concern at OU1 that were evaluated in this study. Again, these results were estimated assuming that contaminant first order degradation rates from Table II will be maintained throughout the life of the plumes.

Table IV. Summary of preliminary remediation goals (PRGs) {9} and estimated clean-up times for contaminants of concern in the western groundwater plume at OU1, Hill AFB, Utah.

Contaminant	First Order Rate (1/d)	Maximum Concentration 3/97 (µg/L)	PRG (µg/L)	Time to Reach PRG (years)
PCE	-0.0055	0.0	5.0	NA
TCE	-0.0010	9.8	5.0	1.8
cis-DCE	-0.0002	648	70	30.5
trans-DCE	-0.0068	1.8	NA	NA
VC	-0.0016	213	2	8.0

As was the for the degradation rate results summarized in Table II, findings from the long-term plume behavior calculations indicate that cis-DCE remains the contaminant driving the overall management requirements at OU1.

<u>Applicability of natural attenuation for OU1</u>. The applicability of natural attenuation at an impacted groundwater site is driven by evidence of contaminant mass destruction based on dissolved plume mass and center of mass calculations described above, and on evidence that this mass removal is due to biologically-mediated processes, and that these biological processes will continue over the duration of the life of the contaminant plumes. Evidence of the biological nature of contaminant loss at OU1 is provided by both parent compound and degradation product data, and terminal electron acceptor data observed throughout OU1.

Parent compound and daughter product analysis for chlorinated solvent impacted sites provides insight into the biological mechanisms governing contaminant loss under site-specific aquifer conditions. The biological fate of chlorinated solvents is summarized in Figure 6 {4}, and provides a basis for evaluating results of groundwater investigations at contaminated sites.
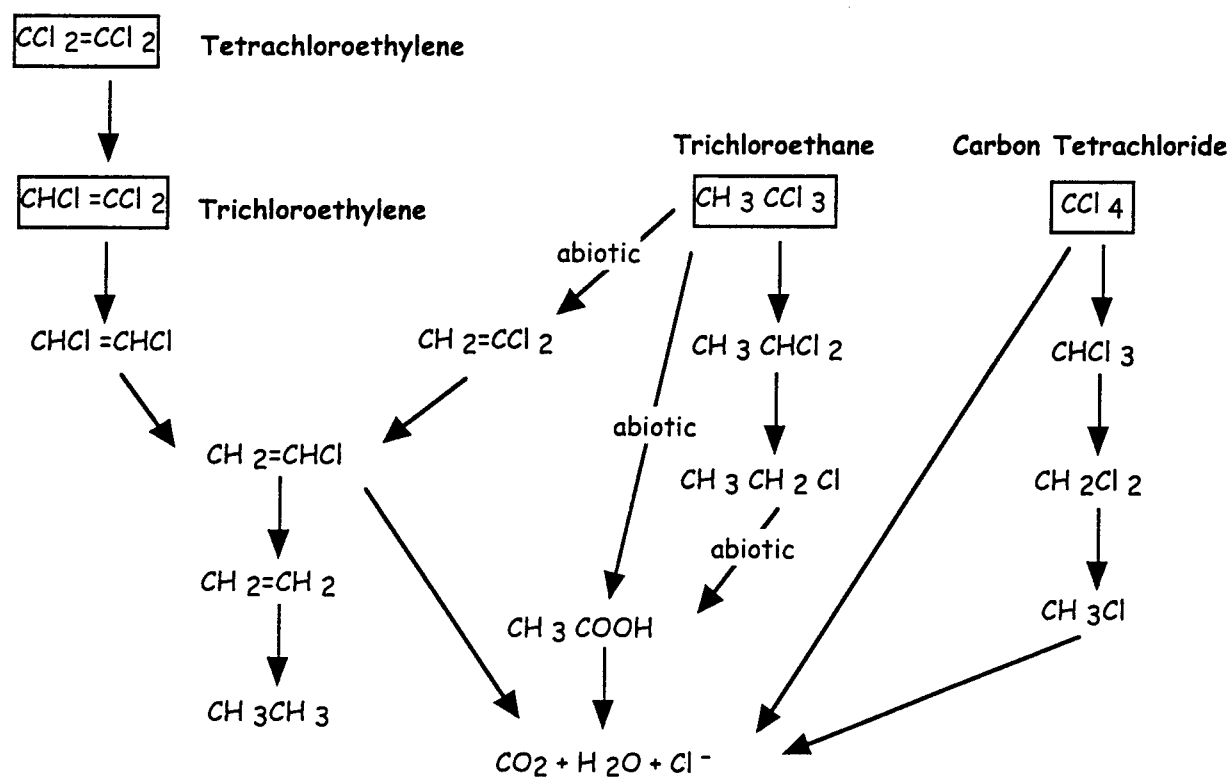

Figure 6. Chlorinated solvent degradation pathways observed in aquifer systems {4}.

3-13

Based on historical records of chemical use at Hill AFB, and waste disposal practices at OU1, it is known that the primary contaminants disposed of at the site were PCE, TCE, and 1,1,1-TCA mixed with fuels and lubricating oils. With this knowledge and pathway information from Figure 6, the detection of cis-DCE, vinyl chloride, and 1,1-DCA throughout the dissolved plume at OU1 indicates the anaerobic dechlorination of the parent material by microorganisms. This dechlorination process should be accompanied by water quality indicators of reducing conditions within the aquifer, i.e., decreased dissolved oxygen, nitrate, and sulfate, and increased dissolved iron and manganese concentrations relative to uncontaminated, background water quality conditions. This relationship is clearly shown in data presented in Figure 7, where significant reductions in all electron acceptors and highly reducing conditions indicated by sulfate reduction occur downgradient of the product area at OU1.
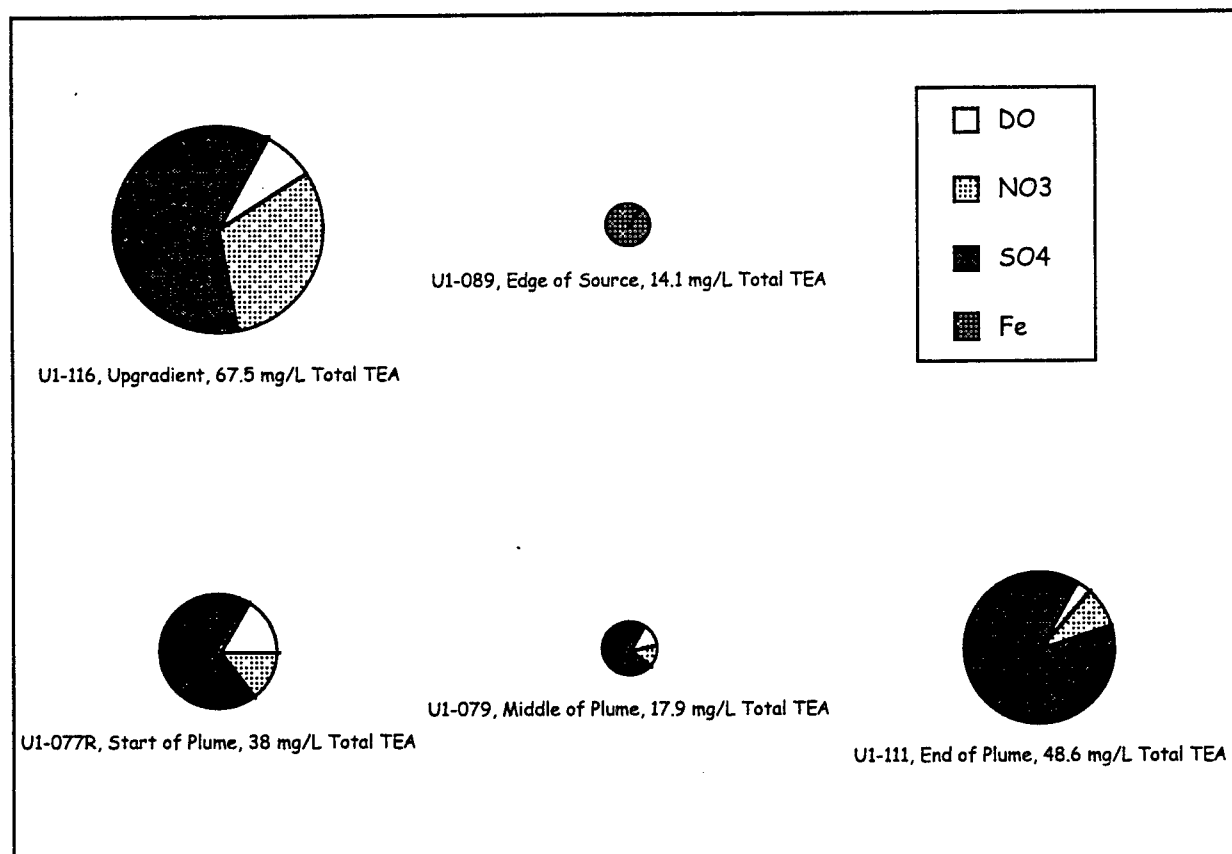

Figure 7. Magnitude and distribution of terminal electron acceptors observed at OU1, during the natural attenuation treatability study conducted March 1997, Hill AFB, UT {7}.

The dechlorination processes taking place throughout the aquifer below OU1 as evident from degradation daughter products and groundwater quality conditions must be driven by some source of

electron donor other than the chlorinated solvents themselves. Under an anaerobic dechlorination pathway the chlorinated solvents act as electron acceptors in the oxidation of a non-chlorinated electron donor. Background concentrations of total organic carbon (TOC) were measured in March 1997 at 3 to 7 mg/L upgradient of the western OU1 plume (U1-115 & U1-116) {6}, falling to less than 2 mg/L at the end of the plume at well U1-111. Near the source area TOC measurements are affected by releases of rapidly biodegradable organic carbon reaching 20 mg/L TOC concentrations at well U1-089.

At many Air Force sites, this required electron donor exists in the form of aromatic and straight-chain hydrocarbons that enter the groundwater from fuel releases. At OU1, however, the level of BTEX and related compounds is quite low in the dissolved plume, apparently being utilized rapidly as they move out of the source area. These compounds appear to be serving as the electron donor driving the rapid dechlorination of parent compounds completely to vinyl chloride immediately adjacent to the source area (notice the relative location of vinyl chloride center of mass shown in Figure 4), but are not believed to be the carbon source driving anaerobic dechlorination away from the source area. It is the native organic matter, measured as TOC, that appears to be maintaining reducing conditions downgradient of the source area at OU1.

It does appear then that natural attenuation is an appropriate plume management approach at OU1, but will require the maintenance of a continued supply of electron donor in the source area to continually maintain reducing conditions and an environment conducive to anaerobic dechlorination if the downgradient, dissolved plume is to continue to degrade anaerobically. If the supply of electron donor is terminated near the source area, background concentrations of TOC may not be sufficient to maintain the entire aquifer anaerobic, resulting in the growth and downgradient mobility of the western dissolved plume at OU1.

Long-term monitoring approach for OU1.

Figure 8 shows the recommended long-term monitoring network to be used for the western plume at OU1. This network consists of 17 sampling locations that will provide verification of degradation processes observed from existing data, and will allow the on-going updating and refinement of the site conceptual model, contaminant degradation rates, plume lifetime estimates, etc. In addition to compliance monitoring data (upgradient and downgradient sampling locations) this sampling network provides both centerline concentration data and Thiessen network data so that estimates of dissolved mass changes over time can continue to be generated (Table V).
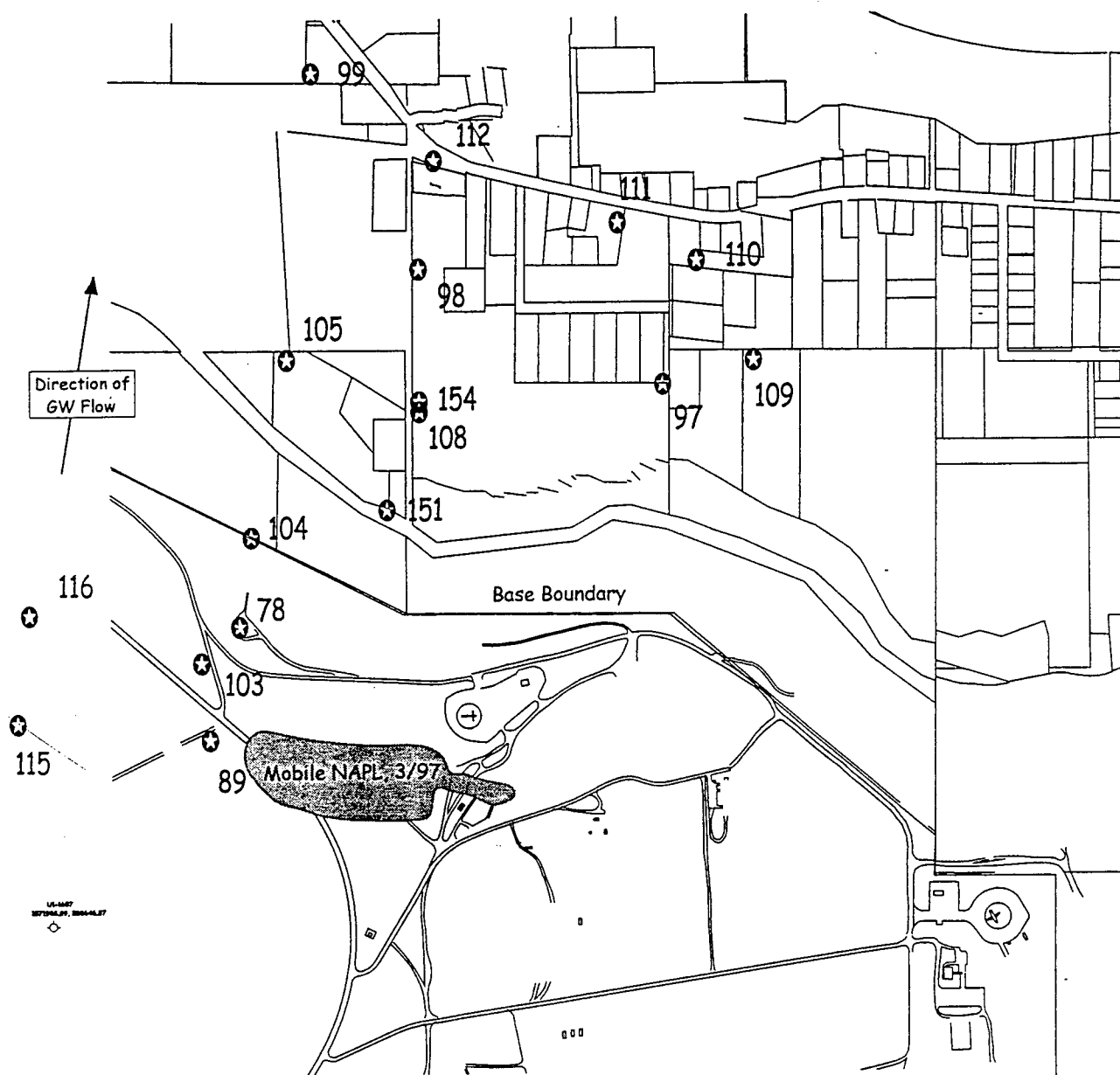
Figure 8. Long-term monitoring well location map, OU1, Hill AFB, UT.

Table V. Proposed long-term monitoring network for compliance and natural attenuation process monitoring for western groundwater plume at OU1, Hill AFB, Utah.

Compliance Monitoring		Natural Attenuation Process Monitoring	
Purpose	Location	Centerline	Thiessen Calculations
Background	U1-115	U1-078	U1-097
Downgradient	U1-099	U1-080	U1-098
	U1-109	U1-103	U1-104
	U1-110	U1-111	U1-105
	U1-111	U1-151	U1-108
	U1-112	U1-154	U1-116

Because of the relatively short lifetime associated with this dissolved plume ($\approx$ 30 years from Table IV), it is recommended that the long-term monitoring network identified in Table V be sampled every 2 years for the suite of natural attenuation parameters relevant for chlorinated solvent sites. These parameters include: water quality/electron acceptor indicators measured in the field - DO, pH, ORP, alkalinity, conductivity, temperature, chloride; electron acceptors measured in the laboratory - nitrate, sulfate, iron, manganese; parent compounds and intermediate products measured in the laboratory - PCE, TCE, cis- and trans-DCE, vinyl chloride, methane, and ethylene; and electron donor concentrations in the laboratory - BTEX, TOC, and TPH. This monitoring will allow verification that natural attenuation processes are effectively reducing contaminant mass and mobility at the site, and will provide data necessary to up-date the modeling of plume behavior.

Conclusions

Based on the findings of this study, the following conclusions can be reached regarding the natural attenuation of chlorinated solvent plumes and the plume management approach recommended for implementation at OU1:

1. Based on dissolved contaminant mass and center of mass estimates for the period from May 1994 through March 1997, the western plumes at OU1 appear to be collapsing in response to anaerobic dechlorination of TCE and its daughter products, and to a source area that has been "eliminated" by weathering and remedial activities at the site. The dissolved plume is no longer being supplied with fresh contaminant, and the assimilation rate appears greater than the flux rate of contaminant from the source area.

2. The dissolved mass data were used to estimate first order degradation rates for the chlorinated alkenes of interest at OU1. Results of these calculations indicated that contaminant half-lives

ranged from less than a year to nearly 5 years. As with many field sites, cis-DCE was the constituent with the lowest degradation rate, and the constituent that will control the length of time required to manage groundwater contamination at this site.

3. Free product samples collected in 1992, and groundwater concentrations measured in 1997 that were in equilibrium with free product do indicate that the source material from OU1 is highly weathered with respect to chlorinated alkenes, supporting conclusion number 1. Further analysis of the product via extraction/purge and trap methods should be conducted so that an adequate determination of current product composition can be made for long-term product weathering and remedial design purposes.

4. Predictions of the long-term behavior of dissolved contaminant plumes at OU1 were based on an extrapolation of contaminant degradation rates estimated from dissolved plume mass changes over time and the assumption that these degradation rates would be maintained over the lifetime of these plumes. cis-DCE remains the contaminant of interest with the longest time to reach PRGs, requiring approximately 30 years to reach clean-up goals of 70 µg/L from maximum 1997 concentration levels in the dissolved plume of 648 µg/L.

5. Electron acceptor concentration distribution observed throughout the site confirms the biological nature of contaminant attenuation at OU1. Rapid transformation to vinyl chloride is taking place immediately adjacent to the source area suggesting that the hydrocarbons identified in the source material are the source of electron donor driving the dechlorination process. Background TOC concentrations are relatively low, however, and a source of electron donor will need to be provided if the source area hydrocarbons are removed prior to the complete assimilation of the chlorinated solvent plume to prevent the growth and downgradient mobility of the western dissolved plume at OU1.

6. A 17 well long-term monitoring network was proposed for this site based on historical data and the current plume footprint. It is recommended that sampling for natural attenuation parameters (parent compound and intermediate product concentrations, electron acceptors, general water quality parameters, and electron donors) be conducted throughout this complete network every 2 years to provide both compliance monitoring data as well as natural attenuation process information necessary to verify that contaminant mass destruction and plume stability continue throughout the life of the plume.

7. It is recommended that plume management at the western plume at OU1 consist of monitored natural attenuation over the duration projected for the dissolved phase. Additional source removal in that area of OU1 is not required, and could in fact be detrimental to the long-term stability of

the chlorinated solvent plume that remains there if the source of electron donor keeping the aquifer reducing is removed.

If further source removal is regulatory driven, then an analysis of alternative electron donors that could be added to the site to sustain dechlorination reactions in the aquifer should be actively pursued. Evaluation of alternative electron donor sources may also be important in accelerating the rate of cis-DCE dechlorination in this dissolved plume. cis-DCE dechlorination is known to be the slowest step in the anaerobic transformation of PCE and TCE to CO_2 and water, and takes place only under sulfate reducing to methanogenic conditions. It may be possible to provide an alternative electron donor source upgradient of this plume at OU1 to drive more of the aquifer more reducing, increasing the volume of aquifer material that could support cis-DCE dechlorination. With an increase in the cis-DCE dechlorination rate, the required plume management time will be reduced, reducing the overall cost of plume monitoring and management required for the site.

References

1. Wiedemeier, T.H., J.T. Wilson, D.H. Kampbell, R.N. Miller, and J.E. Hansen. 1995. Technical protocol for implementing intrinsic remediation with long-term monitoring for natural attenuation of fuel contamination dissolved in groundwater. U.S. Air Force Center for Environmental Excellence, San Antonio, TX.

2. Wiedemeier, T.H., M.A. Swanson, D.E. Moutoux, J.T. Wilson, D.H. Kampbell, J.E. Hansen, and P.Haas. 1997. Overview of the Technical Protocol for Natural Attenuation of Chlorinated Aliphatic Hydrocarbons in Ground Water Under Development for the U.S. Air Force Center for Environmental Excellence. Presented in Proceedings of the Symposium on Natural Attenuation of Chlorinated Organics in Ground Water, EPA/540/R-97/504, U.S. EPA, ORD, Washington, D.C. pp. 37-61.

3. Remediation Technologies Development Forum. 1997. Natural Attenuation of Chlorinated Solvents in Groundwater: Principles and Practices. Prepared by the Industrial Members of the Bioremediation of Chlorinated Solvents Consortium of the RTDF. Beak International, Dow Chemical Company, DuPont Company, General Electric Company, Imperial Chemical Industries, Monsanto Company, Novartis, Zeneca Inc., Version 3.0, August.

4. Dupont, R. R. 1998. Natural Attenuation, In *Innovative Site Remediation Technology, Design & Application: Applied Bioremdiation*, R.R. Dupont, Bruell, Huling, Marley, Norris, and Pivetz, eds. American Academy of Environmental Engineering, Annapolis, MD.

5. Montgomery Watson. 1998. Draft. Statistical Evaluation of Baseline Concentrations for Operable Unit 1. Hill Air Force Base, Utah. Project Number 1166011.88180105. (April).

6. Parsons Engineering Science. 1998. Remediation by Natural Attenuation Treatability Study for Operable Unit 1 at Hill Air Force Base, Utah. Draft. Prepared for AFCEE Technology Transfer Division, Brooks AFB, San Antonio, TX.

7. Montgomery Watson. 1995. Comprehensive Remedial Investigation Report for Operable Unit 1, Hill Air Force Base, Utah. Volume 1. Final. Prepared for EMR, Hill AFB, Utah, Project No,. 2208.0991. (December).

8. Chow, V.T., D.R. Maidment, and L.W. Mays. 1988. *Applied Hydrology*. New York, NY: McGraw - Hill.

9. CH2M-Hill. 1998. Feasibility Study Report for Operable Unit 1 (IRP Sites LF01, LF03, WP02, FT09, OT14, FT81, and WP80). Final. Contract F42650-92-D-0006, Delivery Order 5043. Prepared for Environmental Management, Hill AFB, UT. (January).

A DEVICE FOR EXPERIMENTAL MEASUREMENTS OF
ELECTROSTATIC SHIELDING IN A SPATIALLY NON-UNIFORM PLASMA

C. Lon Enloe
Associate Professor
Integrated Science and Technology Program

James Madison University
MSC 4102
Harrisonburg, VA 22807

A DEVICE FOR EXPERIMENTAL MEASUREMENTS OF ELECTROSTATIC SHIELDING IN A SPATIALLY NON-UNIFORM PLASMA

C. Lon Enloe
Associate Professor
Integrated Science and Technology Program
James Madison University

Abstract

The effects of Debye shielding in a spatially non-uniform plasma are of interest in understanding wake charging phenomena associated with one low-Earth-orbiting spacecraft in the plasma wake of another. This report describes an apparatus for simulating this configuration in a laboratory-based experiment. A graded boom assembly is used to suspend one electrically-biased object behind another, while eliminating the perturbation caused by the boom to the electric fields in the wake region. A versatile set of plasma diagnostics, consisting of a segmented current-collecting probe with a built-in retarding potential analyzer and a hot-filament emissive probe allow the ion density, flow velocity, perpendicular and parallel temperatures, and the local space potential to be determined as the graded boom assembly is placed in a flowing plasma. An automated fitting routine used to determine the space potential is shown to be able to determine the space potential to within ±0.5 V. Comparisons of predicted and measured potential distributions along the graded boom are presented. Ambient and wake measurements of plasma parameters are given for a typical flowing plasma, in particular showing the effects of a finite-sized plasma source on the wake structure in the laboratory.

A DEVICE FOR EXPERIMENTAL MEASUREMENTS OF
ELECTROSTATIC SHIELDING IN A SPATIALLY NON-UNIFORM PLASMA

C. Lon Enloe

Introduction

A conducting body placed in a flowing plasma sets up a spatial non-uniformity in that plasma, the extent of which depends on the ratio of the flow speed to the thermal speeds of the plasma particles. Typically, because of their great disparity in mass, the thermal speeds of electrons and ions are greatly different in a plasma. This allows for the condition of flow speeds that are large compared to the thermal speeds of the ions, yet slow with respect to the thermal speeds of the electrons. Such is the case for a low-Earth-orbiting spacecraft. Assuming that the conducting body in this plasma stream is many Debye lengths across, it will create a highly perturbed wake structure—a void in the plasma ions that may extend downstream for many times the characteristic dimension of the body itself. The addition of another conducting body into this non-uniform plasma structure raises the issue of potential screening or electrostatic shielding in the plasma. In general, the second body in the wake will charge negatively, since it is initially in a region devoid of most ions. As it charges, however, it becomes more attractive to ions and more repulsive to electrons. The equilibrium conditions that determine its charge state are complicated by the non-uniform nature of the plasma in which it is immersed.

The process of plasma wake charging has been investigated numerous times, both experimentally, theoretically, and numerically. [1-8] Many of these studies lead toward one conclusion—plasma wake charging is limited by ion collection from the plasma stream, which in turn depends on how the attractive negative potential penetrates into the ambient flowing plasma. [5-8] Unfortunately, predicting this "potential scoop" can be numerically intense. This report describes an experiment designed to create in the laboratory a spatially non-uniform plasma wake structure, and then to measure the plasma properties of this wake structure and the electrostatic potential structure surrounding a biased object in this wake.

The main body of this report is a description suitable for the general reader. This report includes references to several appendices in addition to the main body. The appendices describe the "nuts and bolts" of the experimental hardware (connector pin-outs, detailed assembly instructions, etc.) that are not of interest not to the general reader, but that are critical to someone working with the experimental hardware. These are included in the copy of this report delivered to the Physics Department of the United States Air Force Academy, where this research was conducted, and are also available separately from the author.

Experimental Setup

The experimental apparatus consists of a test object and a set of diagnostics to determine the space potential and plasma parameters in the vicinity of the object, with associated software to run the experiment. The test object and diagnostics were operated in the 2 m diameter × 2 m long vacuum chamber at the Physics Department of the

United States Air Force Academy. This chamber included an ion gun in a three-grid Kaufman thruster configuration [9] that provided a flowing plasma with variable density and flow speed, essentially forming a "plasma wind tunnel."

Test Object

The test object, consisting of a circular disk to block the plasma flow and a biased sphere suspended behind the disk, was designed to simulate the case of one spacecraft in low Earth orbit following in the wake of another. Unlike the on-orbit case, in the laboratory it was necessary to use a mechanical boom to suspend the sphere behind the disk. So that the mechanical boom would not affect the electric fields in the plasma, however, the boom was designed so that the potential along its length varied to effectively mask its presence from the particles in the plasma.

The concept of a graded boom is shown in Figure 1. This Figure shows the equipotential contours (evenly spaced in voltage) surrounding a sphere biased with respect to a neighboring plate. The contours shown are for the case of the sphere and plate in vacuum. The presence of a plasma will in general change this potential structure—investigating this change is the central theme of this research—but in the region between the sphere and the plate the ions density will be low, as will the electron density, assuming a negatively biased sphere. Therefore, we may use the vacuum solution as a first-order approximation to the electrostatic potential in this region. If the boom can be made so that sections of it are biased at different potentials, and if those potentials are chosen so that they correspond to the potentials that would exist at that location in the absence of the boom, then from an electrical standpoint the boom will not change the local electric field. From an electrical standpoint, the boom would be invisible.
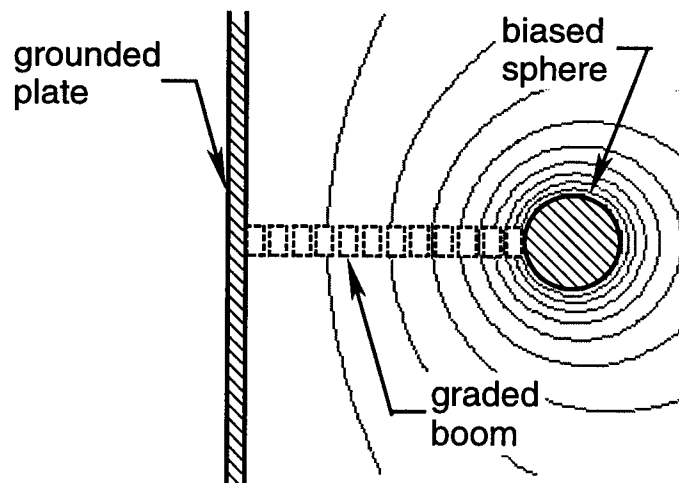
Figure 1. This figure illustrated the concept of a graded boom to suspend an electrically biased sphere in space. If different parts of the boom can be biased at different electrical potentials, those potentials can be chosen so that the boom has no influence on the local electric field.

The cross-section of such an "invisible" boom is shown in Figure 2. In the center of the boom is a solid conducting rod by which the sphere at the end of the boom is connected to the bias supply. An insulating sleeve surrounds this rod. A hollow tube surrounds the insulating sleeve, connected to the same bias supply, but on a different electrical circuit from the sphere. A second insulating sleeve surrounds this tube, and along this sleeve are stacked alternating pairs of conducting rings and resistive spacers. The resistive spacers form a resistive divider chain between the electrically biased end of the boom and the plate, so that each of the conducting rings is at a different electrical potential. The equivalent electrical schematic for the boom and sphere is shown in Figure 3. Because the return current path for the sphere alone is through the plasma, by measuring the current-voltage characteristics of the sphere we may correlate the expansion of the applied potential into the ambient plasma with its effects on the ions in the plasma stream.
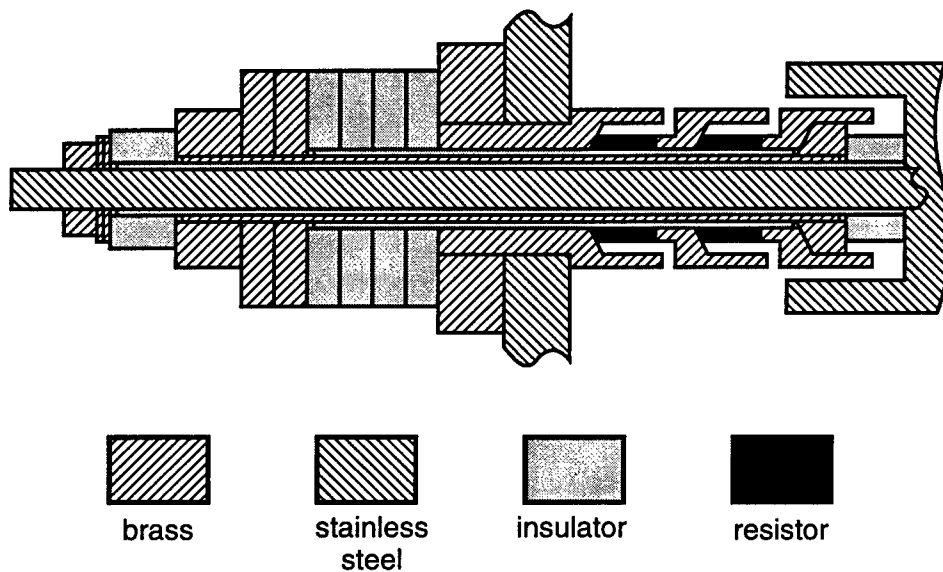
Figure 2. Cross-sectional view of the electrically graded boom used to suspend the sphere behind the disk.
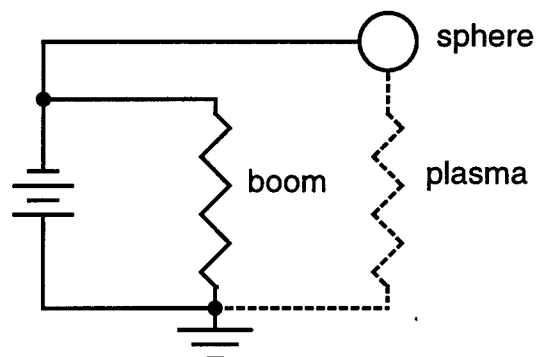
Figure 3. The equivalent electrical schematic for the boom and sphere includes two separate current paths, one of which is completed through the plasma.

As shown in Figure 1, the electrical potential naturally varies non-linearly between the plate and the sphere. Using the method of image charges, one can show that the potential Φ as a function of distance z (where $z = 0$ is the surface of the plate and $z = L$ is the base of the sphere) varies as

$$\phi(z, L, R) = \phi_0 \left(\frac{R}{L+R-z} - \frac{R}{L+R+z} \right)\left(1 + \frac{R}{2L} \right)$$

(1)

where R is the radius of the sphere, L is the separation of between the sphere and the plate (see Figure 4 for the geometry) and ϕ_0 is the potential on the sphere. This function is non-linear, and is shown in Figure 5. This non-linearity implies that the value of the resistance between each of the conducting rungs should be different. For simplicity's sake, a piecewise-linear approximation to the potential as a function of distance is used, so that the boom can be assembled with only two different resistor values. According to the length of the boom, the number of rings and spacers varies, along with the mixture of low-resistance (approximately 5 kΩ) and high-resistance (approximately 40 kΩ) spacers. The number of spacers and the optimum resistor configuration for boom lengths between 0.5 cm and 14.0 cm are given in Appendix A, along with assembly instructions for the boom. As an example, Figure 5 shows the ideal potential as a function of distance compared to the actual potential distribution achieved with the graded boom for the case of a 6-cm separation, which used 12 pairs of disks and spacers.

Figure 4. Geometry to calculate the potential on axis between a biased sphere and a plate, using the image charge method.

Figure 5. The ideal potential distribution between a biased sphere and a plate versus the potential distribution that was achieved with a graded boom using two different values of grading resistors.

Plasma Diagnostics

A set of plasma diagnostics was constructed to measure the plasma parameters in the vicinity of the test object. The diagnostics can be configured to measure either A) plasma potential, using an emissive probe, or B) the density, flow velocity, and parallel and perpendicular ion temperatures of the flowing plasma. The circuitry necessary to operate either of these configurations is housed in a single enclosure with associated power supplies, with the exception of high-voltage bias supplies, which are housed separately. The diagnostic system is under the control of a computer-based data acquisition system based around a National Instruments AT-MIO-16E board. Both configurations, including the necessary connections to the data acquisition system, are shown schematically in Figure 6.
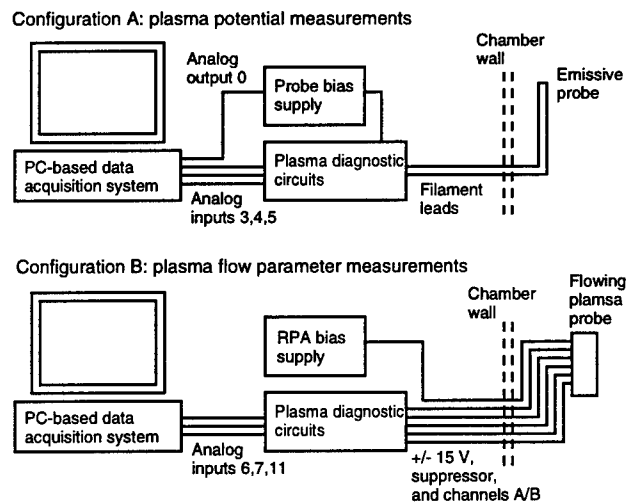
Figure 6. The plasmas diagnostics developed for this experiment could be configured in two ways, in order to diagnose the plasma potential or the density, flow velocity, and parallel and perpendicular ion temperatures.

4-7

Emissive Probe

Placing a hot, electron-emitting filament in a plasma is a common method of determining the electrostatic potential as a function of location within the plasma. [10-15] If the filament is biased to a given potential, the filament will start to emit electrons when the bias potential becomes more negative than the surrounding space potential—hence the common name for this type of diagnostic, the "emissive probe." Because the electrons leaving the probe have a certain distribution of energies, the transition from non-emission to emission is not sharp, so that various techniques have been developed to interpret the emitted current versus voltage characteristics in terms of the local space potential. [13-15] In this experiment, the "inflection point method" is used. [15]

The filament used in this experiment is 0.05 mm diameter tungsten, approximately 3 mm in length. The filament is spot-welded to nickel-wire leads housed in a ceramic tube, as shown in Figure 7. Two filaments are provided in the probe structure, so that if one breaks during a data take, the other may be used immediately without breaking vacuum. Filament currents in the range of 1.0-1.3 A are necessary to heat the filament to emission temperature. Typical electron emission as a function of bias potential is shown in Figure 8. In this case, the probe is located in vacuum between two electrically biased plates, at a space potential of approximately –5 V. As the figure shows, when the probe is biased more negatively that this, electron current is emitted, and in the neighborhood of this potential, the current is linearly proportional to the potential difference. Taking the derivative of this curve would identify two branches of this curve—one in which the slope was zero, and one in which the slope was some negative number. There would be an inflection point in the curve between the two branches, and this point is identified with the space potential of the plasma.

Figure 7. The emissive probe consists of a tungsten filament supported on nickel wire leads in a ceramic housing. Two filaments are available, although only one is used at a time, so that should one break the experiment may be continued without breaking vacuum for repairs.

Taking the derivative of experimental data numerically invariably amplifies any noise in the original data. In this case, we know the form of the derivative we are trying to match—two flat regions, with a transition between them. A convenient function of this form is

$$f(x) = \frac{2}{2 - \exp[-(x - x_0)]}$$ (2)

which commonly occurs in Fermi-Dirac statistics. The parameter x_0 is the midpoint between the two branches of the curve. Integrating this function, with appropriate constants, yields a function suitable to describe the current-voltage characteristics of an emissive probe,

$$I(V) = I_0 \left\{ b - V + \frac{\ln[1 + \exp a(V - b)]}{a} \right\}$$ (3)
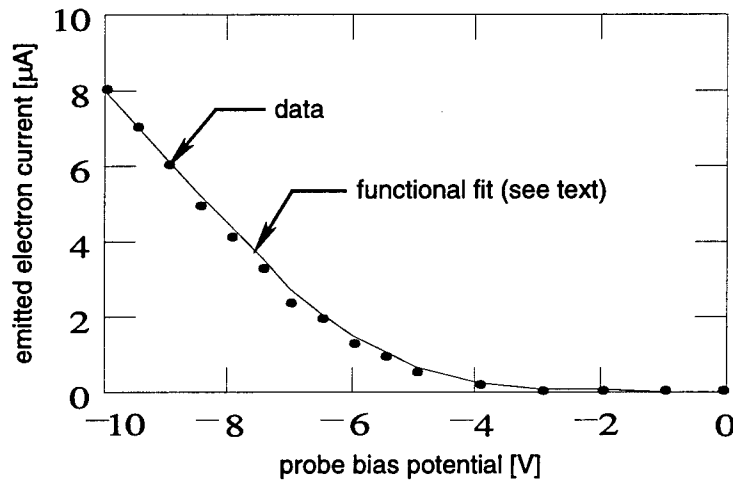
Figure 8. The electron emission from a heated filament placed in a plasma increases as the filament is biased more negatively than its surroundings. The point at which the electron emission begins to be significant in a measure of this space potential.

This function can be fit to the probe data using a non-linear fitting routine, and once the fit is obtained, the parameter b is a direct indication of the plasma potential. Using this technique, the emissive probe was calibrated by varying the space potential at the probe location, sweeping the probe bias potential, and fitting the data to Equation (3). The results show that the parameter b is a valid indication of the space potential, to an accuracy of approximately 0.5 V. This accuracy is consistent with similar results published in the literature. [14]
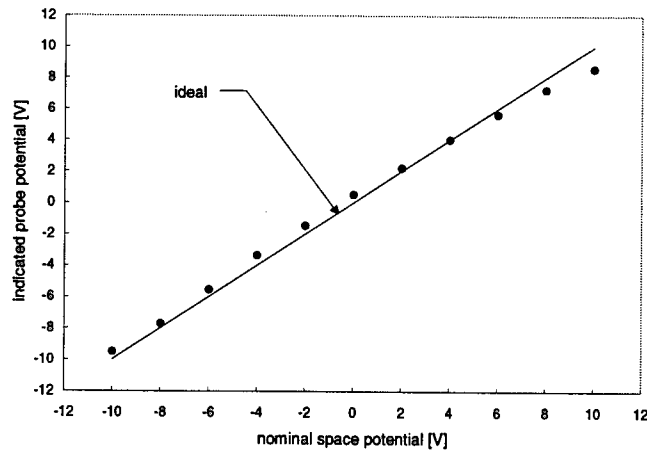
Figure 9. The parameter b obtained by fitting Equation x to the current-voltage curve for an emissive probe is a valid measure of the electrostatic potential at the location of the probe.

To generate the current-voltage curves for the emissive probe, the circuit shown in Figure 10 is used. Because one goal of this experiment is to measure plasma potential over a large range, the probe bias potential is measured using a calibrated voltage divider. The emission current is measured through a current-viewing resistor. Because this resistor floats with the bias potential of the probe, the voltage across it is measured with an isolation amplifier. It is desirable that the smallest electron emission that gives a measurable signal be used, in order to minimize the perturbation of the environment by the probe. A filament current sufficient to yield a signal from the current viewing resistor of 1.0 V (equivalent to an emission current of 10 μA) when the probe is biased –5 V with respect to its surroundings yields optimum results.
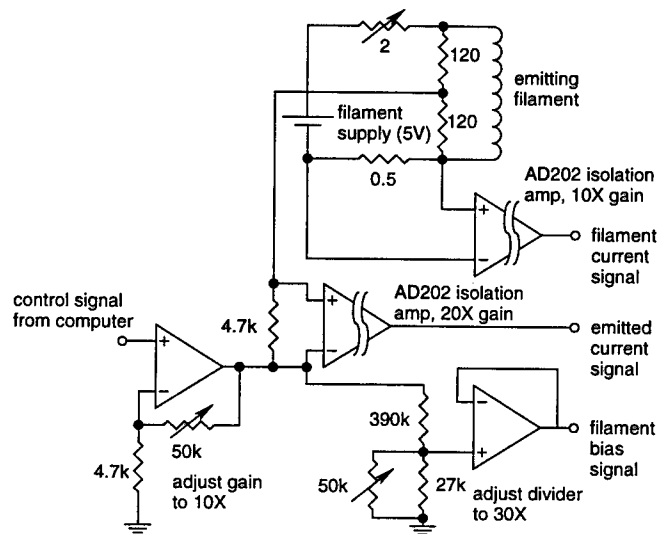
Figure 10. Schematic diagram of the circuit necessary to operate the emissive probe. The details of each of the circuit elements are given in Appendix B.

4-10

Flowing Plasma Probe

A single instrument was developed to determine the density, flow velocity, and parallel and perpendicular ion temperatures of the flowing plasma with and without the presence of the shielding disk. This instrument was based on the author's design for a high-resolution electrostatic analyzer. [16] A cross-section of the instrument is shown in Figure 11.
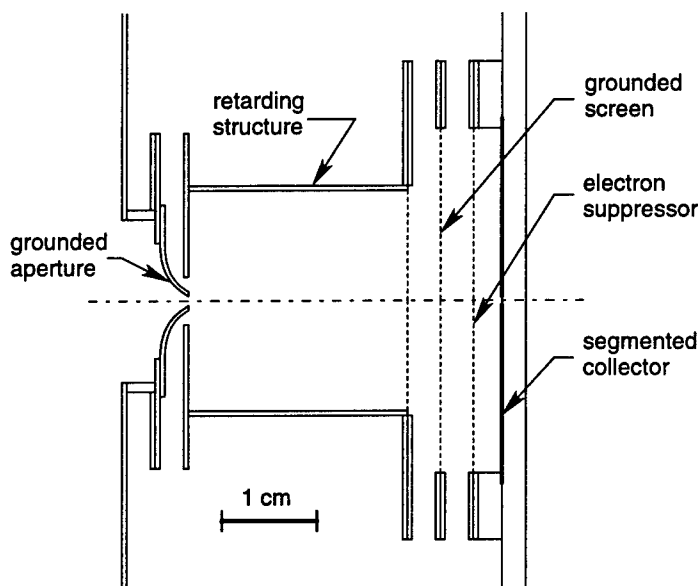
Figure 11. Cross-sectional view of the flowing plasma probe developed to analyze the density, flow velocity, and parallel and perpendicular ion temperatures in the flowing plasma.

In the flowing plasma probe, particles enter the retarding structure through a grounded aperture. The diameter of the aperture is 1.09 mm. The grounded aperture protrudes into the retarding structure, which is biased at the retarding potential Φ_R, through a hole in its front face. The back face of the retarding structures is a fine, transparent metal mesh. The equipotential contours within the retarding structure form nested quasi-spheres. [16] This electrostatic structure is positively biased to serve as an energy high-pass filter for ions, which must have an energy $E = q\Phi_R$ to pass through this filter, where q is the charge of the ion. A grounded mesh serves as an electrostatic barrier between the retarding structure and another mesh biased negatively. This negatively-biased mesh serves to reject electrons from the plasma, and to suppress the emission of secondary electrons, which might otherwise distort the ion current signal, from the collectors. Typically, -15 V is sufficient to suppress these electron populations. There are a total of three meshes, each 90% transparent, between the aperture and the collectors, so that the net transmission of the probe is $T = 0.7$. The collector is divided into two segments along a vertical line so that information about the ion velocity distribution perpendicular to the flow velocity can be obtained.

Ion currents to through the aperture are small (on the order of 1-10 nA), so to reduce noise amplifier circuitry is built into the flowing plasma probe itself. A schematic of the circuit for a single segment is shown in

Figure 12. The circuit consists of a current-to-voltage converted in series with an inverting amplifier with a gain of 270, giving a response of 0.27 V/nA for the probe. The flowing plasma probe is housed in a grounded aluminum box. The electrical connections to the circuit are given in Appendix C.
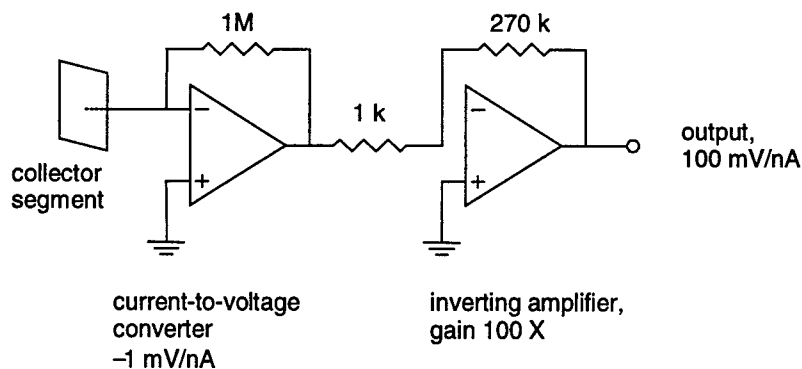
Figure 12. Current-to-voltage converter circuitry used in each channel of the flowing plasma probe.

The flowing plasma probe is inserted into the plasma stream as shown in Figure 13. The coordinates for this experiment are chosen so that the z-axis is in the nominal direction of the plasma flow, the x-axis is horizontal, and the y-axis is vertical. The probe is mounted on a movable table that provides linear motion in the x- and z-directions. In addition, the table can be turned. A clockwise rotation of the table is defined as a positive angle θ.
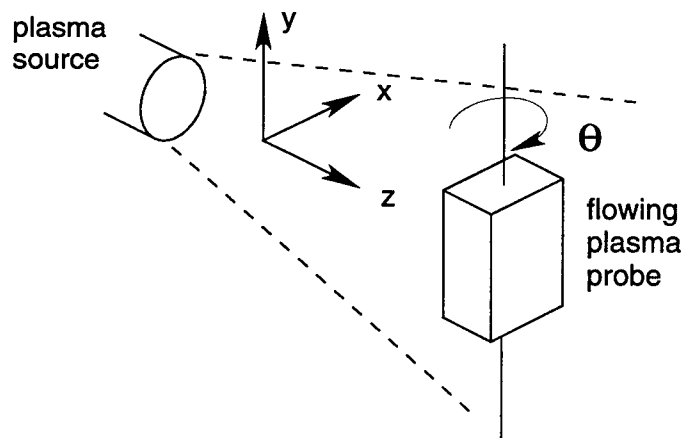
Figure 13. The flowing plasma probe is inserted in the plasma stream. It can be moved linearly in the x-z plane, and can be rotated around its vertical axis.

Control Software

The data acquisition tasks for this experiment are controlled using a computer program written in the National Instruments' "G" language for LabVIEW. The "front panel" (e.g., the user interface) is shown in Figure 14. The software controls the translation/rotation stage inside the vacuum chamber as well as the data acquisition card. The probe (either the emissive or flowing plasma probe) can be moved to a desired location and data acquired at that location. The data can then be saved internally to the program and written permanently to a data file. The details of the "G" code for the control program are given in Appendix D.
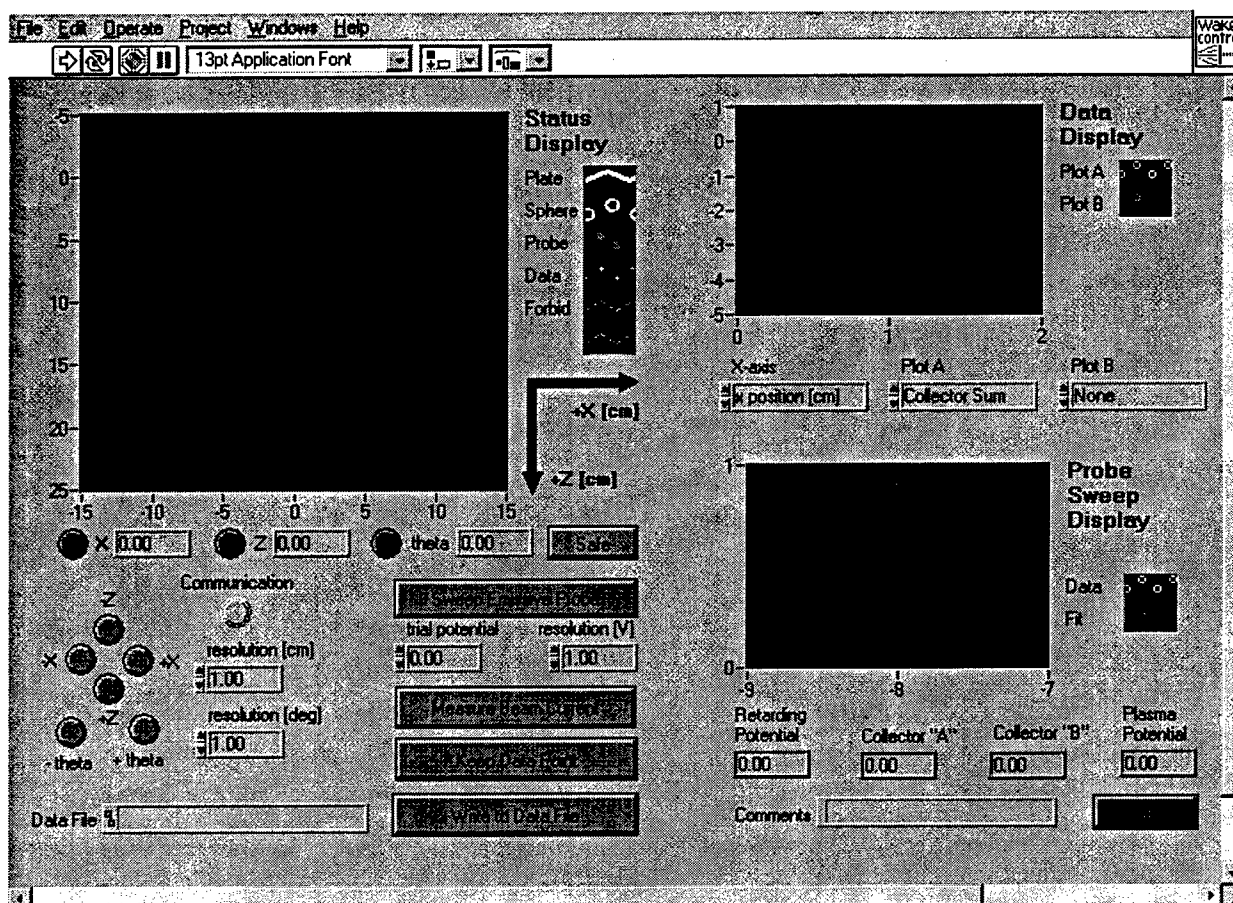
Figure 14. User interface for the software used to take data for the experiment. The control software allows the operator to move the probe (emissive probe or flowing plasma probe) to the desired location and angular orientation, and then to take data from the probe. Data points are stored internally and may be saved to a data file in ASCII format.

Plasma Measurements

Data taken with the flowing plasma probe indicate that a spatially highly non-uniform plasma structure is formed in the wake of the plate, in contrast to a highly uniform plasma upstream of the plate. The ion density, parallel ion temperature, perpendicular ion temperature, and flow velocity can all be determined from the flowing plasma probe.

Retarding Potential Analyzer Measurements

Operating the flowing plasma probe in the mode of a retarding potential analyzer (RPA) establishes the flow velocity of the plasma, which is critical in subsequently determining the density and perpendicular temperature from the probe data. The electric field inside the positively-biased retarding structure (see Figure 11) acts to repel (or "retard") positively-charged plasma ions. Particles can pass through this structure only if they have enough kinetic energy; that is, if

$$\frac{1}{2}mv_z^2 \geq q\Phi_R \qquad (4)$$

where q is the magnitude of the charge of the ion (assumed in this case to be the elementary charge e), m is the ion's mass, v_z is the speed of the ion parallel to the axis of the detector, and Φ_R is the magnitude of the potential applied to the retarding structure.

The output of an RPA can be found from the velocity distribution by integrating the distribution starting with the lowest-velocity particles that can pass the screens and continuing out to infinity. If the distribution is unknown, the procedure is to *differentiate* the RPA output to get the velocity distribution. This works well in theory but in practice is very sensitive to noise. Often a better way to get the distribution is to assume its form and fit the output of the RPA to this form using several parameters. For example, a useful model for ions flowing past a spacecraft is to approximate their parallel velocity distribution as a drifted Maxwellian, given by

$$f(v_z) = \left(\frac{m}{2\pi k T_\parallel}\right)^{\frac{1}{2}} \exp\left[-\frac{m(v_z - v_0)^2}{2kT_\parallel}\right] \qquad (5)$$

where $T_\parallel$ is the parallel temperature of the plasma and v_0 is its flow velocity. Because the RPA is an energy filter, the distribution that really matters is the parallel *energy* distribution, given by

$$f(E) = \sqrt{\frac{1}{4\pi k T_\parallel}} \sqrt{\frac{1}{E}} \exp\left(-\frac{E - 2\sqrt{E_0 E} + E_0}{kT}\right) \qquad (6)$$

where $E_0 = mv_0^2/2$. Using this, the response of an RPA to a drifted Maxwellian input as a function of the retarding potential is given by

$$I(e\Phi_R) = \frac{I_0}{2}\left[1 - erf\left(\frac{\sqrt{e\Phi_R} - \sqrt{e\Phi_0}}{\sqrt{kT}}\right)\right] \qquad (7)$$

where $e\Phi_0 = E_0$, the flow energy, $kT_{\parallel}$ is the parallel temperature of the plasma in energy units, and I_0 is the maximum amount of collected current, which depends on the plasma density, the flow velocity, and the size of the detector aperture. This is well-defined, but clearly non-linear, function can be fitted to the probe data using standard non-linear fitting routines. The result of such a fit are shown in Figure 15. For these data, the nominal beam voltage is 300 V, and the beam current extracted from the source is 10 mA. The data show that the actual flow energy of the beam is $e\Phi_0 = 300$ eV, which gives a flow velocity of $v_0 = 38$ km/s. The parallel temperature of the plasma is $kT_{\parallel} = 0.0095$ eV, which is typical for such ion sources.
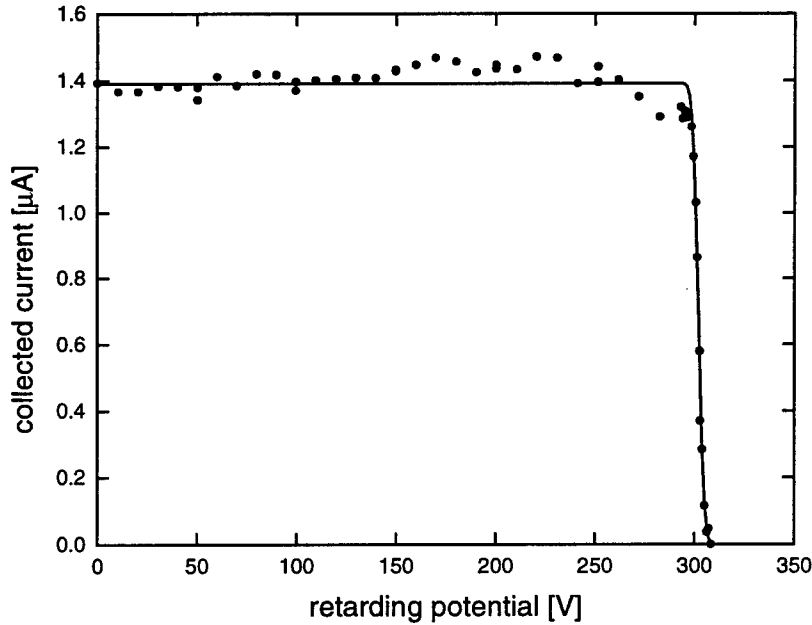
Figure 15. Data from the flowing plasma probe operating in retarding potential analyzer (RPA) mode indicates a beam energy of $e\Phi_0 = 302$ eV (corresponding to a flow velocity of $v_0 = 38$ km/s) and a parallel temperature of $kT_{\parallel} = 0.0095$ eV.

Density Measurements

Once the flow velocity has been established, the plasma density can be determined from the maximum (un-retarded) current I_0 to the flowing plasma probe, along with the probe aperture. The current to the probe is just

$$I_0 = nev_0A \tag{8}$$

where n is the plasma density and A is the cross-sectional area of the probe aperture. The current of $I_0 = 1.4\,\mu\mathrm{A}$ into an aperture area of $A = 9.3 \times 10^{-7}\,\mathrm{m}^2$ gives an unperturbed plasma density for this configuration of $n = 2.5 \times 10^8\,\mathrm{cm}^{-3}$. A scan of the plasma in the x-direction (from one side of the disk to the other, see Figure 13) upstream of the disk shows that the unperturbed plasma density is constant to approximately $\pm 5\%$ across the 30-cm wide area of interest in the vicinity of the disk.

Perpendicular Temperature Measurements

Because of the high flow velocity of the plasma, the motion of the plasma ion will be primarily downstream, in the $+z$ direction. The ions will leave the source, however, with a perpendicular component of velocity. The perpendicular velocity distribution can be diagnosed by rotating the flowing plasma probe and observing the current as it passes from one of the segments of the collector to the other. Which segment any ion will fall on depends on the ion's perpendicular velocity and the orientation of the flowing plasma probe. This situation is illustrated in Figure 16.
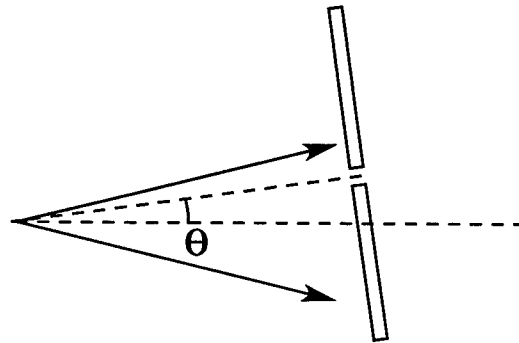
Figure 16. Current to each segment of the collector of the flowing plasma probe depends on the perpendicular velocity distribution of the ions, and the orientation of the probe.

By rotating the flowing plasma probe, we can determine the perpendicular velocity distribution in one direction, so we will assume that the one-dimensional perpendicular velocity distribution is a Maxwellian, so that

$$f(v_x) = \left(\frac{m}{2\pi k T_\perp}\right)^{\frac{1}{2}} \exp\left(-\frac{m v_x^2}{2 k T_\perp}\right). \tag{9}$$

From Figure 16, we see that the relationship between the perpendicular and parallel velocities for any ion (assuming the small angle approximation) is $v_x = v_0 \theta$, so that $dv_x = v_0 d\theta$. The relative amount of current I/I_0 that a segment collects can be determined by integrating the perpendicular velocity distribution up to that velocity v_{0x} that corresponds to the position of the plate separation, so that

$$\frac{I(v_{0x})}{I_0} = \left(\frac{m}{2\pi k T_\perp}\right)^{\frac{1}{2}} \int_{-\infty}^{v_{0x}} \exp\left(-\frac{m v_x^2}{2 k T_\perp}\right) dv_x. \tag{10}$$

In terms of the angle of the detector, this corresponds to

$$\frac{I(\theta)}{I_0} = \left(\frac{m}{2\pi k T_\perp}\right)^{\frac{1}{2}} v_0 \int_{-\infty}^{\theta} \exp\left(-\frac{m v_0^2 \theta^2}{2 k T_\perp}\right) d\theta. \tag{11}$$

We can simplify this expression by introducing the perpendicular thermal velocity

$$v_{th,\perp} = \left(\frac{2 k T_\perp}{m}\right)^{\frac{1}{2}} \tag{12}$$

and defining the variable (a type of Mach number)

$$M = \frac{v_0}{v_{th,\perp}} \tag{13}$$

so that Equation (11) becomes

$$\frac{I(\theta)}{I_0} = \frac{1}{\sqrt{\pi}} \left(\frac{v_0}{v_{th,\perp}}\right) \int_{-\infty}^{\theta} \exp\left(-\frac{v_0^2 \theta^2}{v_{th,\perp}^2}\right) d\theta$$
$$= \frac{M}{\sqrt{\pi}} \int_{-\infty}^{\theta} \exp\left(-M^2 \theta^2\right) d\theta \tag{14}$$

Performing the integral yields another non-linear function,

$$\frac{I(\theta)}{I_0} = \frac{1}{2}\left[\mathrm{erf}(M\theta)+1\right]$$ (15)

that can be fitted using non-linear techniques to the experimental data. Once M is determined, the perpendicular temperature $kT_\perp$ can be determined, and is given by

$$kT_\perp = \frac{mv_0^2}{2M^2}.$$ (16)

Data from an angular scan of the flowing plasma probe is shown in Figure 17. The from the fit to these data and the value of v_0 found previously, we find that the perpendicular temperature is $kT_\perp = 0.27\,\mathrm{eV}$. The finding that $T_\perp \gg T_{\parallel}$ is driven by the perpendicular component of acceleration ions receive in the plasma source. [9]
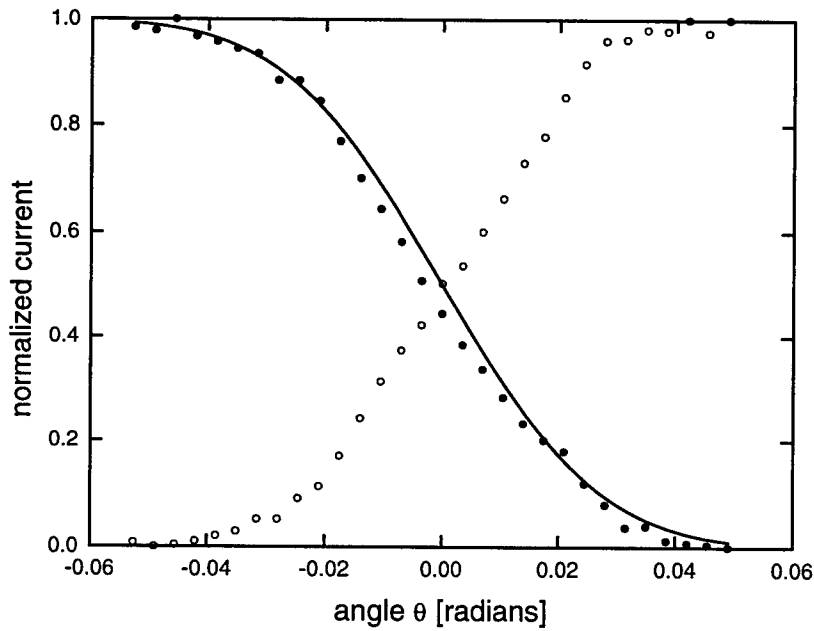
Figure 17. The shift of current from one segment(solid circles) to another (hollow circles) as the flowing plasma probe is rotated in the flowing plasma indicates the perpendicular temperature of the plasma. In this case, this value is $kT_\perp = 0.27\,\mathrm{eV}$.

The flowing plasma probe was scanned throughout the wake region to map the plasma density as a function of position. The results indicate a sharp transition between the wake and the ambient densities. A detailed scan of the wake edge is shown in Figure 18, which give a close-up, cross-sectional slice of the plasma wake edge. These results indicate the effect of the finite source on the wake geometry. There is a relative shallow density gradient from x = 9.5 cm to x = 10.5 cm, at which point the plasma is at its ambient density. The gradient inboard of the 9.5 cm location is extremely steep. This is because the source of the ions, approximately 1 m upstream, is a smaller diameter than the shielding disk. Because the plasma is to a large degree collisionless, ions stream outward from the source. There are essentially no particles with a component of velocity pointing into the wake from the ambient. Therefore, the wake does not fill, and the transition from plasma to wake is sharp. The deep wake structure is equivalent to the umbra of the shadow cast by an extended light source, while the transition to ambient density outboard of this is equivalent to the penumbra. This is a distinctly different structure than that of an object immersed in an infinite plasma, or at least of one originating at a source larger than itself, in which case the wake would tend to fill in downstream of the shadowing body.
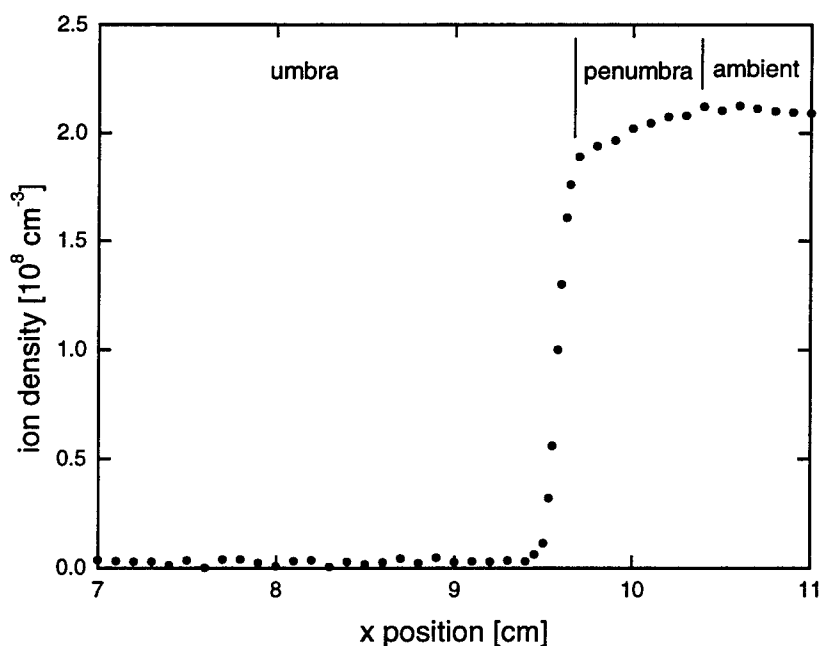
Figure 18. Detail of the wake edge, taken at a distance of 12 cm behind the disk. The transition into the deep wake is sharp because in the laboratory setting, the size of the plasma source is smaller than the shadowing disk.

Summary

It is possible to produce a plasma with a high degree of spatial non-uniformity in the laboratory by flowing the plasma around a shadowing body, thus creating a plasma wake structure. It is further possible to suspend an electrically charged body in this plasma wake by means of an electrically graded structure whose presence minimally perturbs the electric potential in the wake, effectively making the structure invisible to charged particle interactions. It is straightforward to diagnose the ambient and wake plasma parameters using a segmented, current-collecting probe in conjunction with an emissive probe. It is important to realize that a laboratory-produced plasma wake has a significantly different structure from that produced by a body traversing an effectively infinite plasma, such as a satellite on orbit. Nevertheless, a laboratory-produced wake plasma is suitable to test the penetration of electric potentials in a highly spatially non-uniform environment.

References

1. D. E. Hastings, "A review of plasma interactions with spacecraft in low Earth orbit," *J. Geophys. Res.* **100**, 14457-83 (1995).

2. C. L. Enloe, D. L. Cooke, S. Meassick, C. Chan, and M. F. Tautz, "Ion collection in a spacecraft wake: laboratory simulations," *J. Geophys. Res.* **98**, 13635-44 (1993).

3. C. L. Enloe, D. L. Cooke, W. A. Pakula, M. D. Violet, D. A. hardy, C. B. Chaplin, R. K. Kirkwood, M. F. Tautz, N. Bonito, C. Roth, G. Courtney, V. A. Davis, M. J. Mandell, G. B. Shaw, G. B. Giffin, and R. M. Sega, "High-voltage interactions in plasma wakes: Results from the charging hazards and wake studies (CHAWS) flight experiment," *J. Geophys. Res.* **102**, 425-33 (1997).

4. C. L. Enloe, J. T. Bell, D. L. Cooke, D. A. Hardy, R. K. Kirkwod, J. W. R. Lloyd, and M. D. Violet, "The charging hazards and wake studies (CHAWS) experiment," *Rep. AIAA 95-0892,* Am. Inst. of Aeronaut. and Astronaut., Washington, DC (1995).

5. V. A. Davis, M. J. Mandell, D. L. Cooke, and C. L. Enloe, "High-voltage interactions in plasma wakes: simulation and flight measurements from the charging hazards and wake studies (CHAWS) experiment," in review.

6. G. B. Giffin, D. E. Hastings, G. B. Shaw, D. L. Cooke, M. D. Violet, C. L. Enloe, and W. A. Pakula, "A general model for use in LEO high-voltage spacecraft wake engineering," in review.

7. M. J. Mandell, V. A. Davis, D. L. Cooke, M. D. Violet, and C. L. Enloe, "CHAWS wake-side current measurements: comparison with preflight predictions," *Rep. AIAA 95-0489*, Am. Inst. of Aeronaut. and Astronaut., Washington, DC (1995).

8. D.L. Cooke, W. A. Pakula, V. A. Davis, M. J. Mandell, M. F. Tautz, and C. L. Enloe, "Measurement and simulation of high-voltage wake interactions," 1996 IEEE International Conference on Plasma Science.

9. R. G. Jahn, Physics of Electric Propulsion (New York: McGraw Hill, 1968) pp. 143-195.

10. N. Hershkowitz, B. Nelson, J. Pew, and D. Gates, "Self-emissive probes," *Rev. Sci. Instrum.* **54**, 29-34 (1983).

11. M. H.Cho, C. Chan, N. Hershkowitz, and T. Intrator, "Measurement of vacuum space potential by an emissive probe," *Rev. Sci. Instrum.* **55**, 631-632 (1984).

NEURAL NETWORK CONTROL OF WIND TUNNELS
FOR CYCLE TIME REDUCTION

Mark R. Fisher
Assistant Professor
Department of Mechanical Engineering Technology

Southern Polytechnic State University
1100 South Marietta Parkway
Marietta, Georgia 30060-2896

NEURAL NETWORK CONTROL OF WIND TUNNELS FOR CYCLE TIME REDUCTION

Mark R. Fisher
Assistant Professor
Department of Mechanical Engineering Technology
Southern Polytechnic State University

Abstract

Simulation results are given which compare a standard controller and a neural network controller that hold Mach and Reynolds number in a generic wind tunnel model. Results show that the neural network controller reduces Mach number IAE [1] error by 58% and reduces settling time [2] by 29%. These performance improvements mean that desired test conditions can be reached quicker, and therefore the neural network controller can provide higher quality test conditions and reduce testing costs as compared to a standard controller.

NEURAL NETWORK CONTROL OF WIND TUNNELS FOR CYCLE TIME REDUCTION

Mark R. Fisher

Introduction

This paper describes how a neural network offers a practical way to more quickly reach the next test condition in a wind tunnel. The principles of neural network control in this work can also be applied to other projects. This research supports the Technology Project Plan, Job 3912, Phase 2, "Real-Time Optimal Control of Wind Tunnels for Cycle Time Reduction," by Sverdrup Technology and AFOSR.

The Problem: Cycle Time Reduction

Cost savings can be achieved during wind tunnel testing by reducing the time to change from one test condition to another.

Wind tunnels now use a standard feedback control system, which can not produce optimal control for all test conditions and models. The standard controller can be optimized for only one test condition. A crude attempt to get around the problem is to use a table lookup of controller gains as a function of Mach number. However, this method does not take into account other variables. These variables, such as the type of model being tested or its angle of attack, have a profound impact on wind tunnel response.

Because several factors affect the wind tunnel response, a tool is needed that can process several input factors simultaneously. A neural network can easily process several inputs, and so it is ideally suited to help solve the problem of time reduction between test conditions.

The Solution: Neural Network Controller

Figure 1 shows simulation results between a standard controller and neural network controller during transition from Mach number 0.65 to 0.85. The standard controller was optimally tuned for an empty wind tunnel that contained no model. Then a test article model was put in the tunnel and performance was compared between the neural network and standard controller. The following table shows data from figure one used to compute two performance parameters to compare the controllers. The first parameter is settling

time [1] and the second is the integral of the absolute magnitude of error (IAE) [2]. The settling time is the time for the error to drop within 0.00016 of the desired Mach number. The table below shows the settling time for the neural network controller is 11.3 seconds, and the settling time for the standard controller is 15.9 seconds. Thus, the neural net controller reduced settling time by 29%. The IAE error is the sum of the errors at all times. The IAE error for the neural network is 0.00309, and the IAE error for the standard controller is 0.00733. Therefore, the neural network reduces IAE error by 58%.

Time ellapsed from the commanded Mach number change time	Standard Controller Mach	Standard Controller Error	Neural Network Controller Mach	Neural Network Controller Error
6.7	0.85634	0.00634	0.85282	0.00282
11.3	0.84931	0.00069	0.84985	0.00015 (value at settling time)
15.9	0.85016	0.00016 (value at settling time)	0.84989	0.00011
20.6	0.849864	0.00014	0.850005	0.000005
		IAE error = 0.00733		IAE error = 0.00309

Table 1. Standard Controller vs. Neural Network Controller Error

The neural network performs better for the following two reasons.

Reason 1: Ability to Process More Inputs

The standard controller gain shown in figure 2 can only be multiplied by one input. On the other hand, the neural network controller can process any number of inputs. In this simulation, three inputs to the neural network were selected; although more could have been done. Figure 3 shows the inputs were desired test section Mach number, desired test section Reynolds number, and model angle of attack. Multiple inputs make the result from the neural network more accurate over a wider range of test conditions because it can process more factors affecting those test conditions.

Reason 2: Predictive Rather Than Totally Reactionary

The neural network control system speed is limited only by the mechanical speed of the control devices in the wind tunnel because the neural network controller is predictive. The neural network controller immediately outputs final control positions to achieve desired test conditions. On the other hand, the standard feedback controller can not do this. The standard controller must continually readjust its control commands as it approaches desired test conditions, which makes it slower.

Because the neural network controller bases its output only on desired test conditions, it is immune to pressure wave disturbances that fluctuate Mach number during a change in compressor inlet guide vane angle. However, the standard feedback controller is forced to react to these disturbances in Mach number which leads to unnecessary control adjustments.

Neural Network Design

The neural network for Mach number control is shown in figure 4. A sigmoid activation function was used in the neural network. [3] Inputs were scaled between zero and one to make training of the neural network more efficient. [4] Standard back-propagation training was done using 5000 presentations of 990 training cases.

Adjustment Scheme

Although the neural network is faster and more accurate than a standard controller, it is not perfect. As shown in figure 2, the neural network controller initially produced a Mach number of 0.8528 when Mach 0.85 was desired. In order to compensate for this imperfection, adjusted Mach number is computed and subsequently input into the neural network as shown in figure 3. The equation for adjusted Mach number is also shown in figure 3. The adjustment equation computes a ratio of desired Mach number divided by actual Mach number. The ratio is then multiplied times the existing adjusted Mach number. Adjusted Mach number is initialized to the desired Mach number. This equation is extremely effective at homing in on the desired test condition. As shown in figure one and table one, the Mach number is only 0.00015 away from a perfect test value on the second calculation. Usually an accuracy of 0.0005 in Mach number is

acceptable. The adjustment equation is not applied when commanded position exceeds the mechanical limits of the IGVs in order to avoid unnecessary adjustments induced by equipment limits rather than neural network accuracy.

Reynolds Number Control

A neural network similar to that shown in figure 4 was used to control Reynolds number. Although the neural network immediately commanded the correct total pressure needed for a desired Reynolds number, performance was not improved over a standard controller because the ability of the wind tunnel to pressurize is a limiting factor. In contrast, Mach number control is improved because the inlet guide vanes on the compressor move fast enough to respond to a more rapid neural network controller. It is anticipated that if a wind tunnel is equipped with finger flaps, desired Mach number can be attained even faster with a neural network controller due to the rapid change in Mach number caused by finger flaps.

Wind Tunnel Simulation Model

A wind tunnel simulation was written for this study using Saad's 1-D compressible flow equations. [5] The C++ simulation program can be requested from Dr. Frank Steinle, Sverdrup Technology. Work for phase 3 will use a more complex wind tunnel model which captures pressure wave effects on Mach number as IGV angle changes.

Future Plans to Integrate a Genetic Algorithm with the Neural Network

As an actual wind tunnel test progresses, new data will be obtained which can be used to retrain the neural network. Current training methods are so time consuming that training must be done offline. Therefore, a genetic algorithm is being developed to retrain the neural network using the new data. It is hoped that the genetic algorithm will compute new weights and thresholds in the neural network rapidly enough so that retraining will not have to be done offline. This would allow the neural network to be updated with the latest information so as to perform as efficiently as possible.

Conclusions

Multiple wind tunnel parameters have been successfully processed by a neural network, resulting in improved speed and accuracy over a standard controller in reaching the next Mach number. The second calculation made by the neural network controller reaches accuracy well within acceptable limits. The speed of this controller is limited only by the physical limits of the controlled equipment, such as IGVs or pressurization pumps. Because the wind tunnel pressurizes slowly due to pump limits, a neural network controller can not physically make the wind tunnel achieve a total pressure for a desired Reynolds number any faster than a standard controller.

Our current wind tunnel model does not respond dynamically with an inherent unsteadiness of Mach number. A better wind tunnel model, as planned for phase 3, will have an inherent unsteadiness. The genetic algorithm coupled with the fast response from a neural network may well improve the control of unsteadiness.

Neural Network vs. Standard Controller
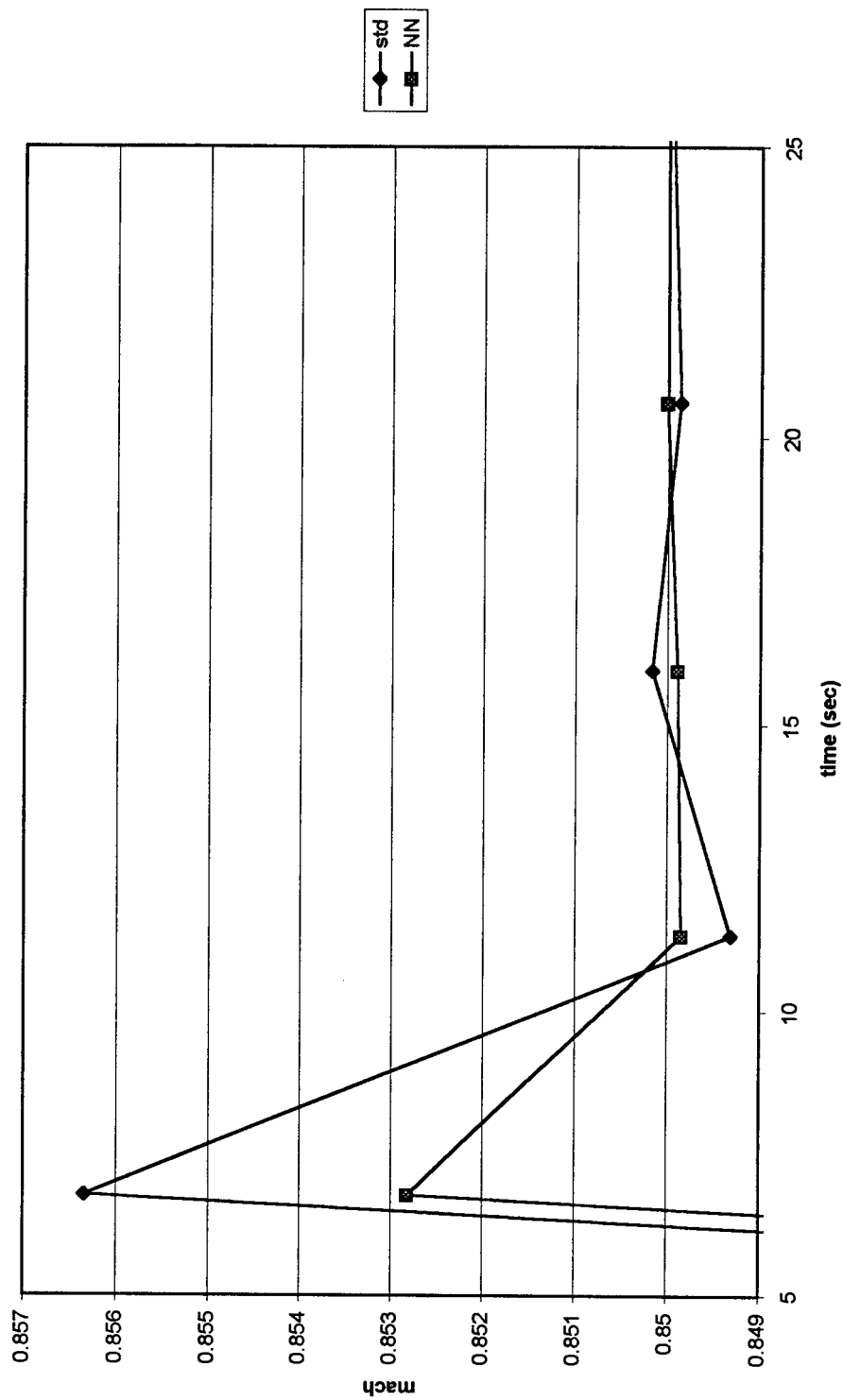
Fig. 1 Neural Network vs. Standard Controller

Fig. 2 Standard Feedback Controller

Fig. 3 Neural Network Controller

The diagram contains the following labels:

Desired mach

adjusted mach = (desired mach / actual mach) * adjusted mach

△1 △2

actual mach

adjusted mach

Neural network

Desired Reynold's number

Model angle of attack

Pressure ratio

wind tunnel
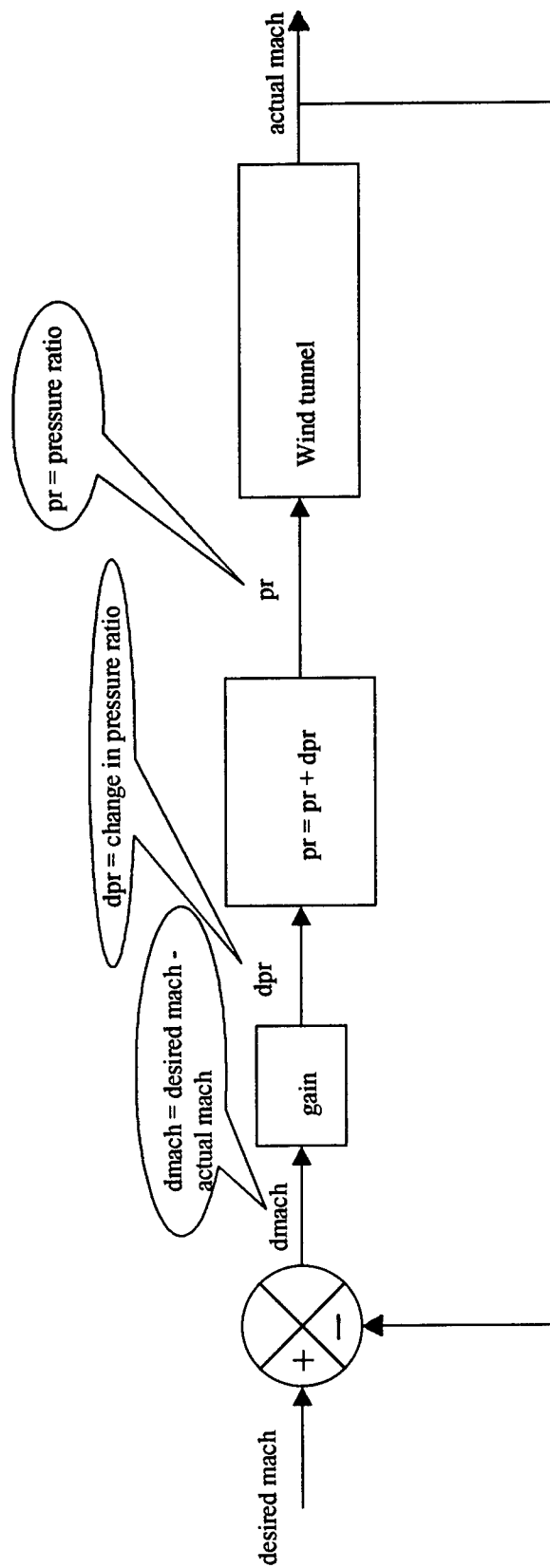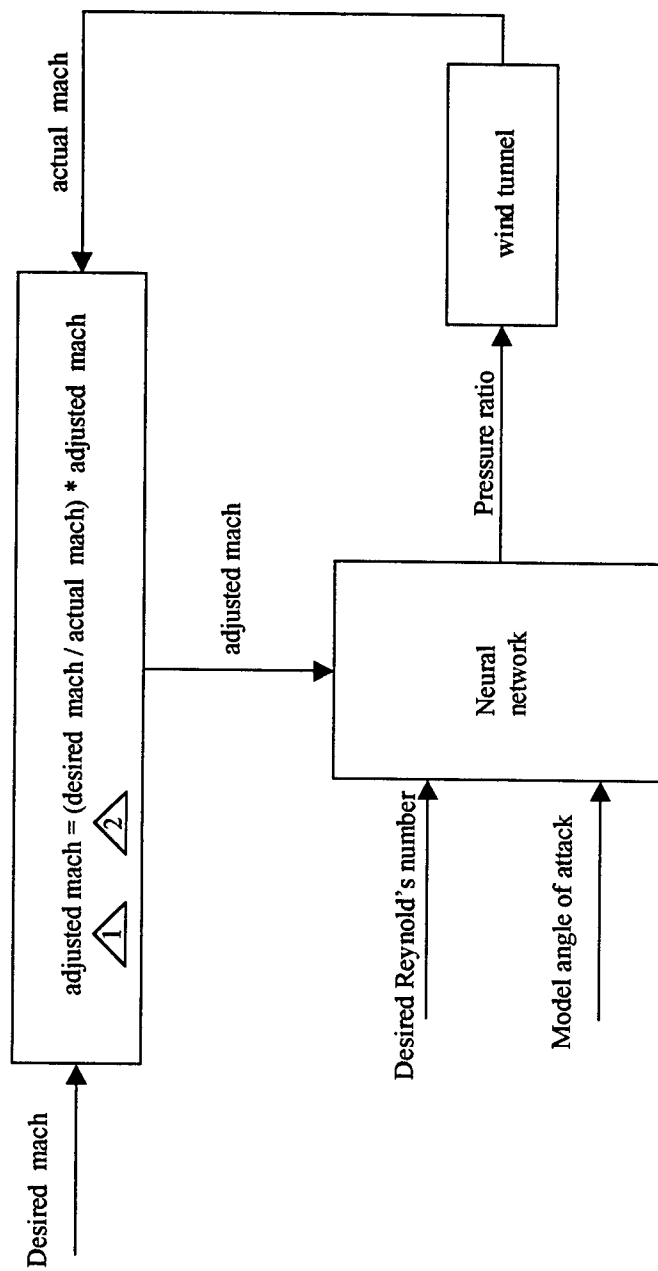
△1 This equation only applies when the commanded pressure ratio = actual pressure ratio in order to avoid adjustments when commands are limited due to mechanical limits.

△2 Adjusted mach is initialized to desired mach.
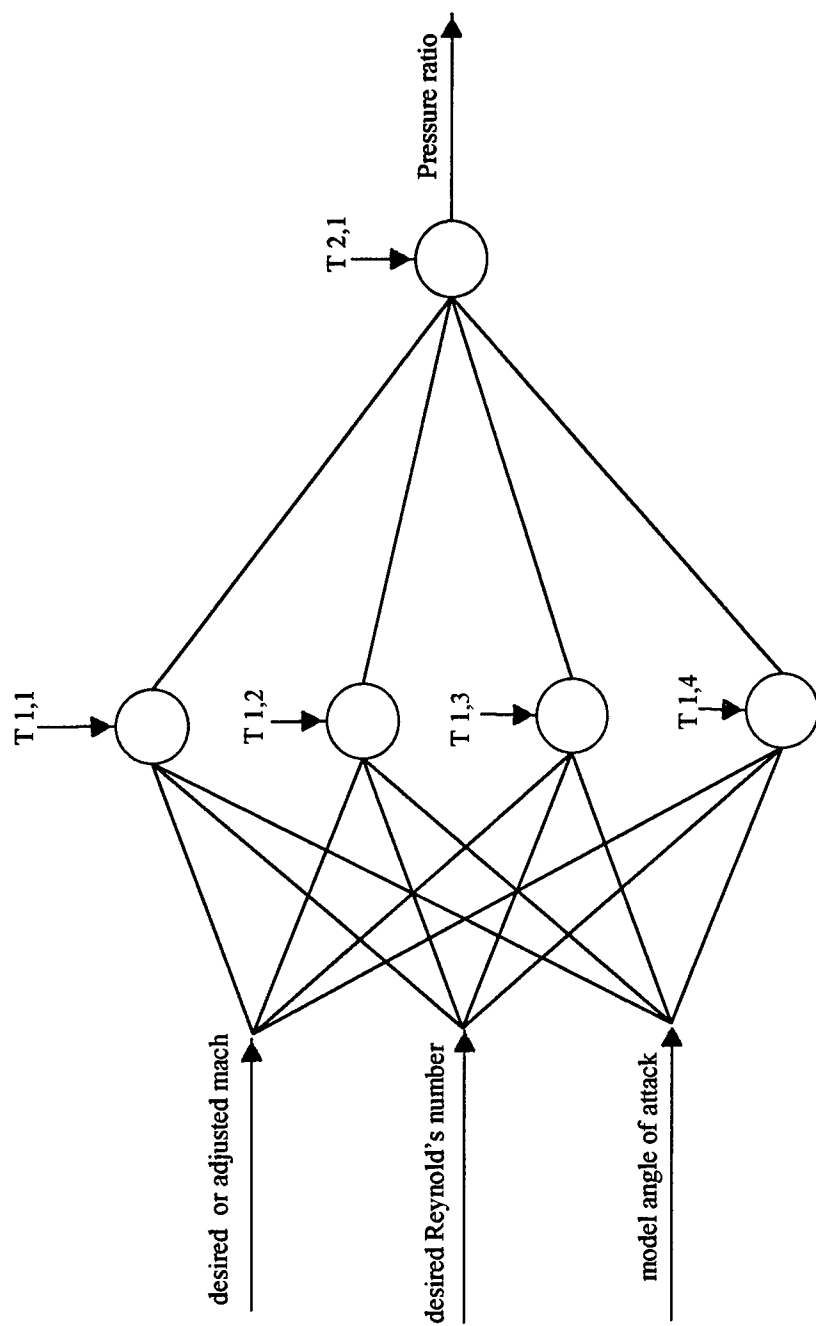
Fig. 4 Neural Network Structure for Mach Number Control
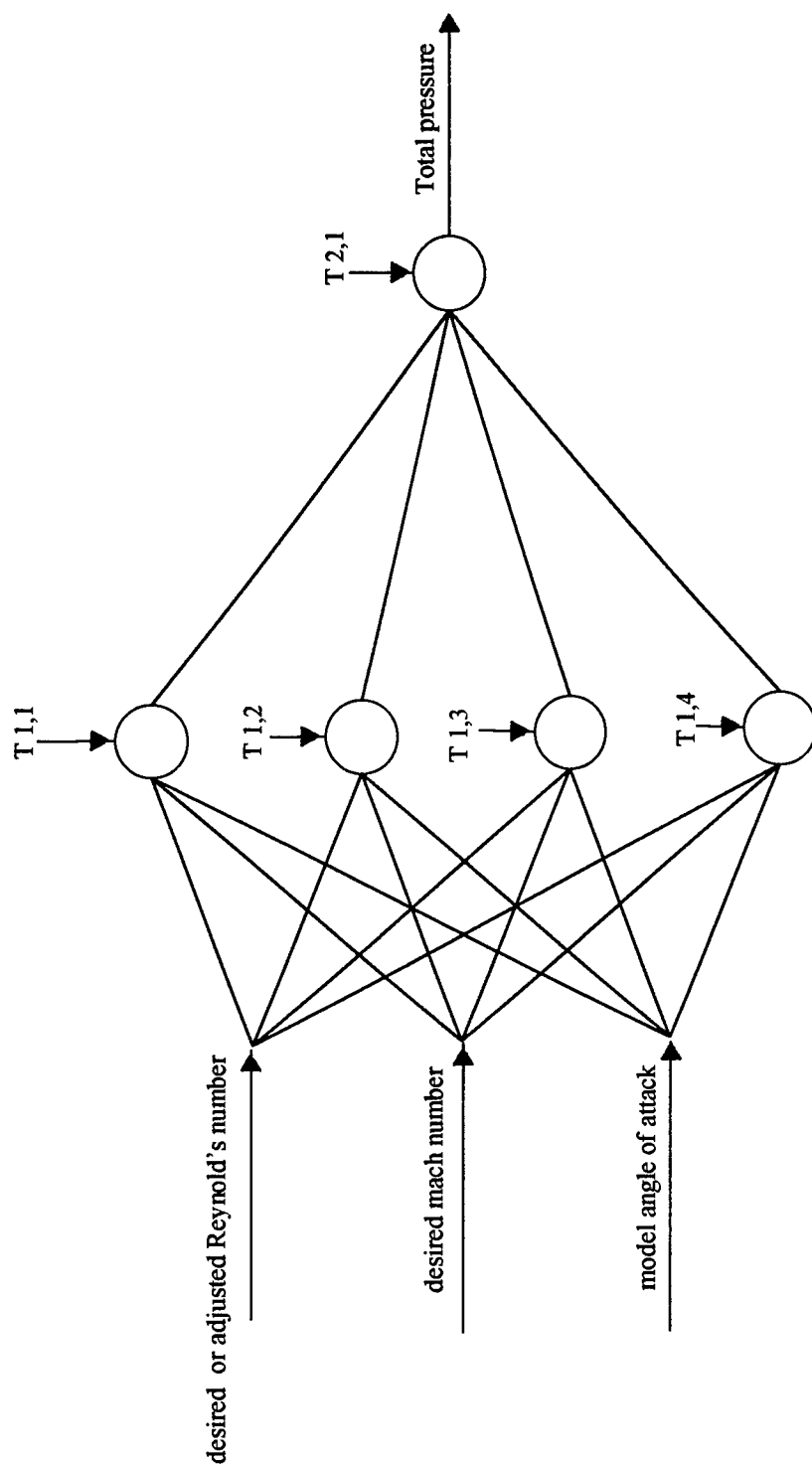
Fig. 5 Neural Network Structure for Reynold's Number Control

Total pressure

T 2,1

T 1,1

T 1,2

T 1,3

T 1,4

desired or adjusted Reynold's number

desired mach number

model angle of attack

References

[1] Dorf, Richard C., <u>Modern Control Systems</u>, 5th ed., Addison Wesley, 1989, pg. 151.

[2] Dorf, pg. 138.

[3] Demuth, H. & Beale, M., <u>Neural Network Toolbox</u>, 1992, The Mathworks, Inc., pg. 2-6.

[4] Demuth, pg. 1-9.

[5] Saad, Michel A., <u>Compressible Fluid Flow</u>, Prentice Hall, 1985, pgs. 271-272.

THERMAL SIGNATURE FOR CIRCUIT CARD FAULT IDENTIFICATION

Sheng-Jen Hsieh
Assistant Professor
Manufacturing Engineering Technology
Department of Engineering Technology and Industrial Distribution

Texas A&M University
College Station, Texas 77843-3367

THERMAL SIGNATURE FOR CIRCUIT CARD
FAULT IDENTIFICATION

Sheng-Jen Hsieh
Assistant Professor
Manufacturing Engineering Technology
Department of Engineering Technology and Industrial Distribution
Texas A&M University

Abstract

This research demonstrates that a thermal signature is an effective tool for fault identification in circuit cards. Experimental results indicate that the mean and variance in heating rate over a period of time are two effective discriminating factors for fault detection. Moreover, results from a preliminary study to identify a correction factor for the thermal signature of identical components in different circuitry seems positive.

The research was carried out in eight steps. First, a means for temperature probing was investigated. Second, fixtures for the circuit card and sensor probe were designed. Third, appropriate data acquisition tools were developed or acquired. Fourth, different fault types were designed. Fifth, experiments were designed and conducted. Sixth, the sampling frequency and run time were determined. Seventh, a discriminating factor was identified. Finally, a prototype was developed to implement these findings.

THERMAL SIGNATURE FOR CIRCUIT CARD FAULT IDENTIFICATION

Sheng-Jen Hsieh

INTRODUCTION

Increases in the number of gates per chip and chips per card make functional fault detection using traditional automated test equipment (ATE) difficult. This is because of the complexity involved in designing comprehensive test programs used for ATE and physical limitations in designing a sufficient number of test points. However, recent advances in thermal imaging techniques, computer-aided data acquisition instrumentation, and temperature sensor technology, have made indirect testing, such as use of a thermal signature for fault detection, more efficient and accurate.

Use of thermal imaging techniques for printed circuit board inspection can be traced back to Jones [1]. This technique was first reported in production testing of Minuteman missile modules. In 1986, another dedicated system for PCB testing, called the Automatic Infrared Test and Inspection System (AITIS), was developed by Hughes for the Air Force Wright Aeronautical Laboratories (AFWAL) [2]. Other similar systems, such as the Army's Infrared Automatic Mass Screening (RAMS) system, were developed at about the same time [3]. Allred [4,5,6] has presented a series of works on the application of infrared thermography for circuit card fault diagnosis. A system called NREDS (neural radiant energy detection system) for repairing circuit cards was developed and is now in place [6].

In the area of chip reliability, Allred [6] used the mean and variance of the heating rate to identify age degradation of EPROM chips in the F16 Digital Flight Control Computer (DFLCC). An infrared defect analysis system (IRDAS) was developed to predict component or assembly faults which could result in early life failure (Anderson [7]).

However, none of the above systems address the issue of the noise factor within the environment. The image capture environment is often characterized as a black box where no noise is allowed, in order to maintain high inspection accuracy. In addition, the above systems require an image profile of good and bad printed circuit boards to function; therefore, traditional bayesian classifiers or neural networks are utilized to discriminate one from another. The accuracy of the inspection is often dependent on the sample sizes used to construct the image profiles. In some conditions, data about defects are difficult to obtain. Moreover, the image profile of a PCB is often a board dependent.

In other words, a new image profile has to be constructed for inspection of a different kind of PCB. No work was found which utilized recent advances in temperature sensor technology and instrumentation for thermal signature acquisition.

Therefore, the objectives of this research were to (1) investigate direct and indirect means for board thermal signature acquisition, (2) use the model-based diagnosis [8,9] concept for thermal image profile construction, (3) identify simple and efficient variables for discriminating defective and non-defective circuit cards, (4) investigate the feasibility of a generic and reconfigurable thermal signature library for circuit card fault identification, and (5) develop a prototype which utilizes the findings from the previous steps.

METHODOLOGY

This research was carried out using (1) resistance temperature detector (RTD) and infrared camera (IR) for thermal signature acquisition, (2) systematic experimental design, hypothesis testing, and statistical analysis techniques to identify discriminating factors for defective and non-defective circuit cards, (3) accelerated test and regression analysis for IC chip aging investigation, and (4) same chip different locations experimentation. The research procedures are described in the following sections.

Thermal Signature Probing and Fixture Designs

Based on production demand, a jet engine frequency control circuit card was chosen for this research. Within this circuit card, an LM101A chip were selected for experiments due to its presence in multiple locations on the same circuit card. An RTD sensor and IR camera, which provide 0.02C° accuracy, were used for thermal signature acquisition. To effectively measure the heat emitted from the IC chip, fixtures were designed to mount the circuit card and sensors in a fixed position; and IC sockets were placed on the board to ease the changing of the chips during the experiments. Figures 1 and 2 show the fixtures designed for the IR and RTD thermal signature capture experiments. In Figure 1, a black ground is used for the experiments to eliminate the potential reflection to the IR camera. Metal studs were anchored to the top of black cardboard for mounting the circuit card to ensure the chip are in same position each time. In Figure 2, two identical fixtures were used to fasten the circuit card and RTD sensor respectively. To ensure that the sensor fully contacts the circuit card, the RTD sensor was loaded within a tube which has a spring inside
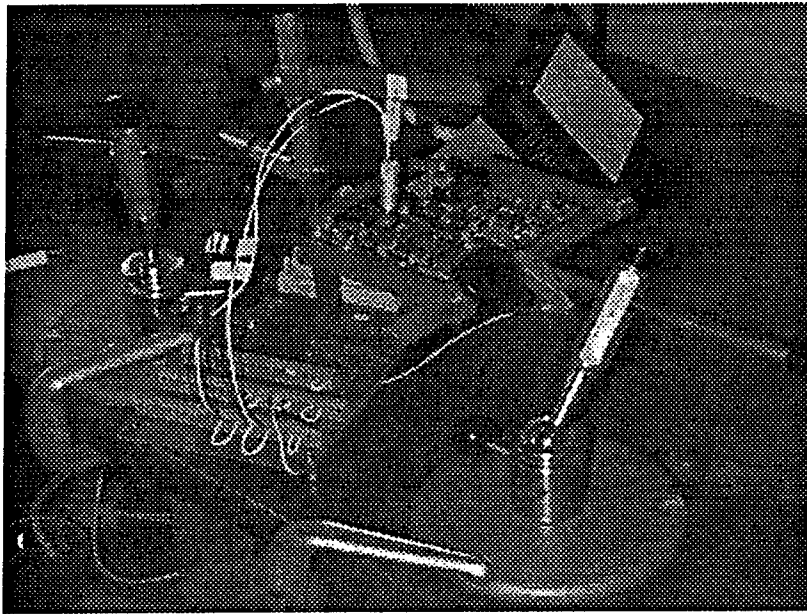
Figure 1. The RTD Sensor Probing Setup.

Figure 2. The Setup for IR Camera Imaging.

it. In addition, an IC test clip was modified to provide a similar function. Figure 3 shows the RTD fastener design, in which the RTD sensor grabs the LM101A chip.

Image Acquisition Tools: Labview Model and WinTES Software

The operating theory behind the RTD sensor is that changes in IC surface temperature will result in changes in resistance within the RTD structure. By knowing the resistance, we can convert the reading into a corresponding temperature. A LabView model, data acquisition module, and circuitry were created, installed and constructed to collect temperature readings at a given frequency and duration. The readings from the input module were voltages. These voltages were converted into first to resistance, and then to temperature values over time using the LabVIEW model. These data were plotted on a control chart as time passed. In addition, an IR camera from Compix Corporation was also chosen for the study. A software package called WinTES was used to collect the thermal signature from the designed experiments.

Model Based Fault Types Design

We applied a model-based diagnosis concept [8,9] for duplication of the defect types, since the defective data are very limited. Several different approaches were applied to produce the defect types. The first approach was to apply high voltage to the pins of the chip; then the chip is inspected against its specifications. Therefore, different types of faults were made. The second approach was to short or open the pin of the chip. The final approach was to stress the chip using the accelerated test method. The chips made using this approach were used for model development and verifications. Figure 4 shows the connection diagram fo an LM101A chip. Table 1 summarizes duplicate faults such as open and short.

Table 1. Various of Duplicate Faults.

	Short	Open	Stress	Stress
Types	P1-P2,P3-P4,P6-P7,P7-P8	P1,P2,P3,P4,P5,P6,P7,P8	Rev.P7-P4	High Voltage & Current

Design and Conduct Experiments

A series of experiments were conducted to (1) determine the appropriate run length and sampling time, (2) ensure the repeatability of the temperature readings over time, (3) construct a discriminating variable for distinguishing between good and bad chips with noise present, and (4) develop an analytic model for chip age degradation

6-6
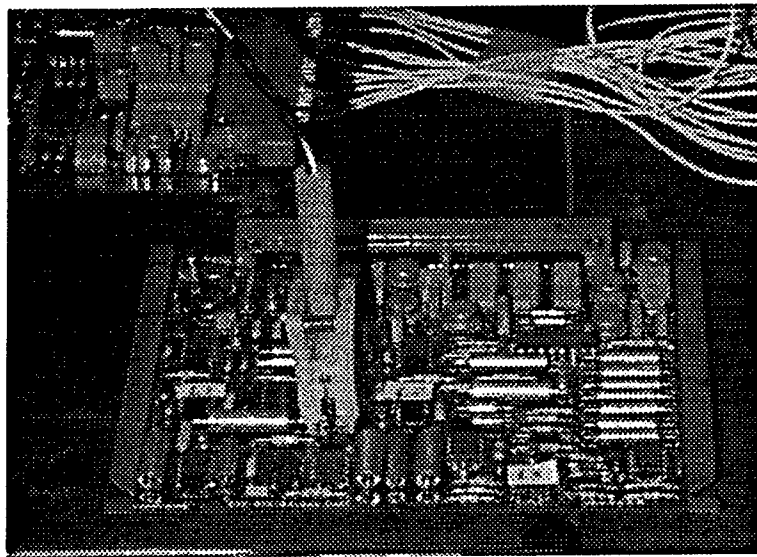
Figure 3. The RTD Fasterner Design.

Connection Diagrams (Top View)

Dual-In-Line Package

TL/H/7752–4

Order Number LM101AJ, LM101J/883*,
LM201AN or LM301AN
See NS Package Number J08A or N08A
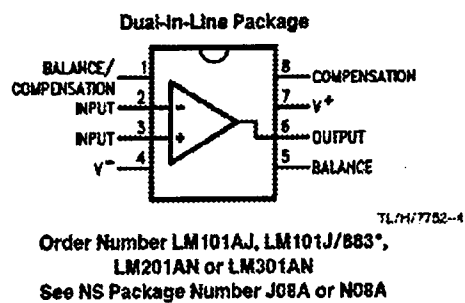
Figure 4. The Connection Diagrams of LM101.

identification. Various hypotheses were proposed for this study, including:

1. Whether there is a time effect to chip thermal signature
2. Whether there is a open fault impact on chip thermal signature
3. Whether there is a short fault impact on chip thermal signature
4. Whether there is an enclosure impact on thermal signature
5. Whether there is a reverse voltage impact on chip thermal signature
6. Whether there is a location impact on chip thermal signature

Find the Discriminating Factors

After conducting a series of experiments, hypothesis testing, and statistical analysis (using ANOVA and F-test), it appeared that the heating rate of the thermal signature of a good chip seems to fall within certain limits, in terms of mean and variation. Heating rate means and variations which fall beyond these limits seem to suggest the subject chip is not a good one. These findings appear to be both similar to and different from Allred's {1998] report. The research context is different: in Allred's work, EPROM chips were used; whereas in this study, operational amplifier chips were used. The measurement variables are similar; i.e., in both cases, mean and variance are used as discriminating variables. However, the definition of heating rate and application environment are different. It is not mentioned clearly what the heating rate is in Allred's work. In this research, the mean and variance of the heating rate are as follows:

$$\text{mean heating rate} = H_{avg} = \sum (Tc_t - Tb_t) / n$$

$$\text{variance of heating rat} = \sum \{ (Tc_t - Tb_t) - H_{avg} \}^2/(n - 1)$$

where t ranges from 1 to n, which is the samples obtained over time. Tc is the chip's temperature and Tb is the board temperature as measured without an enclosure. Since the inspection area did not have an enclosure in this study, Tb is affected by absolute board temperature (i.e. Tb_{abs}) and room/environment temperature (i.e., Te). Often Tb_{abs} temperature is affected by nearby heat sinks and source components on the same board. Moreover, the measurement criteria developed by the author are insensitive to the presence of noise variables. Therefore, the inspection of the circuit card can be done in an ordinary office environment; no special enclosure needs to be used for inspection.

Accelerated Prediction of Chip Life Time

Based on chip specifications and available experiment instruments, the reverse voltage factor was selected to stress the chip. Each sample of chips was divided into three batches. The first batch of chips was used to find the critical point. The second batch was used for different level s of stressing, and the last batch of chips was used for verification. The procedure used for the accelerated test was as follows:

6-8

1. divide chips into lots for experiments, model development, and evaluation;
2. select the factor to be used for stress;
3. stress the chip until it fails;
4. divide the stress time into several different zones;
5. stress the chips for different lengths of time;
6. develop an analytic model;
7. compare the prediction with chips which have been evaluated

Sampling Frequency and Run Time Estimation

Sampling frequency and duration is often very hardware dependent. The resolution and accuracy of the hardware can have great impact on temperature readings. To select an appropriate run time, experiments with a long duration were conducted and plotted for a small sample of good chips. The temperature data were divided into two sections, namely, transition and steady states. After several adjustments on the sampling time of the plot and applied mathematic filter, the cutoff point between transition and steady state was selected. In this case, the time point was 10 minutes. The sampling frequency was limited by the hardware response time. In the case of the IR camera, the sampling time is dependent on the scanning time of the camera; and in this study, 20 seconds of scanning time is used. On the other hand, the sampling time for the RTD sensor was determined to be 10 seconds after several experimental trials.

PROTOTYPE DEVELOPMENT

Modules developed for this prototype include image acquisition, image analysis and interpretation, and online user manual. Within each module, the procedures are shown on the first screen, which is used to remind the users what needs to be done. Figures 5 and 6 show snapshots of the system.

The functions of the image acquisition module are to (1) acquire the thermal signature of the circuit card while it is powering up; and (2) generate images files based on a given scanning interval and duration. These image files are captured through the infrared camera; and the images are represented either in a color or black & white map. In addition, the temperature value associated with each pixel is embedded within the file; this information is useful for image analysis and interpretation. Figure 7 is a snapshot of the image acquisition module. The picture on the right is an image of the circuit card obtained from the infrared camera, and the window on the left is the setting for scanning time, duration, and color bar.

6-9
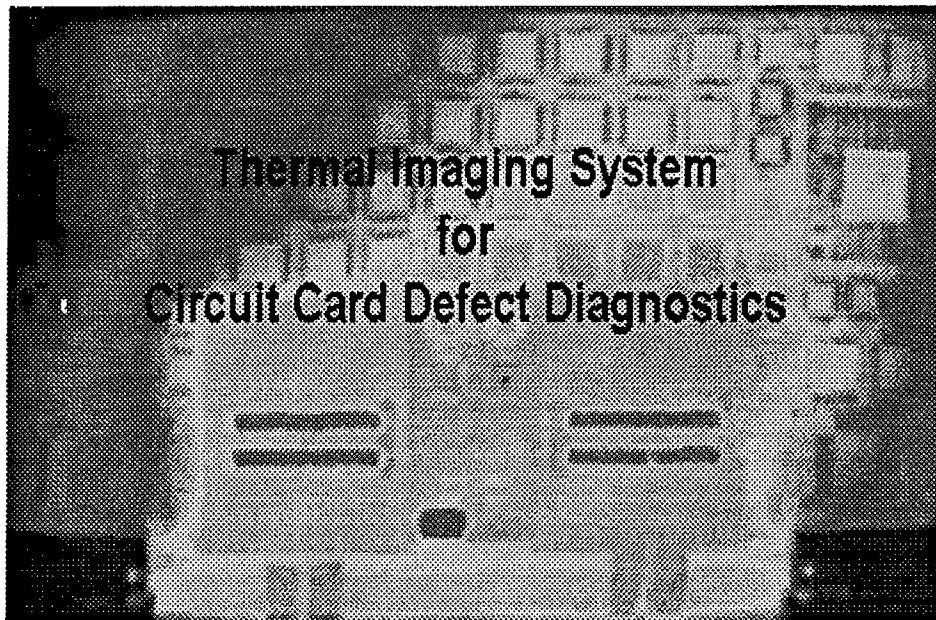
Figure 5. The Snapshot of the Prototype - I.
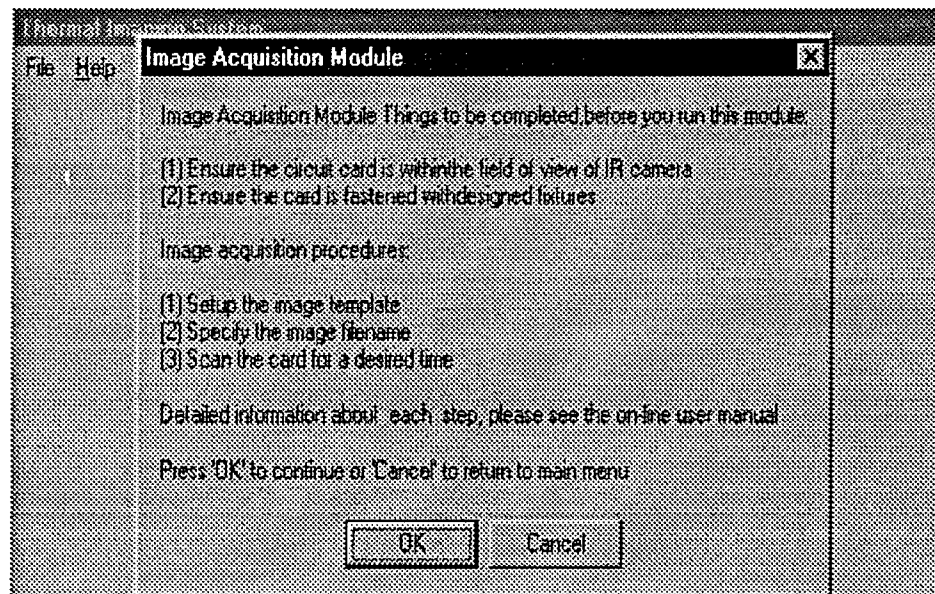
Figure 6. The Snapshot of the Prototype - II.
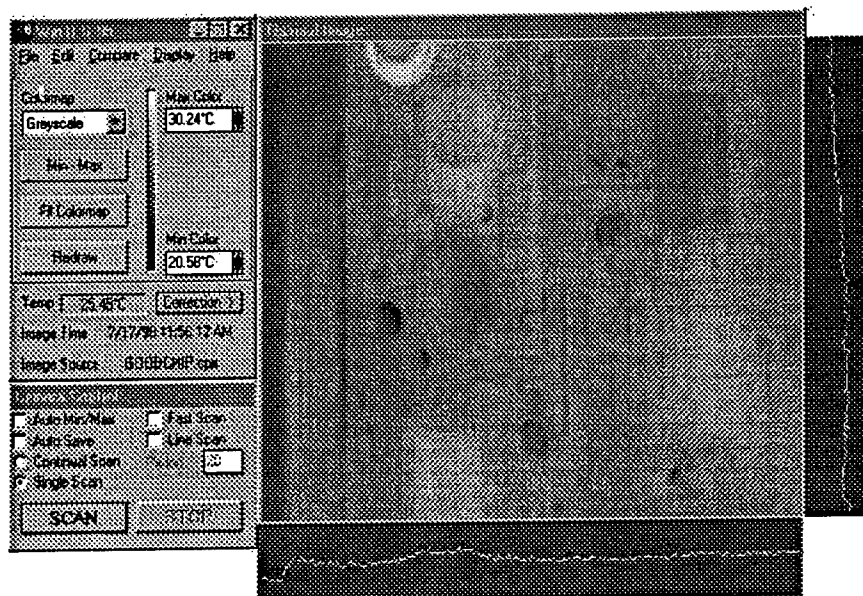
Figure 7. The Snapshot of the Image Acquisition Module.

The functions of the image analysis and interpretation module are to (1) process the images files generated by the image acquisition module, (2) compare the overall mean heating rate and variance with those of a good chip, and (3) indicate whether a chip is good or bad. Figures 8 and 9 are snapshots of this module. The image in the upper-right corner of the screen is the image of the circuit card being inspected. The windows at the bottom show the directory and image files, which allow you to select appropriate files for evaluation. The window in the upper-left corner shows the specification of a good board and the inspection results. If the chip being inspected is a good one, the chip will be highlighted with a green border. However, if the chip is diagnosed as bad, it will be highlighted with a red border. In addition, the upper-left corner window shows the diagnosis results. Figures 10 and 11 are examples for a good and a bad chip.

FINDINGS, CONTRIBUTIONS AND FURTHER RESEARCH

RTD and IR camera are effective tools for visible and functional fault identification. The IR camera is a better tool for thermal signature acquisition; but it is more expensive. The difference between board and chip temperature is a good variable for discriminating between defect-free and defective chips. Contributions of this research include (1) studying multiple types of component faults in a circuit card with noise variables present; (2) developing a simple and

6-11
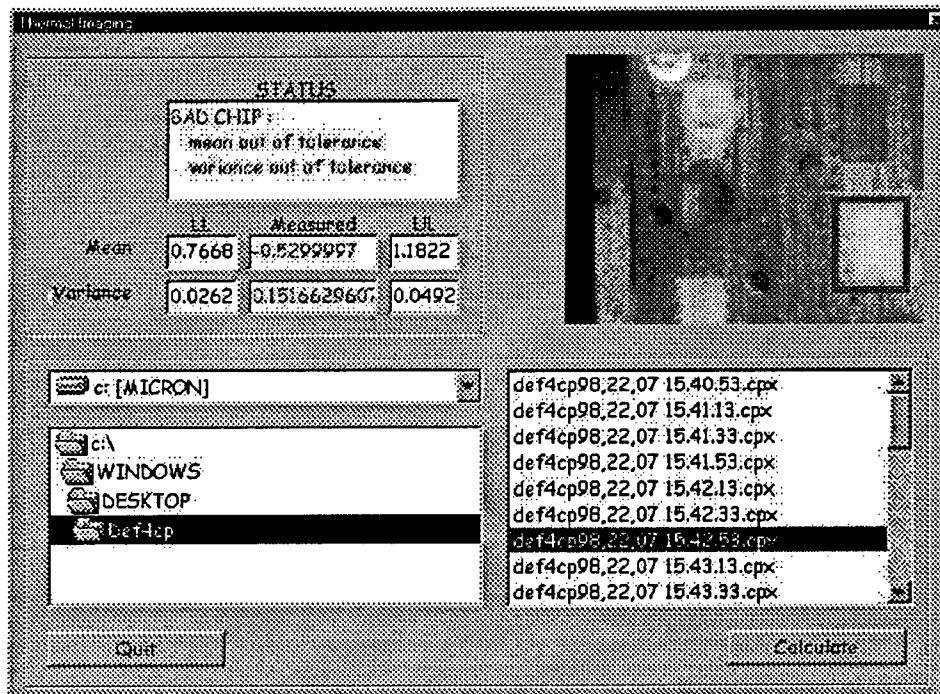
Figure 8. The Snapshot of the Image Analsis Module -- Bad Chip.
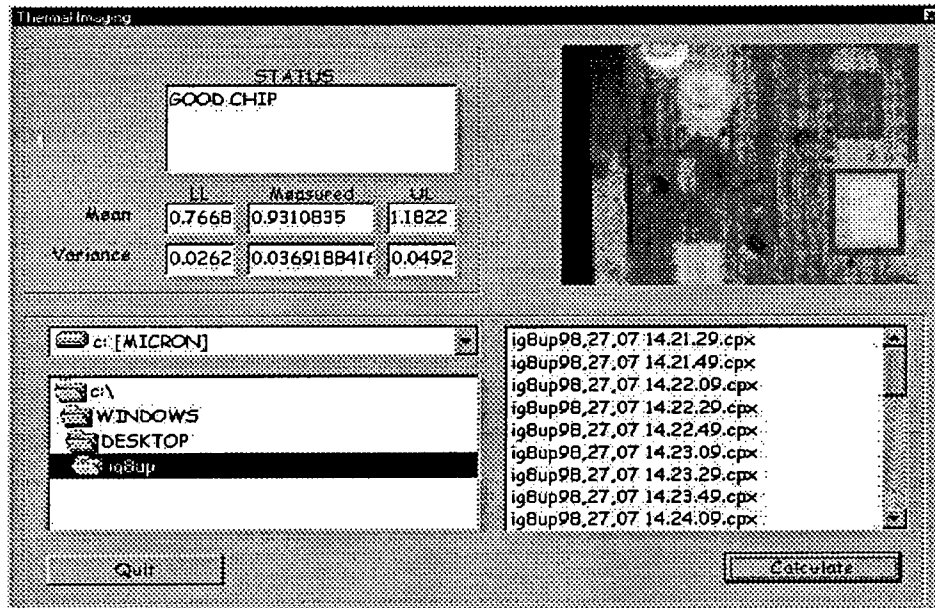
Figure 8. The Snapshot of the Image Analsis Module -- Bad Chip.

efficient approach to circuit card fault diagnosis. This study also lays significant foundationd for future work in: (1) developing a generic and reconfigurable thermal signatures library for multiple circuit card fault diagnosis; thereby eliminating the need for prior testing of known-good cards; (2) circuit card life time prediction and preventative maintenance; and (3) smart sensors for on-line real time circuit card fault diagnosis.

REFERENCES

[1]   R.Ward Jones, "An infrared tester for printed circuit boards and microcircuits," Automation in Electronic Test Equipment, Vol. VII, Goodman, N.Y. University Press, May 1969.

[2]   Keith V. Pearson, "Printed circuit board fault detection and isolation using thermal imaging techniques," SPIE Vol. 636-Thermal Imaging, 1986, pp. 122-125.

[3]   H.Kaplan, P.Hugo, R.Zelenka, "The Infrared Automatic Mass Screening (IRAMS) system for printed circuit board diagnostics," Conference Proceedings, AUTOTESTCON'86, pp. 301-306.

[4]   L.G. Allred, T.R. Howard and G . Serpen, "Thermal imaging is the sole basis for repairing circuit cards in the F16 flight control panel," Conference Proceedings, AUTOTESTCON'92, pp. 455-458.

[5]   L.G. Allred, T.R. Howard, G. Serpen, "Thermal imaging is the sole basis for repairing circuit cards in the F-16 flight control panel," Conference Proceedings, AUTOTESTCON'96, pp. 418-424.

[6]   L.G. Allred, T.R, "Identification of age degradation in EPROM chips using infrared thermography," AeroSense, SPIE, April 1998, pp. 418-424.

[7]   R.A. Anderson, P.N. Cholakis, "Effective analysis of electronic circuit manufacturing with infrared imaging," Advanced Imaging, October 1995, pp. 92-95.

[8]   Saxena, S. and Unruh, A., "Diagnosis of semiconductor manufacturing equipment and processes," IEEE Transactions on Semiconductor Manufacturing v 7 n 2 May 1994 , pp. 220-232.

[9]   Abu-Hanna, A., Jansweijer, W., Benjamins, R., and Wielinga, B., "Functional models in perspective: their characteristics and integration in multiple model-based diagnosis," Applied Artificial Intelligence v 8 n 2 Apr-Jun 1994 , pp. 219-237.

ACKNOWLEDGMENTS

STUDIES ON THE AMPHETAMINE DERIVATIVES AND ANALYTICAL STANDARDS

S. Bin Kong, Ph.D.
Associate Professor
Department of Chemistry

University of the Incarnate Word
4301 Broadway
San Antonio, TX 78209

7-1

STUDIES ON THE AMPHETAMINE DERIVATIVES AND ANALYTICAL STANDARD

S. Bin Kong, Ph.D.
Associate Professor
Department of Chemistry
University of the Incarnate Word

Abstract

Synthesis of amphetamine derivatives are described with retrosynthetic analysis and synthon /disconnection approach. The schemes were studied from economic and technological considerations that take into account the following: The starting material availability, number of steps, technological difficulties and controlled substance regulations. The chemical synthesis in this research were also involved with identification and quantification of chlorobenzorex.

STUDIES ON THE AMPHETAMINE DERIVATIVES AND ANALYTICAL STANDARD

S. Bin Kong, Ph.D.

Introduction

The derivatives of amphetamines were analyzed by synthon and disconnection approach. We began to work with 3-clobenzorex. There were several ways to make the compounds with the following consideration.

      1) Stability of the ion fragmentation.

      2) The fragmentation could be positively charged or negatively charged.

      3) The synthetic steps should be short as possible.

      4) Use the concept of functional group inversion.

The molecules that affect as adrenergic and central nerve system stimulants were also studied and listed (Table 1 and 2). Retrosynthetic analysis were employed(Table 3 and 3a) and synthesis of the derivatives were investigated (Table 4) along with metabolic pathways via identification of the chemicals with mass spectra.

Table 1. Adrenergic stimulant studied.
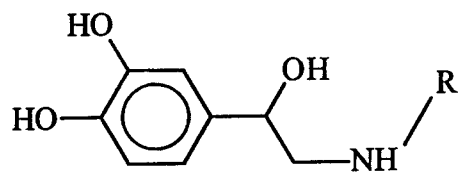
R = Me, Epinephrine
H,   Norepinephrine
isopropyl, Isoproterenol
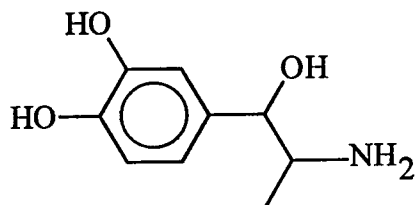
Levonordefrine
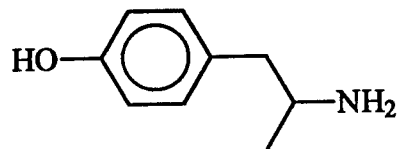
Hydroxyamphetamine

7-4

Table 2. Central nerve system stimulants studied.
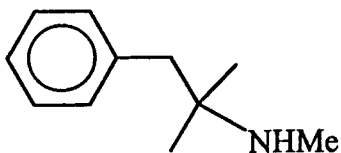
Mephentermine
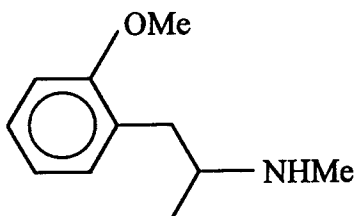
Methoxyphenamine
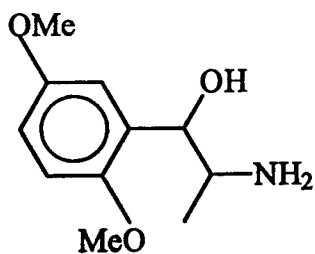
Methoxamine
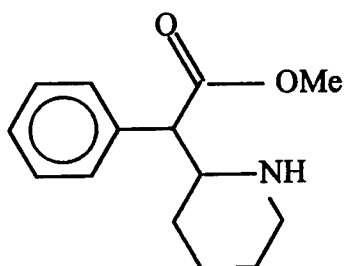
Methylphenidate   7-5

Table 3. Retrosynthetic analysis of amphetamine derivatives.
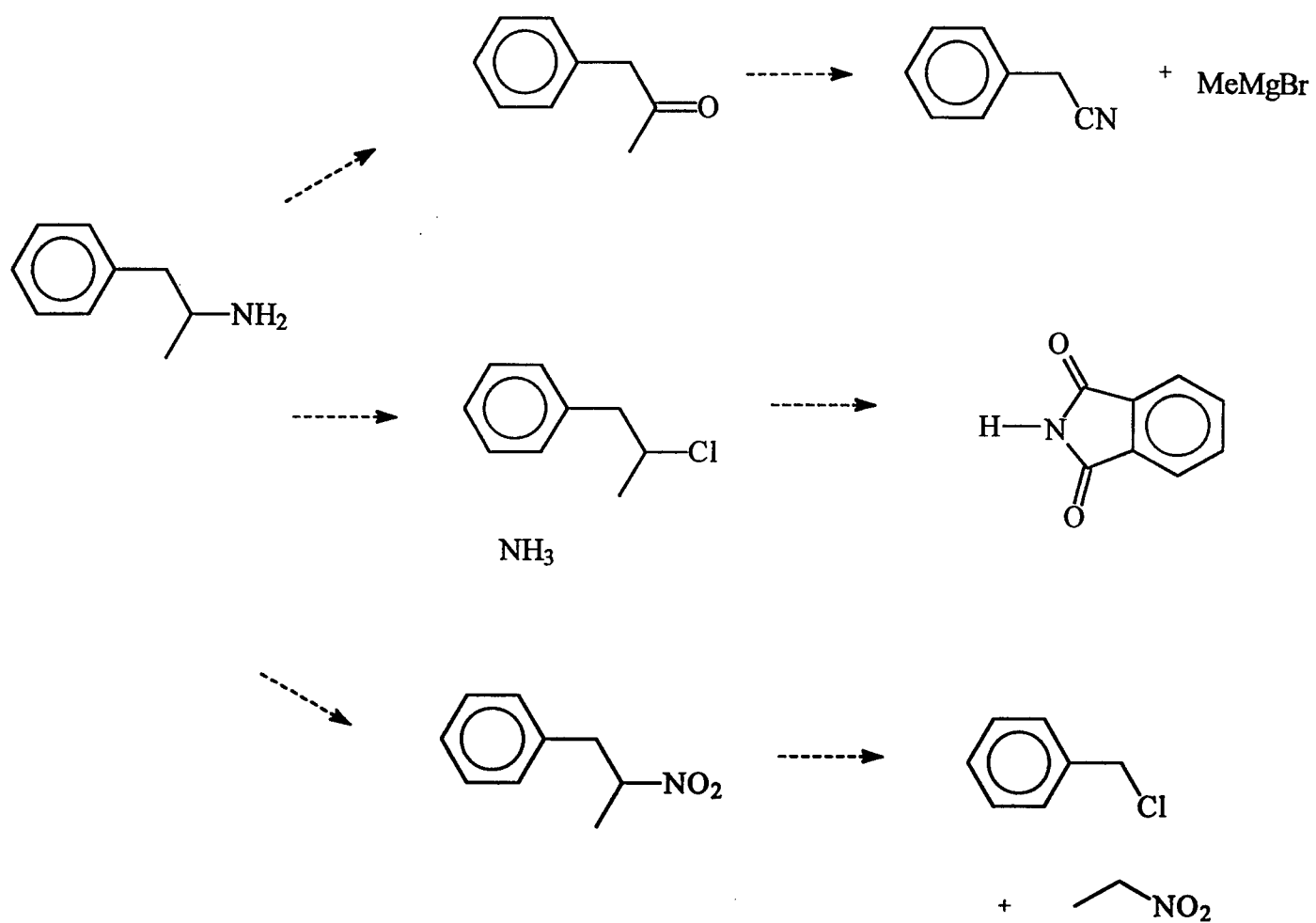
Table 4. Synthesis of amphetamine derivatives.
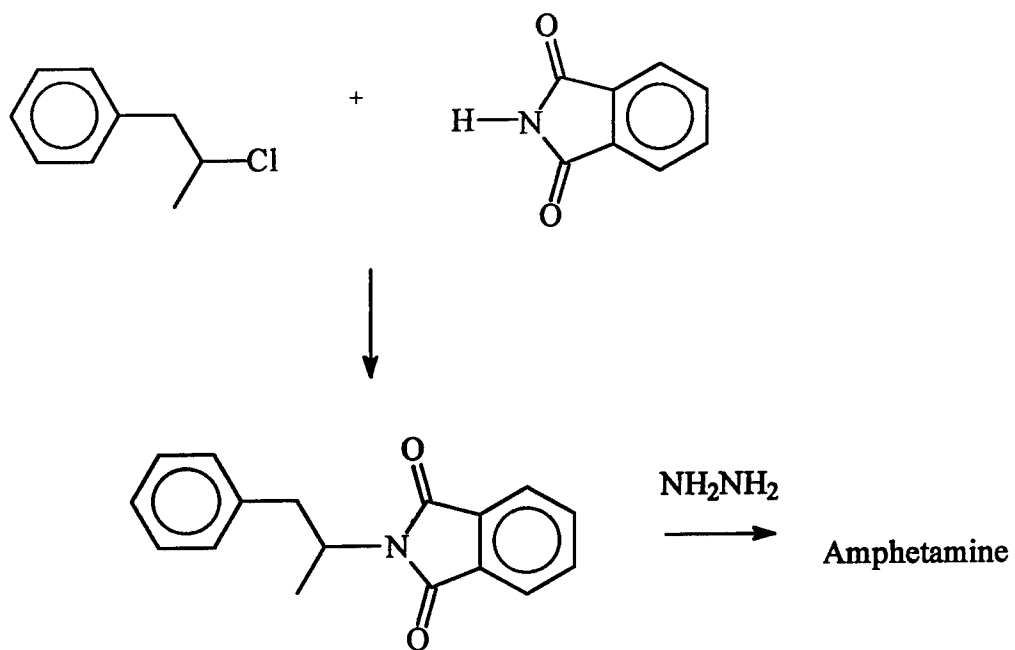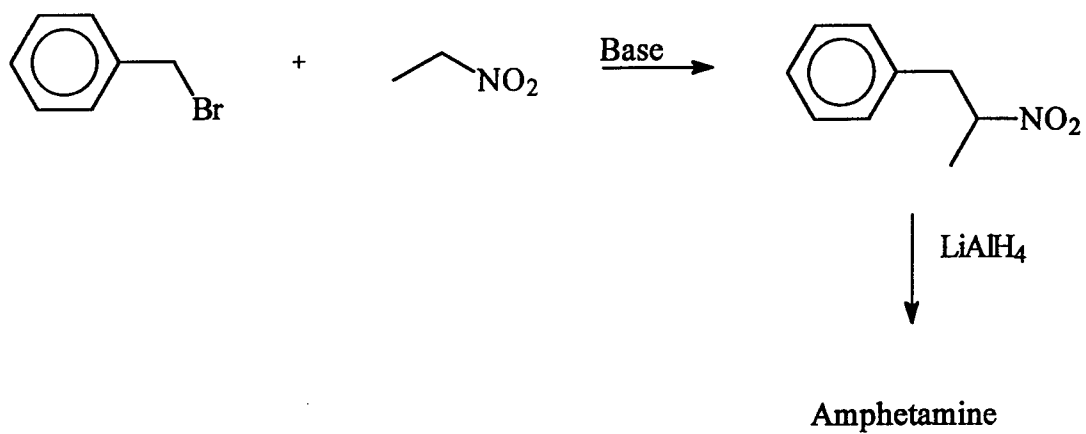
Table 5. Clorbenzorex derivatives (Target Molecules)

(TM 1)

(TM2)

(TM3)

(TM4)

Amphetamine
as starting material

7-8
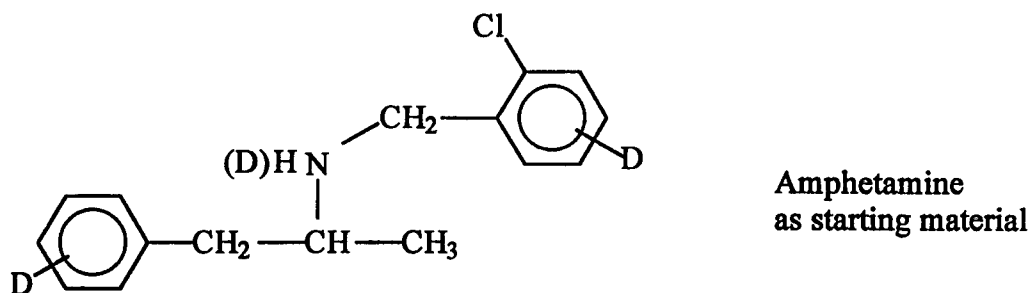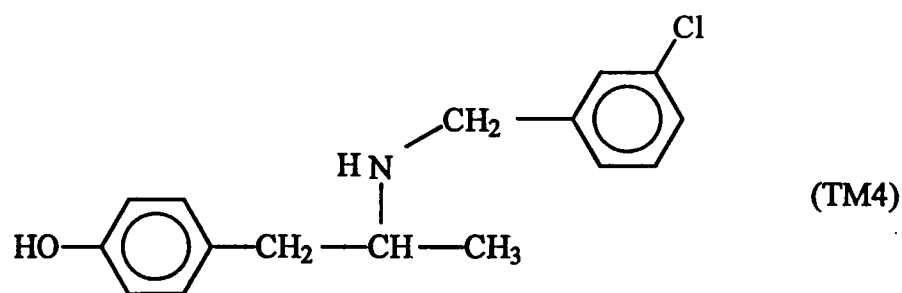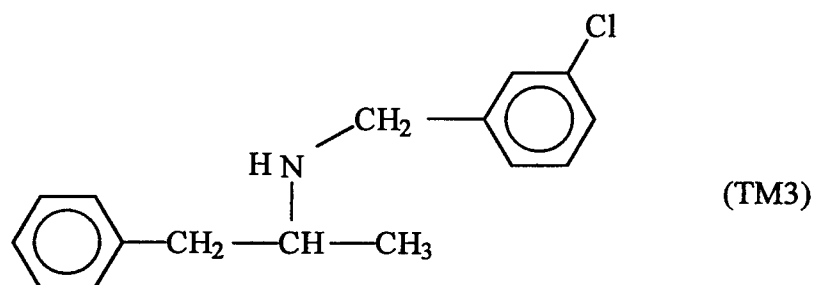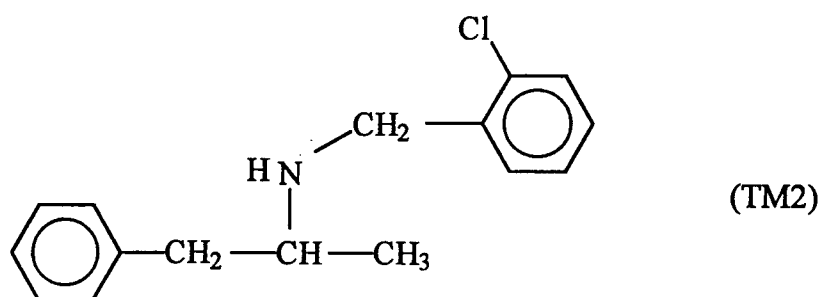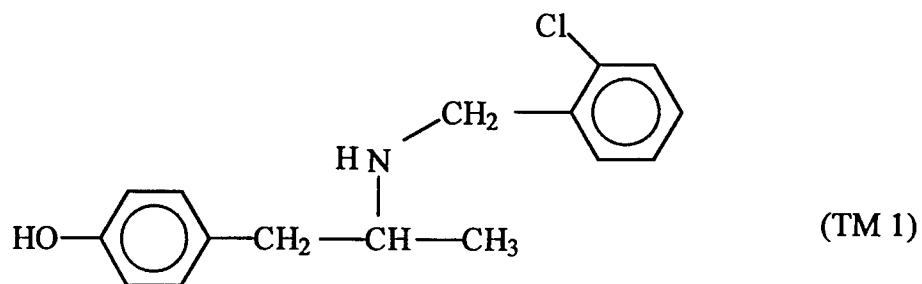
Table 6. Synthesis of Clorbenzorex (1).

K$_2$CO$_3$

reflux

benzene

(1)

+

+

1) EtOH

2) NaBH$_4$

(1)

Cl

Cl

Cl

Cl

—NH$_2$
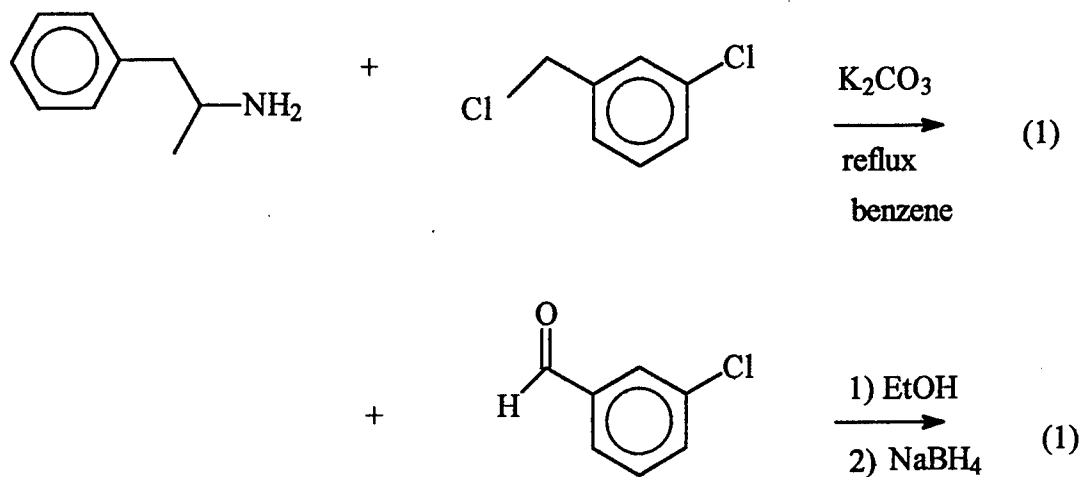
Both above reaction came with 2 major products. MS interpretation could be as following:

Cl

—NH

MW 259

7-9

MW 259

m/z 168

m/z 125

m/z 91
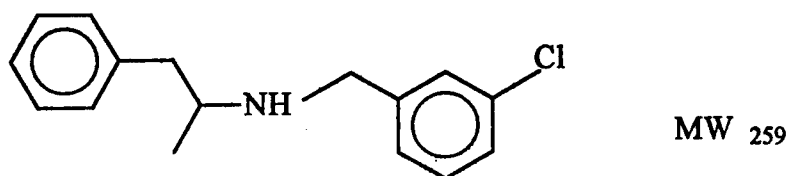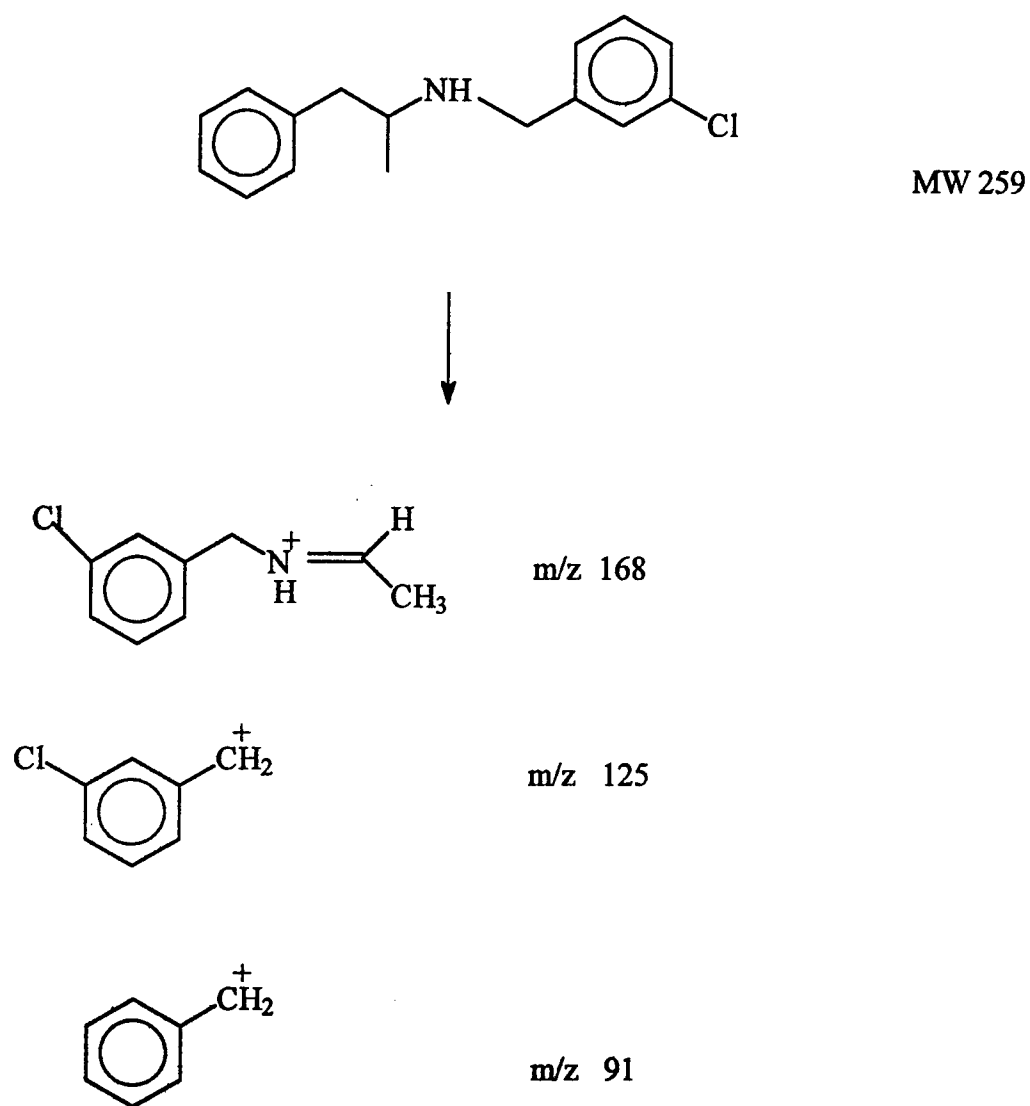
Figure 1. Possible fragmentation pattern.

I tried to reduce the product with sodium borohydride to a double bond but the reaction didn't go, which means that m/z is not the structure below.
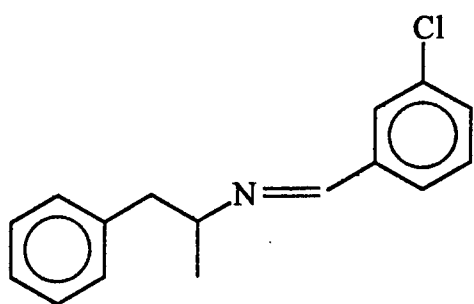
mw = 257

I should have investigated the data from EI or should study further on this result with high resolution Mass data. The chromatogram and the mass data are attached.
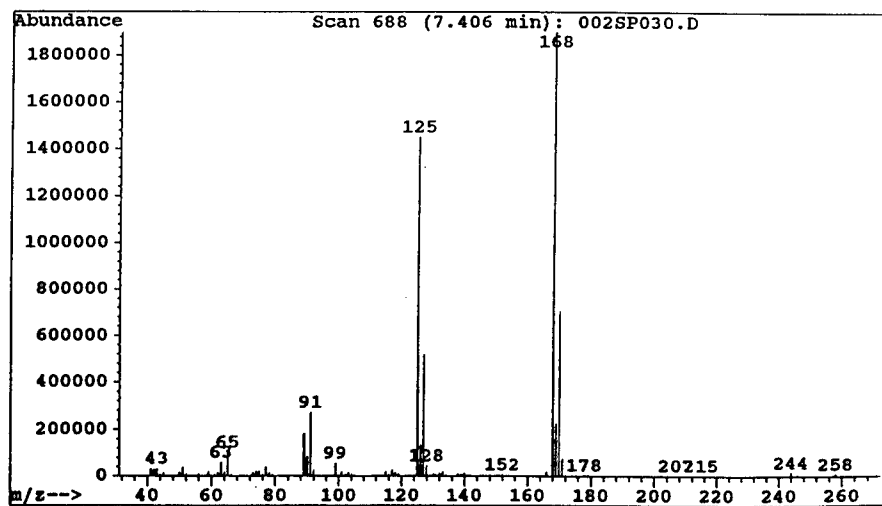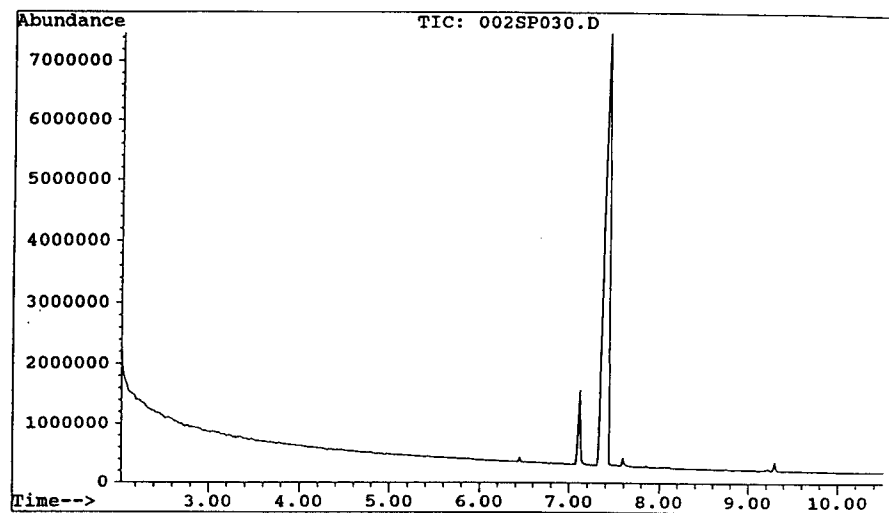
Figure 2. Mass spectrum of 3-chlorbenzorex
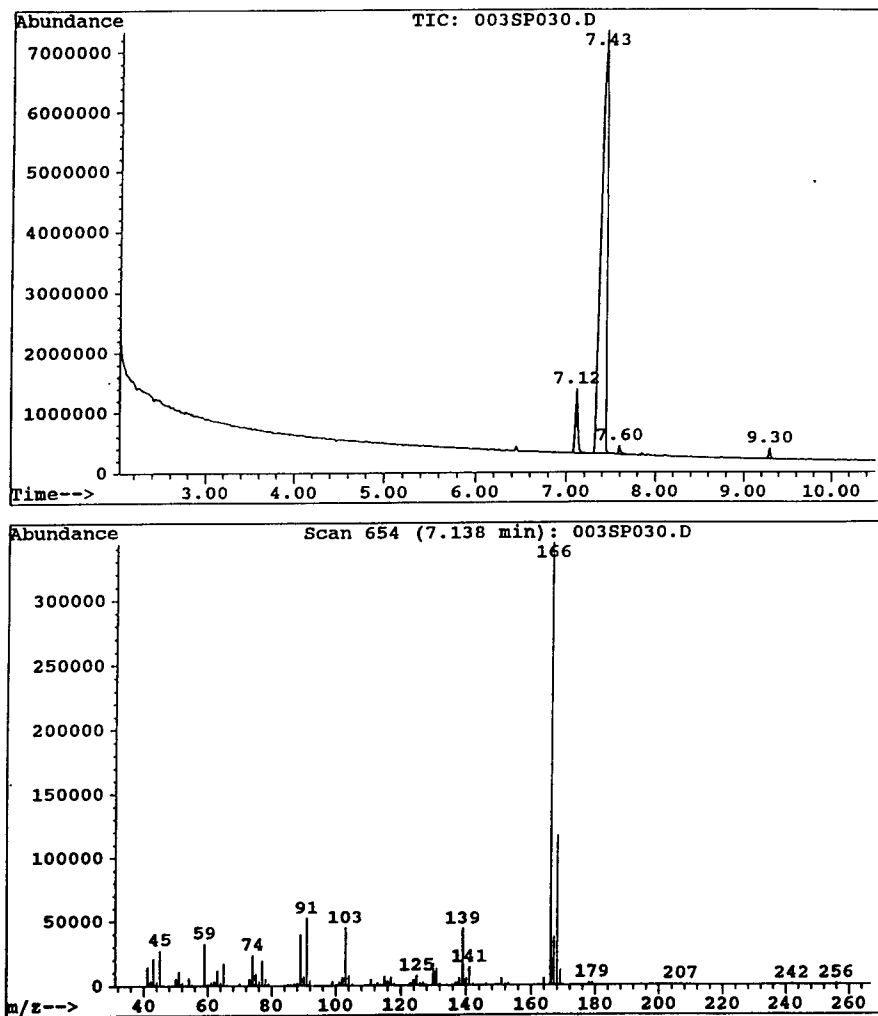
Figure 3. Mass spectrum of 3-Chlorbenzorex side product.
Unknown

Discussion

Electron Ionization (EI) was used for mass analysis. EI played the major role in the routine analysis of small molecules in this research. Its technique is straightforward and the databases contain the EI mass spectra of over 50,000 compounds were used through the summer. However, it is difficult to analyze side products of the synthesis even if the backgrounds are subtracted due to the degree of fragmentation. It limited the chemist to small molecules well below the mass range of common bioorganic compounds. Chemical Ionization(CI), electrospray ionization(ESI) or fast atom/ion bombardment(FAB) can be useful tools for future investigation. The usefulness of EI decreased significantly for compounds that didn't produce molecular ion peak. The requirement that the sample be thermally desorbed into the ionization source often leads to decomposition prior to vaporazation. The principal problems associated with thermal desorption in EI in our case were possibly the thermal decomposition, and in many cases, excessive fragmentation. Too much fragmentation often resulted in no observable molecular ion with 3-chlorbenzorex derivatives. If we combine the data derived from EI and CI with GC/MS/IRD, that could be very useful for analyzing many volatile chemicals.

Mass spectra

It was difficult to identify the chemical components with mass spectra only in many cases due to the overlapping of the retention times of molecules and unidentifiable peaks with possibly different column and detector conditions of the GC-Mass spectrometer. I was beginning to get familiar with the GC-Mass when summer tour was over. Even if we try to change the column conditions, carrier gas or flow rate, the interpretation could be tricky, despite making background subtractions. We should consider other ionization methods such as CI or methods for accurate weight determination. I should mention the synthesis of 3-clobenzorex and the GC-Mass spectra. There were two compounds (RT 7.12 and 7.43). The former had fragmentation pattern with 45, 59, 74, 91, 103, 125, 139, 166 (base peak), 179, 207, 242 and 256. The latter had 43, 65, 91, 99,

125, 168, 244, and 258. The clobenzorex were synthesized (Table 5) with two different methods (Table 6), which resulted the same GC data. The fragment at 166 is still mystery and should be studied further in detail with CI.

Conclusion

Identification of metabolite intermediates can be done more efficiently if we use GC/FT-IRD/MS.
Chemical Ionization(CI) should be applied along with EI. To characterize biodegraded molecules which can have high molecular weights, FAB , electron spray(ESI) or other methods could also be considered. To solve the problem above, we also need to synthesize individual standards of derivatives. I need more time to be familiar with the GC-Mass spectrometer that I used during the summer, LC-Mass and the research subject. Further study is necessary.

Future Work

This summer, we have characterized and synthesized 3-chlorobenzorex as a standard to identify the chemical components as a basis for future research. We will use these data for chemical and biodegradation studies in the following years. After we establish the routine procedure and identification of related chemicals, we can proceed to other samples such as Sydnocarb, LSD and other controlled substances for metabolite studies. Identification and quantitation studies should be also possible.
(Table 7)

References

R. P. Iyer and A. V. Prabhu, Synthesis of Drugs, A Synthon Approach, Sevak Publications, Bombay, India (1985).

O. Vinar, et al., A survery of phychotropic medications not available in the United States Neurophychopharmacology, Vol. 5, No. 4, 201(1991).

J. A. Tarver, Amphetamine positive drug screens for use of clobenzorex hydrochloride. Journal of Analytic toxicology, Vol. 18, p183 (1994).

R. de la Torre, R. Badia, G. Gonzalez, M. Garcia, M. J. Pretel, M. Farre and J. Segura, Cross Reactivity of stimulants found in sports drug testing by two fluorescence polarization immunoassays., Jour. Of Analytical Toxicology, Vol. 20, 165 (1996).

S. Valtier, S. B. Kong and J. T. Cody, A Procedure for Identification and Quantitation of Clobenzorex, Society of Forensic Science & Toxicologist Meeting, Abstract Paper, Albuquerque, New Mexico(1998).

R. Young, N. A. Darmani, E. L. Elder, D. Dumas and R. A. Glennon, Clobenzorex: Evidence for amphetamine like behavioral actions., Pharmacology Biochemistry and Behavior, Vol. 56, N0. 2, 311(1997).

J. Litermans, A. Benakis and R. Ratouis, Synthese du chlorhydrate de cholrobenzyl methyl phenethylamine marque en position 7 par C-14 (Chlorhydrate de Clobenzorex).

Acknowledgement

Table 7. Retrosynthesis of future target molecules.

Prenylanine
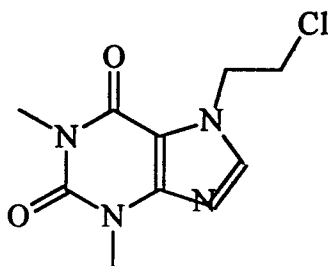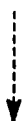

CHO — CH$_2$CH

NH$_2$CH$_2$CH$_2$ —CH
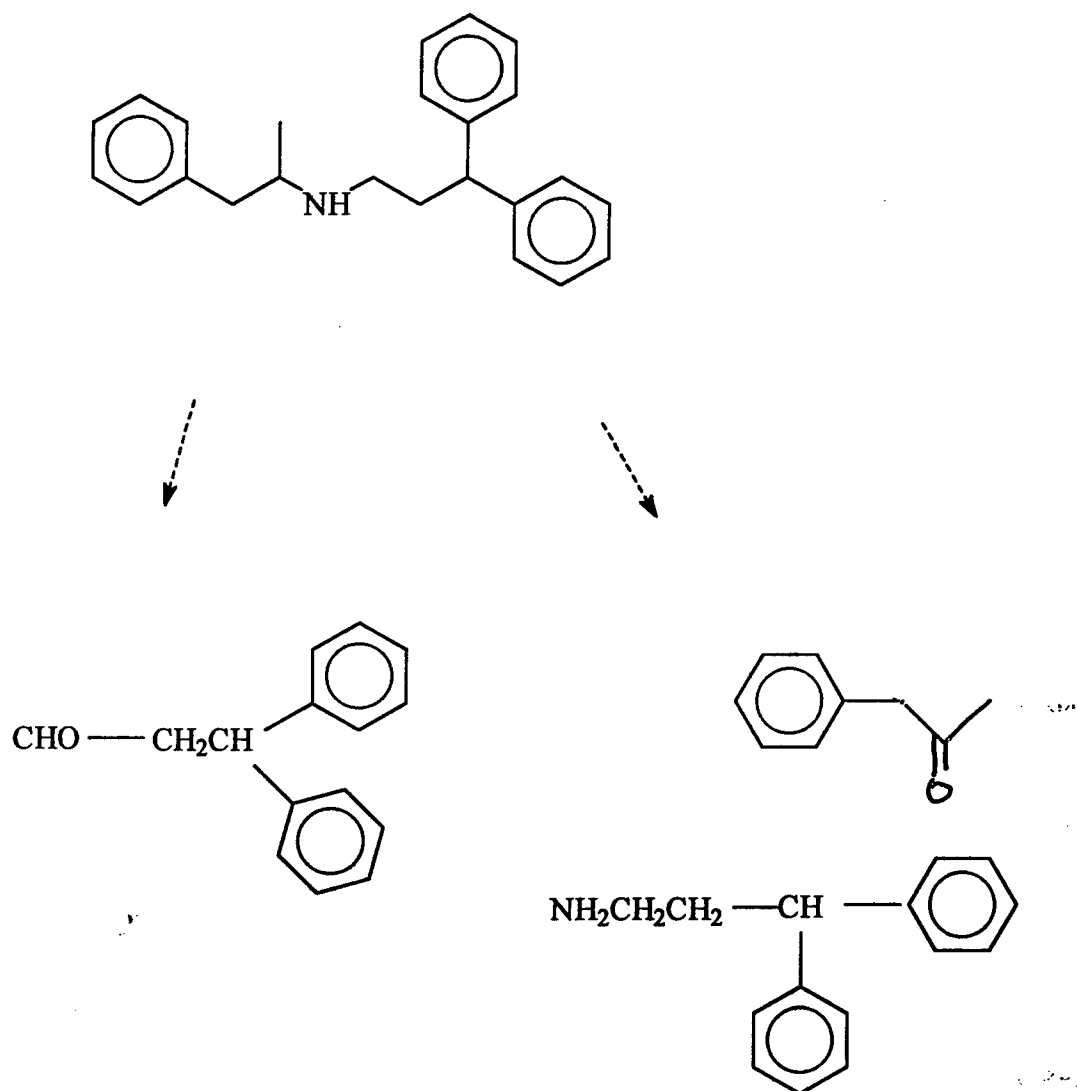
**3,3-diphenylpropylamine
Aldrich 13629-8 (5586-73-2)
FW 211.31, mp:29-31, 25g/$39.50**
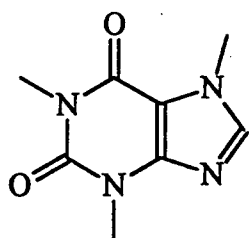
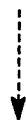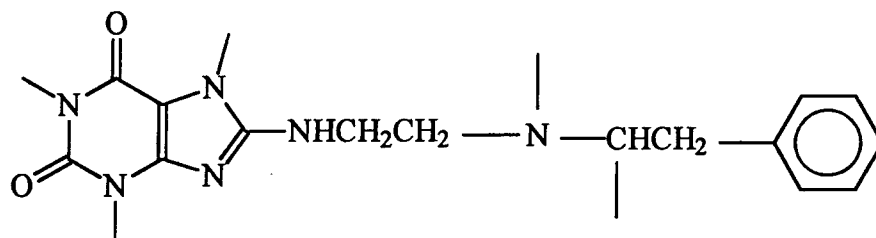7-17

Fenethylline ·
Merck #3901
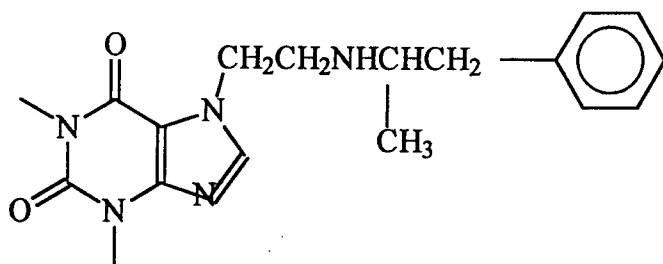
Preparation from 7-(- chloroethyl)theophylline and amphetamine
German patent 1,123,329 (1962) to Degusa. CA 57, 5933C (1962)
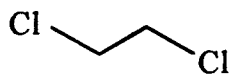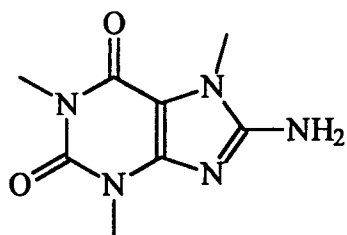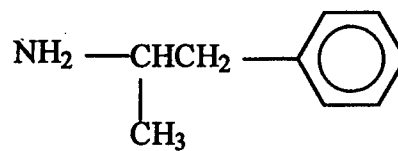

+ Amphetamine

Acros Organics, 15575-0050
7-(2-Chloroethyl)theophylline, 97%
(5878-61-5)
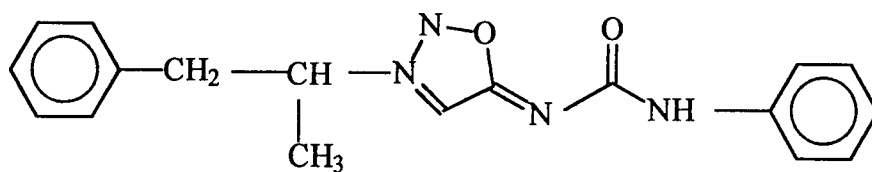5g/31.80, FW 242.66, mp 124-125
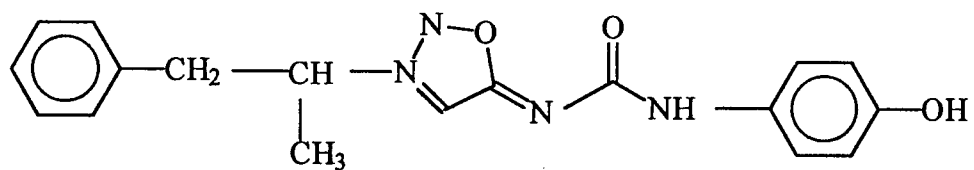
7-18

Fencamine
Merck #3894

Caffeine
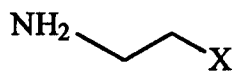
7-19

Mesocarb

Hydroxymesocarb (K220)

Dihydroxymesocarb

FILTERED-RAYLEIGH SCATTERING
IN REACTING AND NON-REACTING FLOWS

Kevin M. Lyons
Assistant Professor
Department of Mechanical and Aerospace Engineering

North Carolina State University
Box 7910
Raleigh, NC 27695-7910

FILTERED-RAYLEIGH SCATTERING
IN REACTING AND NON-REACTING FLOWS

Kevin M. Lyons
Assistant Professor
Department of Mechanical and Aerospace Engineering
North Carolina State University
Box 7910
Raleigh, NC 27695-7910

Abstract

Investigations into Filtered Rayleigh Scattering for large scale velocity field measurements in AEDC high speed wind tunnels were continued during the summer 1998 program. The injection seeded Nd:YAG laser was optimimized for measurements, refining the alignment and cooling system of the laser and assessing its temperature stability, tunability, mode hopping characteristics and other pertainent optical requirements. An iodine cell used in the collection optics was also constructed and tested in the laboratory. The main accomplishments of the research were the measurement of the one component of the velocity in a seeded laboratory air jet. At the current state, the technique is a qualitative velocity measurement technique. Work will be done in the next few months to design calibration schemes for quantitative measurement. The results indicate that filtered-Rayleigh scattering is a promising technique for tunnel applications and more work will be done in the coming year (1999) in making tunnel measurements feasable as well as improving measurement accuracy. Additionally, it is the PI's intent to apply the technique in reacting flows of fundamental interest.

FILTERED-RAYLEIGH SCATTERING
IN REACTING AND NON-REACTING FLOWS

Kevin M. Lyons

Background

In the history of experimental fluid mechanics and combustion, a wide variety of techniques have been used to study both large-scale and small-scale features of reacting and non-reacting flows. These techniques can be divided into categories based on the nature of the method employed. Measurements of scalars such as temperature have been made using thermocouples by physically probing the environment of interest. Velocity measurements have been made by hot wire anemometers, again by perturbing the flow with a probe. All of the methods classified as techniques that physically probe a medium have drawbacks related to the intrusive nature of the measurement. In addition, data obtained from physical probes need to be corrected in order to be made quantitative; for example, thermocouples need to be corrected for conduction and radiation effects. Also, as the measurement environment gets more hostile, it becomes more and more difficult to build probes that are able to withstand high temperatures and pressures and to remain accurate in the presence of particulates.

A category of techniques that has seen much fruitful use in fluid mechanics and combustion is that of optical diagnostics. Shadowgraphy and Schlieren photography have been applied widely in fluid mechanics, particularly in the area of compressible flow. These methods are sensitive to changes in refractive index and hence density, and have the advantage that they allow two-dimensional measurements to be made (Merzkirch 1987). These techniques have the draw back that they are line-of sight, i.e. the detector records images integrated through the measurement volume. With two spatial dimensions well resolved and one poorly resolved, applications of these techniques are limited.

Probably the best known and most widely applied optical technique used to

measure velocity in flows is laser Doppler velocimetry (LDV). The technique obtains its name from preliminary experiments where the Doppler shift of light incident on moving particles in a flow was detected; the shift is indicative of one component of the flow velocity in the resolution volume. Today's velocimeters, while referred to as laser "Doppler" anemometers, do not in general employ the same principles. Using these instruments, intensity gratings are created in the flowfield by the intersection of two laser beams. As a particle travels through the bright fringes in the grating, a time trace of the scattered light is detected. Since the spacing in the grating is known from the wavelength of the laser and the orientation of the beams, one component of the velocity can be found. Instruments are commercially available that use these principles for measuring all three components of the velocity. These instruments have frequently been used to determine velocity statistics at a point. The advantages of the current LDV instrumentation is the high data rate (> 10 kHz) and ease of optical alignment. The major drawback is the single point nature of the technique, being unable to instantaneously characterize turbulent flow structures and the need for particle seeding. Heitor et al. 1993 surveys recent advances in laser Doppler velocimetry techniques and instrumentation.

A variety of molecular tagging techniques have been used to determine velocity fields in gas flows using laser-induced fluorescence and phosphorescence of molecules in the flow. Velocity field visualizations in subsonic gas flows have been obtained by laser-induced phosphoresce of biacetyl molecules (Hiller et al. 1984). This technique is restricted to applications in low speed flows and due to the uncertainty in phosphorescence lifetime of the biacetyl molecule, the accuracy of the velocity measurement is poor. Velocity profiles in a sonic jet have been obtained by Raman excitation and laser-induced electronic fluorescence of oxygen molecules (RELIEF) (Miles et al. 1989). These studies have resulted in velocity measurements of one component along a line. Another class of velocity measurement techniques, better termed spectroscopic techniques, rely on the Doppler shifted absorption curve of molecules such as iodine and sodium. These and other similar

8-4

techniques have met with varying degrees of success. The shortcoming in all of these approaches is the difficulty in measuring more than one component of the velocity. Additionally, most of these techniques are not suitable for application in reacting flows. However, their major strength is that no particulates need to be added to the flow as markers, as is required in LDV or PIV.

Seeding flows with small particles and subsequently tracking their motion is an approach taken by many to both qualitatively and quantitatively investigate fluid motion. Van Dyke's *An Album of Fluid Motion* has many examples of light scattering from smoke particles in air to visualize flowfields. Particle streak velocimetry has been used to investigate velocity fields by recording scattered light from moving particles interrogated by light sources of long enough duration to result in streaks rather than particle images. This technique allows the determination of the velocity field by knowledge of the length of the streak and the duration of the laser pulse. However, its general applicability and accuracy are questionable since it depends on measurement of the length of individual particle streaks by visual or computer-aided inspection.

In recent years studies of velocity fields in various flows have been made using particle image velocimetry (PIV). By using strobed laser light to illuminate a plane within a particle seeded flow, multi-exposed images are recorded, which contain information about the displacement of the particles. Processing this data yields the in-plane velocities within the illumination sheet. The time interval between pulses is adjusted according to flow velocity in order to optimize the measurement of the particle displacement. Though many PIV studies to date examine laminar flow fields, this technique does have the ability to yield quantitative information with high spatial resolution about two-dimensional velocity fields in turbulent flows, and is being presently applied to such flows. Investigations of steady and turbulent flows have been made including uncertainty estimates in turbulent flows. Measurements of velocity fields and vorticity in a plane have been made in a motored

internal combustion engine. This study is encouraging in that it demonstrates application of PIV to practical devices.

Techniques Suitable for Large Scale Tunnel Facilities

Although the techniques discussed above have produced many important results in laboratory and small scale device diagnostics, most of them are unsuitable for large scale wind tunnel/model testing applications. Firstly, most require the detector to be in close proximety to the laser sheet, which is difficult to accomplish in most tunnel/model geometries. Also, the addition of particulates to the flow, as required in LDV and PIV, limits the number of tunnels that can be probed with such techniques. Filtered Rayleigh Scattering is a promising technique that can be used to make quantitative measurements of velocity by using the doppler shifted scattered light from particulates (and/or molecles in the flow). In addition, in order to desciminate the scattered light at the doppler shifted wavelength from the background laser light, the absoption spectra of an iodine vapor cell is used due to its sharp-cut properties and its shape in the vicinity of the operational wavelength of the Nd:YAG laser. The theory and basic details are contained in many papers and monographs, among them Elliott and Samimy (1996) and Forkey (1996).

Achievements During Summer 1998

A)   An injection seeded Continuum Nd:YAG was optimized for the proposed measurements. This involved precise alignment of the diode laser used to seed the main YAG laser in order to reduce the laser linewidth by an order of magnitude.

B) An iodine cell to be used in the Filtered Rayleigh experiments was constructed and tested. The cell was made of a 4 inch diameter Pyrex tube 12 inches in length with imaging quality flat glass ends that were fused to the Pyrex. A sidearm was installed in the Pyrex tube through which 5 grams of iodine was inserted. The cell was then evacuated and the sidearm sealed. Heat tape was then applied to the cell, as well as to the sidearm

independently, and each of the regions were controlled separately. The sidearm temperature was below the cell temperature (nominally 30 C compared to 80 C for the cell) and effectively controlled the number density of iodine in the vapor. Once the cell was temperature stabilized, absorption measurements were using aa unintensified CCD detector to detect scattered light from a jet interrogated by a laser sheet from the seeded laser. Reproductions of numerically predicted iodine absorption were made and compared to previous results (Forkey 1996).

In addition, relative velocity measurements were attempted in a high speed jet seeded with a fogging agent. Although the results were qualitative, many of the problems associated with making quantitative measurements were investigated in a preliminarly manner. The future will see these issues in A) and B) reinvestigated in the research follow-on program, as well as make preparations for the full scale tunnel test anticipated to be in late 1999.

C) Other Efforts

Some of the issues discussed concerned experimental setup, data processing, background suppression and system calibration. Based on these conversations, along with the current literature on flowfield assessment (Arnette et al. 1995, McKenzie 1996, Miles and Lempert 1997), the filtered-Rayleigh technique seems promising as a technique for assessment of velocity fields in large scale facilities such as 16T at AEDC. Although currently the filtered Rayleigh technique requires particle seeding to obtain adequate signal levels, it is anticipated that the technique will be applicable in the future in unseeded flows with the advent of higher energy pulse lasers (Miles and Lempert 1997).

The PI is in the process of analyzing some Rayleigh scattering measurements along with a student (Kyle Watson, NCSU) and Wright-Patterson AFB personnel (Jeff Donbar) and ISSI scientists (Cam Carter). The Figure shows turbulent diffusion flame images with the hot zone (dark) surrounding a nonreacting core (light). These results were obtained by Kyle Watson and Cam Carter at Wright Laboratories. We are in the process of examining

this leading edge of the flame in more detail and will pursue this work in the next year both at N.C. State and in our ongoing collaboration with Wright-Patterson AFB and AEDC.

Future Work

The future work in 1999 involves a number of engineering/ image acquisition issues, including:

A) Testing the system by looking at larger fields of view.

B) Taking steps to environmentally seal cameras to be able to operate in ambient tunnel conditions.

C) Working on software to facilitate data processing and analysis.

D) Application in Reacting Flows.

Theses issues are to be addressed during 1999 during either the Summer Research Program, at the faculty members university in conjunction with a student or at both times. The intentions are that if enough progress can be made by 8/99, preparations for a full scale run should begin in early 1999 and a run attempted possibly in Fall 1999.

References

Arnette, S. A., Samimy, M. and Elliott, G. S., AIAA Jl. 33, 430 (1995)

Eckbreth, A., *Laser Diagnostics for Combustion Temperature and Species,* (Abacus Press, Cambridge, MA 1988).

Elliott, G. S. and Samimy, M., AIAA96-0304, Reno (1996).

Forkey, J. N., Ph.D. dissertation #2067-T, Princeton University (1996).

Laufer, G., *Introduction to Optics and Lasers in Engineering,* (Cambridge 1996)

McKenzie, R. L., Applied Optics 35, 948 (1996)

Merzkirch, W., *Flow Visualization,* 2nd ed. (Academic Press, Orlando 1987).

Miles, R. B. and Lempert, W. R., Annual Review of Fluid Mechanics, 26, 285 (1997)

Watson, K., Lyons, K. M., Donbar, J. and Carter, C. D., to appear Comb. Flame (1999)